UNIVERSITY OF CYPRUS

DEPARTMENT OF BIOLOGICAL SCIENCES

Defective polycystin 2 increases cellular proliferation in the PKD2 (1-703) transgenic rat subsequent to the appearance of renal cysts

PANAYIOTA KOUPEPIDOU

PhD THESIS

MAY, 2009

Panayiota Koupepidou

UNIVERSITY OF CYPRUS

DEPARTMENT OF BIOLOGICAL SCIENCES

Defective polycystin 2 increases cellular proliferation in the PKD2 (1-703) transgenic rat subsequent to the appearance of renal cysts

PANAYIOTA KOUPEPIDOU

Thesis submitted for the degree of Doctor of Philosophy at the Department of Biological Sciences, University of Cyprus.

Panayiota Koupepidou

BOARD OF EXAMINERS

Professor Constantinos Deltas, University of Cyprus

Assistant Professor Pantelis Georgiades, University of Cyprus

Lecturer Paris Skourides, University of Cyprus

Professor Konstantinos Siamopoulos, University of Ioannina

Dr Aristidis Charonis, Biomedical Research Foundation of the Academy of Athens

Panayiota Koupepidou

ABSTRACT

The main characteristic of Autosomal Dominant Polycystic Kidney Disease (ADPKD) is the formation of bilateral fluid-filled cysts that eventually destroy the renal parenchyma and lead to chronic renal failure. Although the genes responsible for ADPKD are known, the mechanisms of disease initiation and progression are not completely understood. To date, abnormal cell proliferation is thought to be a major pathogenic feature of the disease. Cysts are thought to arise from tubular epithelial cells mainly through increased proliferation, but other processes including apoptosis, differentiation, alterations in epithelial cell polarity and fluid secretion are thought to be contributing factors. Studies have provided evidence of abnormal proliferation in both cystic and noncystic epithelia of human ADPKD and in animal models resembling ADPKD. Several proteins and pathways known to regulate proliferation have been shown to be deregulated in cell culture systems and animal models of Polycystic Kidney Disease (PKD).

In this study the role of polycystin-2 (PC-2) in PKD cellular proliferation was addressed by using primary cultures of Tubular Epithelial Cells (TECs) from 7.5 week old transgenic rats overexpressing a mutated form of PC-2, the protein product of PKD2. These cultured cells displayed increased proliferation as assessed by increased levels of proliferating cell nuclear antigen (PCNA), c-myc, cyclin-dependent kinase 2 (cdk2), decreased levels of $p57^{kip2}$ and abnormal cell cycle profile as compared to their normal counterparts.

However, the contribution of PC-2-induced abnormal proliferation to cyst initiation remained unclear. To further address this issue gene expression profiling of whole kidney homogenates from rats at an early stage of the disease, at 0, 6 and 24 days, was performed. Although cysts appear as early as 0 days, deregulation of proliferation-related genes occurs after 24 days. Instead, pathways including the renin-angiotensin system, the Wnt, focal adhesion, glutathione metabolism and basal transcription factors are altered at these early time points. This demonstrates that abnormal cell proliferation is probably not a primary event in the initiation and formation of cysts but is probably involved at later stages in disease pathogenesis.

Panayiota Koupepidou

ΠΕΡΙΛΗΨΗ

Το κύριο χαρακτηριστικό της Αυτοσωματικής Επικρατούσας Πολυκυστικής Νόσου των Νεφρών είναι η δημιουργία αμφοτερόπλευρων κύστεων γεμάτων με υγρό που καταστρέφουν το νεφρικό παρέγχυμα και οδηγούν σε χρόνια νεφρική ανεπάρκεια. Παρόλο που τα γονίδια που ευθύνονται για τη νόσο είναι γνωστά, ο μηχανισμός γένεσης και ανάπτυξης των κύστεων δεν είναι απόλυτα κατανοητός. Μέχρι σήμερα, ο αυξημένος κυτταρικός πολλαπλασιασμός θεωρείται ένα από τα κύρια παθογενετικά χαρακτηριστικά της ασθένειας. Πιστεύεται, ότι οι κύστεις προκύπτουν από τον αυξημένο πολλαπλασιασμό των σωληναριακών επιθηλιακών κυττάρων, παρόλο που και άλλες διαδικασίες όπως η απόπτωση, η διαφοροποίηση, οι αλλαγές στη πολικότητα των επιθηλιακών κυττάρων και έκκριση υγρού παίζουν σημαντικό ρόλο στη δημιουργία των κύστεων. Έρευνες έχουν δείξει αυξημένο κυτταρικό πολλαπλασιασμό σε κυστικά αλλά και μη κυστικά επιθήλια σε ιστούς ασθενών αλλά και σε ζωϊκά μοντέλα που μοιάζουν στον τρόπο εκδήλωσης της ασθένειας στον άνθρωπο. Επιπρόσθετα, σε τέτοια μοντέλα ζώων αλλά και σε συστήματα κυτταροκαλλιεργειών, παρατηρείται απορρύθμιση ενός σημαντικού αριθμού πρωτεϊνών, οι οποίες καθορίζουν και συντονίζουν τον κυτταρικό πολλαπλασιασμό.

Η μελέτη αυτή επικεντρώνεται στην εξέταση του ρόλου της πολυκυστίνης-2 (PC-2) στον κυτταρικό πολλαπλασιασμό που παρατηρείται στην πολυκυστική νόσο των νεφρών. Για το λόγο αυτό, χρησιμοποιήθηκαν πρωτογενή σωληναριακά επιθηλιακά κύτταρα από διαγονιδιακούς αρουραίους ηλικίας 7.5 εβδομάδων, στα οποία υπερεκφράζεται μια μεταλλαγμένη μορφή της πολυκυστίνης-2. Τα κύτταρα αυτά επέδειξαν τόσο μια αυξημένη ικανότητα πολλαπλασιασμού, όσο και αντικανονικά προφίλ κυτταρικού κύκλου, συγκρινόμενα με τα αντίστοιχα φυσιολογικά. Η αυξητική ικανότητα των κυττάρων καταγράφηκε και σαν αύξηση των ενδοκυτταρικών επιπέδων του PCNA, του c-myc και του cdk-2, αλλά και σαν μείωση του $p57^{kip2}$.

Παρόλα αυτά, η συμβολή της πολυκυστίνης-2 στον αυξημένο κυτταρικό πολλαπλασιασμό κατά την εμφάνιση των κύστεων παραμένει αδιευκρίνιστη. Με τη χρήση πειραμάτων μικροσυστοιχιών έγινε μια προσπάθεια περεταίρω εξέτασης του τρόπου δράσης της πολυκυστίνης-2, στα οποία έγινε ανάλυση της συνολικής γονιδιακής έκφρασης με τη χρήση ομογενοποιήματος ολόκληρου νεφρού, από τους ίδιους διαγονιδιακούς αρουραίους στα πρώτα στάδια της κυστογένεσης, και συγκεκριμένα ηλικίας 0, 6 και 24 ημερών. Έτσι

Panayiota Kouppari

φάνηκε πως παρόλο που οι κύστεις εμφανίζονται στις 0 μέρες, η απορύθμιση των γονιδίων που σχετίζονται με τον πολλαπλασιασμό παρατηρείται μετά από τις 24 ημέρες. Ταυτόχρονα, στις πρώτες ώρες γέννησης φάνηκε να επηρεάζονται μονοπάτια όπως το σύστημα ρενίνης-αγγειοτασίνης, το μονοπάτι του Wnt, των εστιακών σημείων πρόσδεσης, ο μεταβολισμός της γλουταθιόνης και οι μεταγραφικοί παράγοντες έναρξης. Αυτό αποδεικνύει πως ο αυξημένος πολλαπλασιασμός στην πολυκυστική νόσο των νεφρών δεν επάγεται απευθείας από την γένεση ή την δημιουργία των κύστεων, αλλά είναι πιθανόν να ξεκινά σε μεταγενέστερα παθογενετικά στάδια της νόσου.

Panayiota Koupepidou

ACKNOWLEDGEMENTS

This work would have not been possible without Prof. Constantinos Deltas. I would like to express my deep and sincere gratitude to him for his supervision, advice, and encouragement.

I am deeply indebted to Dr Kyriacos N. Felekkis, a truly committed and able scientist, for his guidance, stimulating suggestions and critical comments both on the experimental work and the writing of this thesis.

I would also like to warmly thank the following colleagues and associates, in no particular order, for their invaluable help and support over the past 6 years:

- All the members of the Laboratory of Molecular and Medical Genetics of the University of Cyprus and especially Gregoris Papagregoriou for his critical comments and suggestions on the manuscript.
- Prof Norbert Gretz, and his team members, Dr Bettina Kranzlin, Dr Li Li, Dr Carsten Sticht and Maria Saile for their rats and their work on gene expression profiling.
- Dr Leonidas Tsiokas and Dr Chang-Xi Bai for the plasmids and electrophysiology experiments.
- Dr Ralph Witzgall for the rat model.

The Research Promotion Foundation and the University of Cyprus must also be acknowledged for providing the funds for my experimental work.

I cannot end without thanking my family, on whose constant encouragement and love I have relied throughout these years. It is to them that I dedicate this work.

Panayiota Koupepidou

TABLE OF CONTENTS

Panayiota Koupepidou

Panayiota Kouppepidou

Panayiota Koupepidou

LIST OF FIGURES

Parayota Koupenio

Panayiota Koupepidou

LIST OF TABLES

Panayiota Kouppoidou

Panayiota Koupepidou

LIST OF ABBREVIATIONS

μ	micro (10^{-6}, μg, μl, etc)
^{o} C	degrees centigrade
aa	amino acid(s)
ADPKD	autosomal dominant polycystic kidney disease
ANOVA	analysis of variance
ASO	antisense oligomer
ARPKD	autosomal recessive polycystic kidney disease
ATP	adenosine triphosphate
BBS	Bardet-Biedl syndrome
BCA	bicinchoninic acid
bp	base pairs
BSA	bovine serum albumin
BUN	blood urea nitrogen
cAMP	cyclic adenosine monophosphate
CDK	cyclin dependent kinase
cDNA	complementary deoxyribonucleic acid
CFTR	cystic fibrosis transmembrane conductance regulator
CHO	chinese hamster ovary
CKI	cyclin-dependent kinase inhibitor
CMA1	chymase1
CMV	cytomegalovirus
c-myc	avian myelocytomatosis viral oncogene homolog
Cp	crossing point
Cpa3	carboxypeptidase A3
C-terminus	carboxy terminus
d	day(s)
DCT	distal convoluted tubule
D-MEM	Dulbecco's modified eagle medium
ECL	enhanced chemiluminescence
EDTA	ethylenediaminetetraacetic acid
EGF	epidermal growth factor
EGFR	epidermal growth factor receptor

Panayiota Koupepidou

EGTA	ethylene glycol tetraacetic acid
ER	endoplasmic reticulum
ERK	extracellular signal-regulated kinase
ESRD	end stage renal disease
FBS	fetal bovine serum
g	gram(s)
GAPDH	glyceraldehyde-3-phosphate dehydrogenase
GOI	gene of interest
GPS	G protein-coupled receptor proteolytic site
GSK3	glycogen synthase kinase 3
HA	haemagglutinin
HEK293	human embryonic kidney cell line
HEPES	4-(2-hydroxyethyl)-1-piperazineethanesulfonic acid
HLH	helix-loop-helix
HPRT	hypoxanthine-guanine phosphoribosyltransferase
HRP	horseradish peroxidase
IGF	insulin growth factor
IRAP	insulin-regulated membrane aminopeptidase
JAK	Janus kinase
kb	kilo-base pairs
kDa	kilodalton
L	liter(s)
m	milli (ml, mg etc)
M	molar
MAPK	mitogen-activated protein kinase
MCKD	medullary cystic kidney disease
MDCK	Madin-Darby canine kidney
Mfap3	microfibrillar-associated protein 3
min	minute(s)
mRNA	messenger ribonucleic acid
mTOR	mammalian target of rapamycin
Nek8	never in mitosis A-related kinase 8
NPHP	nephronopthisis
NRK52E	normal rat kidney epithelial cells

Paraskevi Koupepidou

N-terminus	amino terminus
p	probability
p	short arm of a chromosome
PACS	phosphofurin acidic cluster proteins
PAGE	polyacrylamide gel electrophoresis
PBS	phosphate buffered saline
PC	polycystin
PCNA	proliferating cell nuclear antigen
PCR	polymerase chain reaction
PCT	proximal convoluted tubule
PFA	paraformaldehyde
PI	propidium iodide
PIGEA14	polycystin-2 interactor, golgi- and ER-associated protein
PKD	polycystic kidney disease
PKHD1	polycystic kidney and hepatic disease 1
PVDF	polyvinylidene fluoride
q	long arm of a chromosome
REJ	receptor for egg jelly
RG	reference gene
RNA	ribonucleic acid
rpm	revolutions per minute
RT	reverse transcription
RT-PCR	reverse transcriptase PCR
SBM	SV40 enhancer, β-globin promoter, myc
s.d.	standard deviation
SD	sprague dawley
SDS	sodium dodecyl sulphate
SEM	standard error of the mean
STAT	signal transducers and activators of transcription
TEC	tubular epithelial cell
TGFα	transforming growth factor alpha
TIMP	tissue inhibitor of metalloproteases
TRP	transient receptor potential
WT	wild type

Panayiota Koupepidou

1 INTRODUCTION

1.1 Physiology of the kidney and structure of the nephron

The kidney is a vital organ that performs an excretory, regulatory and secretory function. Humans have two kidneys which are located about two inches above the body's midline just below and behind the liver in the upper abdomen and behind the lower ribs. The primary function of the kidney is to maintain the proper balance of water and minerals (including electrolytes) in the body. Additional functions include the filtration and excretion of waste products from the processing of food, drugs, and harmful substances (toxins), the regulation of blood pressure and the secretion of certain hormones (such as erythropoietin, renin and 1, 25-Dihydroxyvitamin D3).

The end product of the kidney's function is urine, which flows from the kidneys through the ureter into the bladder, from where it is eliminated through the urethra. The kidney consists of two distinct regions, an outer cortex and an inner medulla. The cortex has a granular appearance and the medulla is composed of renal pyramids, which are coned-shaped structures. The base of each pyramid touches the cortex and the tip of each pyramid – a region known as the renal papilla – projects into the renal sinus (an internal cavity within the kidney). Adjacent renal pyramids are separated by cortical tissue called renal columns which extend into the medulla. Ducts within each renal papilla discharge urine into calyces that merge to form the renal pelvis, which is connected to the ureter (**Figure 1a**).

The basic functional unit of the kidney is the nephron. Its main function is to regulate the concentration of water and soluble substances by filtering the blood, reabsorbing what is needed and excreting the rest as urine. There are about 1 million nephrons in each human kidney. Each nephron consists of (1) a glomerulus, which is surrounded by a thin-walled bowl-shaped structure, called the Bowman's capsule, (2) the proximal convoluted tubule (PCT), (3) the descending and ascending limbs of the loop of Henle, and (4) the distal convoluted tubule (DCT). Each nephron is connected to a collecting duct. The cortex contains the glomeruli, the proximal and distal tubules, the cortical collecting duct tubules and the peritubular capillaries. The pyramids of the medulla are made of the long loops of

Panayiota Koupepidou

Henle, the medullary collecting ducts and the *vasa recta* (long, straight capillaries that parallel the loop of Henle) (**Figure 1b**).

A

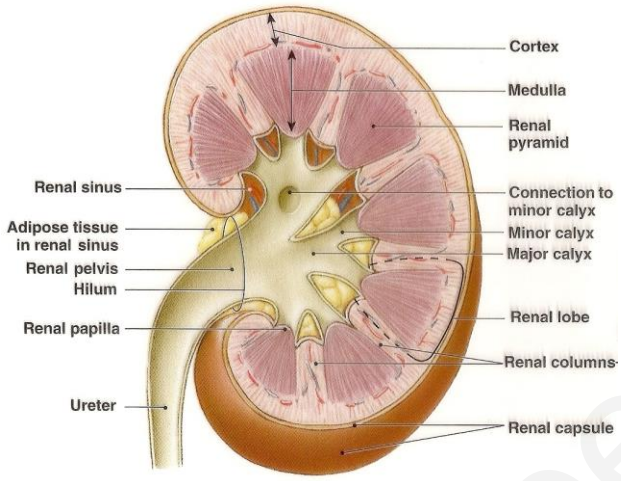

B

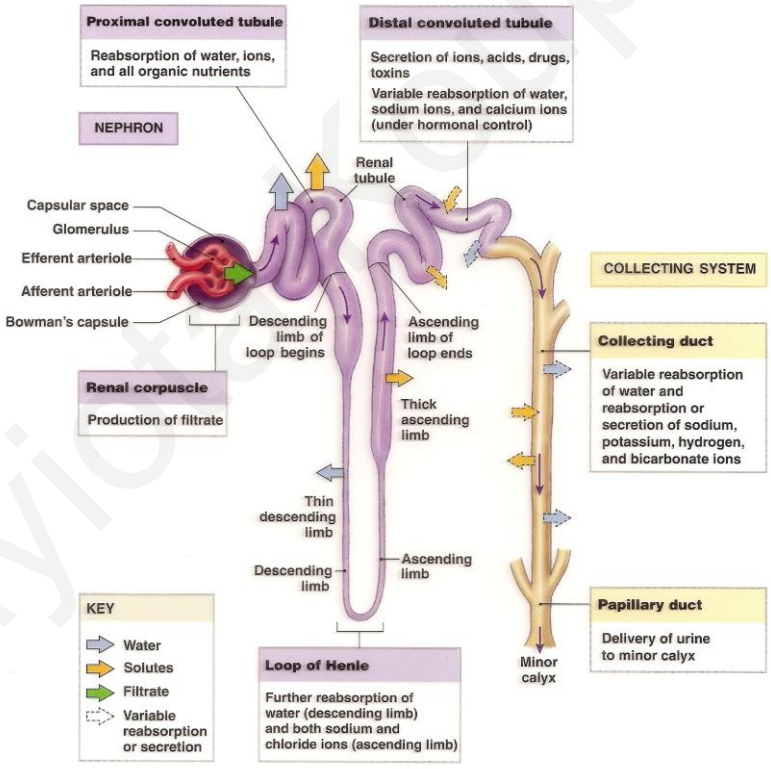

Figure 1: A diagrammatic representation of a section of a kidney
(A) and the structure of a nephron showing the major functions of each segment (B) [taken from [1]].

The glomerulus is a capillary tuft that receives its blood supply from an afferent arteriole of the renal circulation. As blood flows through the kidneys, approximately 20% of the plasma is filtered through the glomerular wall into the Bowman's capsule. The glomerular

Panayiotakopepidou

membrane only allows filtration of fluid and small molecules. This glomerular filtrate is then processed along the tubules to form urine. The renal tubule is responsible for reabsorbing all the useful organic nutrients that enter the filtrate, reabsorbing more than 90% of the water in the filtrate, and secreting into the tubule any waste products that failed to enter through filtration at the glomerulus. The lining of the PCT is a simple cuboidal epithelium whose apical surfaces bear microvilli. At the site of the PCT, the tubular cells absorb organic nutrients, ions, water and plasma proteins (if present) from the tubular fluid and release them into the peritubular fluid (the interstitial fluid surrounding the renal tubule). The limbs of the loop of Henle consist of a thin and a thick segment, which refers to the height of the epithelium: the thick segments have a cuboidal epithelium whereas a squamous epithelium lines the thin segments. The thick descending limb pumps sodium and chloride ions out of the tubular fluid. The thin segments are freely permeable to water, but not to solutes. Water moving out of these segments helps concentrate the tubular fluid. The DCT has a smaller diameter than the PCT and its epithelial cells lack microvilli. At the site of the DCT three processes occur: (1) the active secretion of ions, acids, drugs and toxins, (2) the selective reabsorption of sodium and calcium ions from tubular fluid and (3) the selective reabsorption of water, which assists in concentrating the tubular fluid. The collecting system transports the tubular fluid from the nephron to the renal pelvis, adjusts the fluid's composition and determines the volume of urine[1].

1.2 Cystic diseases of the kidney

The cystic diseases of the kidney refer to a set of single-gene disorders that frequently progress to end-stage renal disease (ESRD) due to progressive tubular cystic expansion and loss of normal renal structure and function. They are transmitted both as autosomal dominant and autosomal recessive. Although they share common features such as the development of fluid-filled cysts and progressive impairment of renal function, they are distinguished by different ages of onset, variable rates of renal disease progression and a diverse range of extra-renal manifestations. The most prevalent of these disorders is the Autosomal Dominant Polycystic Kidney Disease (ADPKD). The two distinct types of Medullary Cystic Kidney Disease (MCKD) are also inherited as autosomal dominant traits (a third locus has been implicated due to the lack of linkage to the other two loci in some families). They are caused by mutations in either the *MCKD1* or *MCKD2* gene, and are characterized by bilaterally shrunken kidneys, cysts restricted to the renal medulla and the

Panayiota Koupepidou

corticomedullary region, salt wasting and polyuria. Some cases present with hyperuricaemia, manifested as gout. Recessive disorders include the Autosomal Recessive Polycystic Kidney Disease (ARPKD), caused by mutations in *PKHD1* (Polycystic Kidney and Hepatic Disease 1), the juvenile, the infantile and the adolescent forms of Nephronophthisis (NPHP) and the Bardet–Biedl syndrome (BBS). ARPKD is characterized by bilateral renal cysts that derive from collecting ducts and start to develop *in utero*. Cysts in ARPKD result from the expansion of the collecting duct and remain in contact with the nephron of origin. About 30% of patients die perinatally, although most patients reach ESRD in infancy, early childhood or adolescence. The *PKHD1* gene encodes polyductin/ fibrocystin, which has a role in terminal differentiation of the collecting duct and biliary system. Nine different genes have been identified to cause Nephronopthisis and twelve genes have been identified to cause the Bardet-Biedl syndrome. Cysts in NPHP mostly arise from the corticomedullary border of the kidneys and renal pathology typically consists of tubular basement membrane disruption, tubular atrophy, cyst development and interstitial infiltration along with fibrosis[2-4].

1.3 The primary cilium as a unifying organelle in cystic diseases of the kidney

Every tubular epithelial cell, with the exception of intercalated cells of the renal collecting tubule, has a primary cilium on its apical surface. The primary cilium is an antenna-like organelle that consists of a ciliary membrane that is continuous with the cell membrane and a central axoneme composed of nine peripheral doublets of microtubules, but lacks the central microtubule structure (9+0) found in motile cilia (9+2). The cilia axoneme originates from the basal body, a centriole-derived microtubule organizing centre. Primary cilia act as sensory cellular organelles to detect a wide variety of stimuli outside the cell.

The cilium has received much attention lately, as a convergence of data indicated that the products of almost all genes mutated in cystic diseases of the kidney in humans, mice and zebrafish were found to localise in primary cilia, basal bodies or centrosomes[5]. Also, inactivation of Kif3a, a protein involved in maintenance of renal ciliary structure has resulted in cystic kidney disease [6]. Defects in structure or function of the primary cilium could possibly be involved in the mechanisms of developing cystic disease of the kidney. The exact molecular function of cilia and their role in cystic diseases of the kidney is still unknown although they have been implicated in mechanosensation. It has been observed

Panayiota Koupepidou

that bending of renal cilia by fluid flow results in an increase of intracellular calcium $[Ca^{2+}]_i$ [7]. However, little is known about the downstream signaling pathways regulated by this mechanosensation, and how defects in the structure and function of primary cilia contribute to the development of a cystic phenotype. It is thought that they may play a role in regulation of the cell cycle, the Wnt signaling pathway and the establishment of planar cell polarity and that they may be important in the regulation of tubule lumen diameter [8].

1.4 Autosomal dominant polycystic kidney disease

The main characteristic of ADPKD is the formation of bilateral fluid-filled cysts in renal tubules and collecting ducts, which progressively enlarge and lead to the destruction of the normal renal parenchyma and finally cause renal failure. Interstitial inflammation, fibrosis and tubular apoptosis appear to be involved in renal deterioration [9]. ADPKD cysts derive from every segment of the nephron [10]. Cysts are out-pouches of the tubule wall, lined by a single layer of epithelium that expand and finally close off from the nephron of origin. While cysts remain in continuity with the nephron, intracystic fluid may derive from glomerular filtrate. However, when cysts expand and lose their connection to the nephron, they grow to a large size by continued cell proliferation and by the secretion of fluid into the cyst lumen [11].

ADPKD is genetically heterogeneous and can arise by mutations in either of two genes, *PKD1* or *PKD2*, which encode for polycystin-1 (PC-1) and polycystin-2 (PC-2), respectively. About 85-90% of the cases of the autosomal dominant form are caused by mutations in the *PKD1* gene (type I disease – ADPKD1) and 10-15% of the cases are due to mutations in the *PKD2* gene (type II disease – ADPKD2). Linkage studies have revealed a very small percentage of families that do not link to either loci [12], and so there is an implication for a third locus, but such has not been identified yet.

ADPKD is one of the most common human inherited monogenic diseases with a prevalence of 1:1000. It is a systemic disease affecting multiple organs and cell types. Early symptoms include hypertension, polyuria, back pain, recurrent urinary tract infections and renal stones [2,10]. Apart from kidney cysts, patients develop cysts in the liver, pancreas and intestine and may present with colonic diverticulitis, intracerebral or aortic aneurysms and heart valve defects [13].

Panayota Koupepidou

The clinical manifestation of type I and type II disease is very similar, although there are differences in that ADPKD2 is a milder disease [14]. It has a lower prevalence of hypertension and a later age of onset at ESRD (ADPKD1 mean age: 54.3 years and ADPKD2, mean age: 74 years) [14,15]. Interestingly, within both ADPKD1 and ADPKD2, there is a wide range of intrafamilial variability, both in the severity of renal disease and extrarenal abnormalities, which indicates that modifier genes and environmental factors possibly influence the course of the disease [16-18]. Modifier genes could regulate cyst initiation or disease progression by influencing polycystin-mediated signal transduction pathways, cyst fluid accumulation or other molecular features associated with ADPKD [19]. Several candidate modifiers have been proposed both in humans and PKD animal models, but no modifier has ever been proven to have a strong association with the disease [20].

1.5 Molecular genetics of ADPKD

The *PKD1* gene was identified by positional cloning in 1994. It is located on chromosome 16p13.3-p13.2, spans a region of 52kb, is encoded into a transcript of 14.2kb and translated into a protein of 4302aa, with an expected molecular weight of 462kDa [21-24]. The *PKD2* gene is located on chromosome 4q21-q23, spans a region of 70kb, is encoded into a transcript of 5.4kb and translated into a protein of 968aa, with a molecular weight of 110kDa [25,26].

Genomic duplication of the 5' region of *PKD1* has complicated the characterization of the gene structure and the identification of mutations in the *PKD1* gene. About 70% of the *PKD1* genomic sequence, encompassing exons 1 to 33, is duplicated at 6 other sites on the chromosomal region 16p13.1 [27]. These homologous genes have approximately 95% similarity to *PKD1* and are transcribed into mRNA, but they are not translated into proteins, and hence were named pseudogenes [28].

More than 200 mutations have been identified in the *PKD1* gene and they are of various types, including missense/ nonsense mutations, splicing defects, small deletions, small insertions, gross deletions, gross insertions and complex rearrangements [www.hgmd.cf.ac.uk]. Mutations at the 5' end of *PKD1* appear to be associated with an earlier onset of the disease than mutations at the 3' end [29]. More than 70 mutations have

Παναγιώτα Κουρεπίδου

been identified in the *PKD2* gene and they are mainly missense, nonsense mutations and gross deletions [[30], www.hgmd.cf.ac.uk].

It has been observed in ADPKD, that although all epithelial renal cells have the same inherited germinal mutation, only a small number (~1%) of the nephrons becomes cystic [31]. In an effort to explain the focal nature of cyst formation and the slowly progressive course of ADPKD, several laboratories have proposed that a somatic second hit or loss of heterozygosity may be required for cystogenesis to occur (the two hit hypothesis) [31]. This is a model in which one mutation (first hit) is inherited in one PKD allele, and another somatic mutation (second hit) is required in the wild type allele for cysts to form. This phenomenon has been revealed by several laboratories in both ADPKD1 and ADPKD2 [32-35]. It was also shown that in cystic DNA from a kidney of an ADPKD1 patient, somatic mutations occurred not only in the *PKD1* gene of certain cysts, but also in the *PKD2* gene of other cysts or vice versa, generating a trans-heterozygous state with mutations in both genes [36,37]. The role of trans-heterozygous mutations in *Pkd1* and *Pkd2* has also been investigated in mouse models of polycystic kidney disease, with trans-heterozygous mice developing more renal cysts compared to singly heterozygous mice. The somatic events in the other ADPKD gene appear to be analogous to the effects of modifying genes that increase the risk of cyst development rather than influence cyst initiation [38]. Somatic mutations have also been found on hepatic epithelial cystic cells [35]. Therefore, it can be concluded that while the pattern of inheritance of the disease is dominant, the disease acts like a recessive one at the cellular level.

Although the 'two-hit' hypothesis is the mutational mechanism proposed for ADPKD, it could not explain why not all epithelial cells isolated from cysts have been proven to have a somatic mutation, or why the polycystins have been detected by immunohistochemistry in many cyst-lining epithelia [39]. Other mechanisms are thought to contribute to the ADPKD development, including the gene-dosage effect or the dominant-negative mechanism. Therefore, the loss of heterozygosity model may not be the sole mechanism for cyst formation. The dosage level of functional PC-1 has been proven to be important since mouse models expressing reduced levels of PC-1 develop cysts [40,41]. Additionally, transgenic lines overexpressing a *Pkd1* transcript at different levels reproducibly develop a disease phenotype, implying the importance of the gene dosage effect mechanism [42,43]. Recently, Rossetti et al. identified three families with incompletely penetrant *PKD1* alleles

Panayiota Kouppoudou

resulting in mild cystic disease. This study suggests that the dosage of functional PC-1 is probably critical in cyst initiation [44]. Additional proof has been given by overexpression of a human truncated PC-2 (1-703) in Sprague Dawley rats, which gives rise to polycystic kidney disease that resembles human ADPKD despite high levels of functional endogenous PC-2 [45]. One of the possible mechanisms of cyst formation could be that precise levels of the polycystin proteins (or even a precise ratio between the two polycystins) have to be maintained in the cell and overexpression or a reduced dosage level of either of the two could lead to cystogenesis. Another possible mechanism could be that the mutant protein acts by a dominant negative manner, acting antagonistically to the wild type allele and producing an abnormal biologic activity.

There are still unanswered questions as regards to cyst initiation and formation and it seems that cystogenesis is probably due to a much more complex mechanism than the requirement of the somatic inactivation of a normal allele of the PKD genes. It cannot be ruled out however, that the second hit might be a later event more important for cyst expansion and progression rather than the initiation of the disease [46].

1.6 The polycystins and their function

1.6.1 Polycystin-1

PC-1 is a transmembrane protein spanning the membrane 11 times with its N-terminus in the extracellular space and the C-terminus in the cytoplasm [22,23]. PC-1 is thought to be a receptor with an as yet unidentified ligand, owing to its huge extracellular N-terminus that contains various distinct protein motifs, which includes two leucine-rich repeats (LRR), flanked by cysteine-rich domains, a C-type lectin domain, a WSC (named after the cell wall integrity and stress component proteins 1-4 found in *S. cerevisiae*) domain, a low-density lipoprotein-related domain (LDL), 16 immunoglobulin-like domains called PKD repeats [47], a receptor for egg jelly (REJ) domain and a G-protein coupled receptor proteolytic site (GPS) domain (**Figure 2**) [reviewed in [48]]. These extracellular motifs may function in protein-protein or protein-carbohydrate interactions, supporting a role for PC-1 in cell-adhesion and cell-matrix interactions [22-24]. The leucine-rich repeats of PC-1 interact with collagen I, laminin and fibronectin [49], whereas the C-type lectin domain binds carbohydrates in a Ca^{2+}-dependent manner and collagens I, II and IV *in vitro* [50]. The

Paraskota Koupepidou

extracellular portion of PC-1 can undergo cleavage at the GPS domain in a process that requires the REJ domain [51].

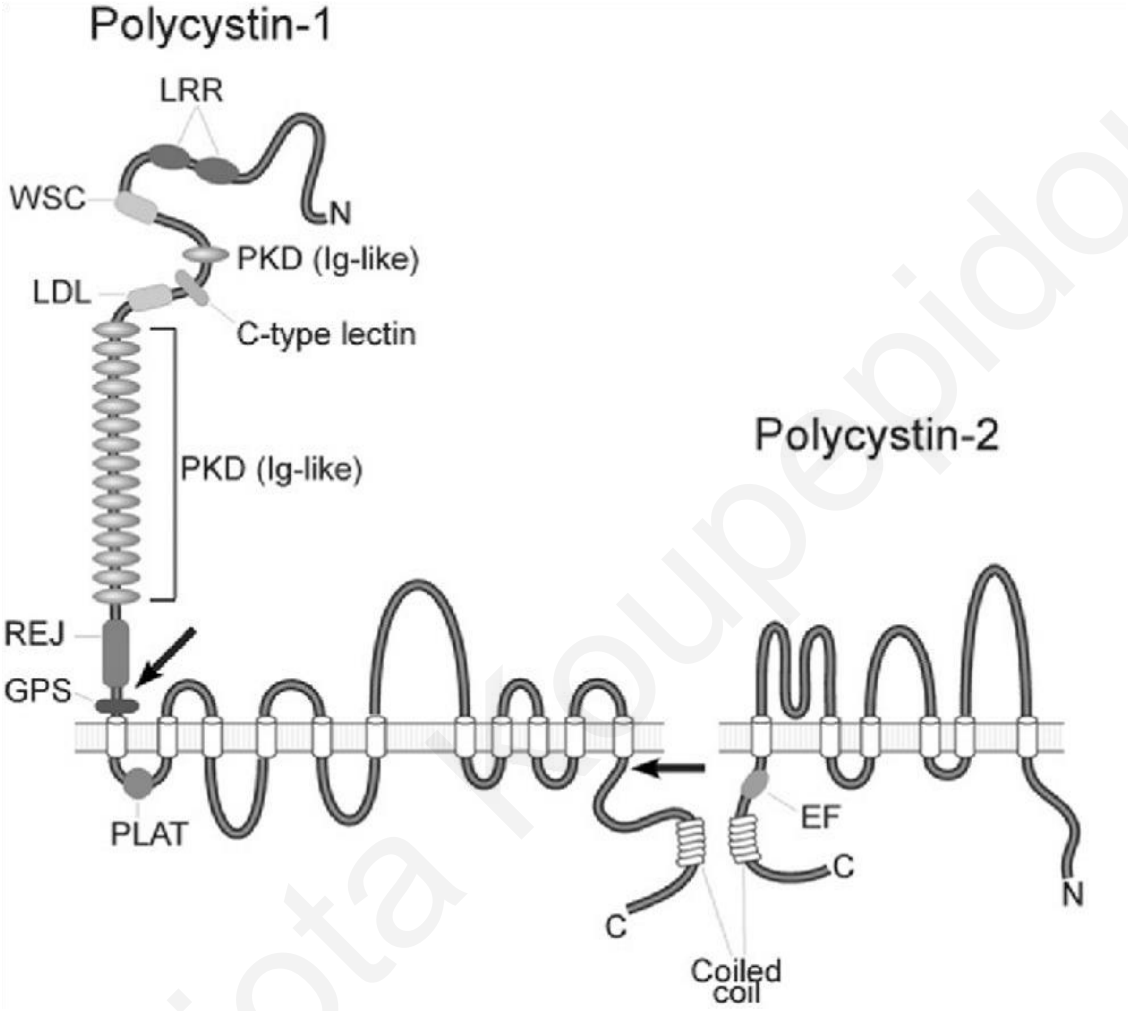

Figure 2: Graphical representation of the structures of polycystin-1 and polycystin-2.
LRR: Leucine-rich repeats, WSC: cell-wall integrity and stress-response component, PKD (Ig-like): Ig-like domains, LDL: low-density lipoprotein domain, REJ: receptor for egg jelly, GPS: G-protein coupled receptor proteolytic site, PLAT: lipoxygenase domain, EF: EF hand domain. Arrows indicate the sites at which polycystin-1 can undergo cleavage [taken from [52]].

On the intracellular site of the first transmembrane domain there is a PLAT – lipoxygenase domain. The intracellular C-terminus includes a coiled-coil domain, several predicted phosphorylation sites [23], and a presumed binding sequence for heterotrimeric G proteins [53]. The intracellular C-terminal portion of PC-1 has also been shown to undergo cleavage, in which the C-terminal tail was released (a process called regulated intramembrane

proteolysis – RIP) and translocated to the nucleus, where it could affect cell gene transcription [54].

PC-1 has been detected in tight junctions, adherens junctions, desmosomes, focal adhesions, apical vesicles and primary cilia [55-58]. It has been shown to interact with PC-2 through their C-termini [59], and other proteins including RGS7 (a member of the Regulators of G protein signaling proteins) [60], components of the intermediate filament network [61] and was found to form a complex with E-cadherin (an essential epithelial cell adhesion molecule) and its associated cytoplasmic catenins [62].

1.6.2 Polycystin-2

PC-2 is also a transmembrane protein, spans the membrane 6 times and both its N- and C-termini are intracellular [25]. The transmembrane region is homologous to PC-1 and to voltage-activated and Transient Receptor Potential channel (TRP) subunits [63]. The C-terminus of PC-2 contains an ER-retention signal, an EF-hand motif, and a coiled-coil domain (**Figure 2**) [25,64,65]. The N-terminus contains an RVxP motif responsible for cilial localization [66]. The subcellular localization of PC-2 has been an area of controversy. PC-2 has been found to localize to the plasma membrane [67-69], the endoplasmic reticulum (ER), which is its predominant location [70,71], the primary cilium [72] the centrosome [73] and the mitotic spindle in dividing cells [74]. The specific localization of PC-2 is determined by distinct recognition motifs and the function of PC-2 depends on its intracellular location. PC-2 forms a receptor-operated, non-selective cation channel in the plasma membrane [56,75], a novel intracellular Ca^{2+} release channel in the ER activated in response to increases in intracellular Ca^{2+} concentration [71,76] and a mechanosensitive channel in the primary cilium [reviewed in [77]].

PC-2 has been found to from a homodimer [59] and to interact with TRPC1 (a transient receptor potential channel protein) [78], the CD2-associated protein (CD2AP) (an adapter protein that attaches membrane proteins to the cytoskeleton) [79], HAX-1 (a protein associated with the cytoskeleton) [80], tropomyosin-1 (an actin microfilament component) [81], troponin I (an angiogenesis inhibitor) [82], IP_3R (Type I Inositol 1, 4, 5-Triphosphate Receptor) [83] and Nek8 (Never in mitosis A-related kinase 8) [84]. Functional significance of all these interactions, however, still remains elusive.

Panayiota Koupepidou

1.6.3 Functional interaction of polycystins

The similar disease profiles caused by mutations in *PKD1* and *PKD2* suggested that the polycystins probably function in common signaling pathways. The differential subcellular localisations of polycystins also suggested that apart from their common functions, both proteins might have independent functions.

The coiled coil domain in the C-terminus of PC-1 is responsible for the interaction with PC-2 [56,59,85,86]. The first report on the functional expression as a channel activity of PC-2 provided evidence that PC-1 and PC-2 interact to form a functional heteromeric complex *in vitro* [56]. In this study it was shown that PC-2 alone cannot form a functional channel in Chinese Hamster Ovary (CHO) cells, and that channel activity was not observed when PC-1 truncation mutants were used, implying that co-assembly of both proteins is required for PC-2 channel function in the plasma membrane [56]. It was also reported that the R742X *PKD2* mutant, which does not bind PC-1 translocates to the plasma membrane but does not display channel activity, suggesting that *PKD2* channel function requires PC-1 [56]. Another study, however, presented contradictory results displaying that the same R742X *PKD2* mutant displays channel activity [87]. Since the initial report on the channel function of PC-2 several studies using different systems have characterized the channel properties in more detail [75,76,88].

1.7 Cell biology of PKD

Although polycystins were identified more than a decade ago to be the causative proteins for ADPKD, the mechanism of cyst formation still remains elusive. Cysts arise from various tubular segments and are lined by a single layer of epithelium. The most important abnormalities of the tubular epithelium lining the cysts are [1] disturbance in the balance between tubular cell proliferation and apoptosis [89-93], [2] abnormal fluid secretion [89], [3] alterations of tubular basement membrane constituents and the associated extracellular matrix [94], [4] alterations of epithelial cell polarity with apical mislocalisation of key receptors and enzymes [95], and [5] abnormal ciliary function [96,97].

Panayiota Koupepidou

The polycystins have been found to regulate a confusing plethora of molecules and pathways, including the Wnt, β-catenin, mTOR, JAK/STAT, MAPK/ERK, AP-1, cAMP, Ca^{2+}, G-proteins and G-protein coupled receptors [10,98]. The integration of these pathways that possibly function in parallel, in a highly coordinated manner probably participate in an interplay within renal tubular cyst formation and progression; disruption of any of these, that control essential cellular functions such as proliferation, apoptosis, adhesion and differentiation, may potentially lead to a cystic phenotype. The proposed mechanisms of cyst formation are discussed in the following sections.

1.7.1 Alterations in epithelial cell polarity and abnormal fluid secretion

Although tubular epithelial cells typically absorb fluids, studies have supported the presence of fluid secretion in PKD [89] and have suggested a role of cyclic adenosine monophosphate (cAMP) in this process. The accumulation of fluid, after the cysts have lost their connection to the tubules, occurs by transepithelial fluid secretion [89]. Typically, tubular epithelial cells are polarized, with a well-defined apical and basolateral side, with coordinated distribution of specific receptors, transporters and channels. In human ADPKD cyst-lining epithelia, the epidermal growth factor receptors (EGFR) and the Na^+/K^+-ATPase, which is a sodium pump, are abnormally sorted to the apical (luminal) cell membranes rather than the basolateral membrane, and the Na^+, K^+, $2Cl^-$ symporter is misplaced to the basal surface of the epithelia [95,99]. The EGFR was found to be overexpressed and mislocalised in both human PKD and animal models of PKD [100]. As cystic fluid contains EGF and TGFα which are ligands of the EGFR, this is thought to promote a signalling cascade that results in cell proliferation [99]. The mispolarization of the Na^+/K^+-ATPase could account for the observation that cyst fluids aspirated from ADPKD patients contained abnormally high levels of Na^+ ions [95]. Abnormally high levels of Cl^- ions have also been observed, which suggested that the cystic fibrosis transmembrane conductance receptor (CFTR) played a role in fluid accumulation [101]. Additional studies have implicated that increased cAMP levels mediated the chloride secretion via CFTR [102]. Although abnormal polarity is frequently associated with renal cysts, it did not appear to be a prerequisite for cystogenesis or for the progressive cyst enlargement as there are cystic animal models with properly localized channels [45].

Panayiota Koupepidou

Apart from the apico-basolateral polarity of epithelial cells, there exists another level of polarity which describes a second polarity axis in the plane of the epithelium, called the planar cell polarity (PCP) pathway (also called noncanonical Wnt pathway) [8]. It is unknown, however, what role does the PCP play in the kidney. It was proposed that during renal development, the tubular epithelial cells must be correctly oriented with respect to a longitudinal axis of the tubule, when the tubule elongates by directed cell migration and cell division [103]. This is thought to be disrupted in PKD, giving rise to a dilated tubule or cyst. It has also been suggested that primary cilia regulate the PCP in the kidney, but the mechanism is not known. It has been reported that in response to fluid flow, the ciliary protein inversin (encoded by the gene responsible for NPHP2), seems to facilitate a switch from canonical to noncanonical Wnt signalling [104].

PC-1 was demonstrated to form a complex with the essential cell adhesion molecule E-cadherin and its associated cytoplasmic catenins, suggesting a role in the stabilisation of adherens junctions and the maintenance of a fully polarised renal epithelial cell [62]. This complex was found to be disrupted in primary cells from ADPKD patients with loss of E-cadherin and its substitution by N-cadherin [105]. The impairment of the PC-1/E-cadherin complex could result in altered cell-cell adhesion and defective signal transduction.

1.7.2 Alterations of tubular basement membrane constituents and the associated extracellular matrix

Alterations of tubular basement membrane constituents and the associated extracellular matrix have also been proposed to be a possible pathogenic mechanism of cyst initiation or expansion. The cystic epithelia from a rat model and human patients of ADPKD have been reported to contain increased levels of basement membrane components, such as laminin, fibronectin, type IV collagen and heparan sulphate proteoglycan, resulting in basement membrane thickening [106,107]. Alterations have also been identified in the balance of matrix metalloproteinases and their specific inhibitors (tissue inhibitor of metalloproteinase-TIMP) [108,109].

Paraviota Koupepidou

1.7.3 Abnormal ciliary function

As mentioned in section 1.3, the primary cilium has received much attention in the cystic diseases of the kidney world as it was shown that most of the cystogenic proteins reside to the primary cilium, basal bodies or centrosome [5]. PC-1 and PC-2 have been found to localise to primary cilia in renal epithelial cells where they might function in sensory transduction, such as shear fluid stress [7,55,72]. In the mammalian kidney, cilia were proposed to act as mechanosensors sensing the flow in the tubular lumen by bending and eliciting a Ca^{2+} influx, which resulted in an increase in intracellular Ca^{2+} [110,111]. This flow-mediated increase in $[Ca^{2+}]_i$ occurred via the polycystin1/2 complex localized on the primary cilium, as a mutation in the *PKD1* gene resulted in defective ciliary polycystin localization and loss of flow-induced Ca^{2+} signaling in human ADPKD primary cyst epithelial cells [112]. The role of the primary cilium on kidney epithelia still remains vague. However, studies have shown that loss of ciliary function and/or formation resulted in cystic diseases of the kidney, which meant that it probably plays a role in PKD pathophysiology [96]. The first evidence for cilia involvement in cystogenesis came from the *orpk* mouse model of ARPKD, that arose from a mutation in the Tg737 gene (encodes a cilial protein – Polaris), and characterized by dilation of the proximal tubules and cystic lesions in the collecting ducts [113]. Additional evidence was provided by a mouse model with kidney specific inactivation of KIF3A (a subunit of kinesin-II), where cyst formation followed the loss of cilia in the kidneys [6]. The localisation of cystin (protein disrupted in the *cpk* mouse model of PKD) and inversin (disrupted in NPHP2) to the cilium further supported the role of the cilium in the pathogenesis of cystic diseases of the kidney [114,115].

Although evidence suggested that the primary cilium plays an important role in the pathogenesis of PKD, the molecular function of renal epithelial cilia is unknown. It has been suggested that they may play a role in the establishment of tubule lumen diameters, in cell cycle regulation, the Wnt signaling pathway, and the establishment of planar cell polarity [8].

1.7.4 Disturbance in the balance between proliferation and apoptosis

Apoptosis was found to be a pathologic feature of PKD, destroying much of the renal parenchyma. However, apoptosis would unlikely be the sole cellular pathophysiologic

Panayiota Koupepidou

mechanism for ADPKD as the kidneys would rather become hypoplastic instead of enlarged. Increased apoptosis levels have been observed in human ADPKD [92,116-118], but they were also found to be a feature of animal models of PKD. These included the cpk mouse model of ARPKD [117], transgenic mice overexpressing the proto-oncogene c-myc (SBM mice) [119], mice lacking the transcription activating protein AP-2β (AP-2β) [120], Bcl-2 deficient mice [121], and the Han:SPRD rat [122]. Apoptosis was detected in kidneys of humans with ADPKD regardless of renal function, but not in normal kidneys [117].

Abnormal epithelial cell proliferation is thought to be a key feature of cyst formation and renal enlargement in ADPKD. This increase in cell proliferation appeared to be a consistent feature in human PKD and in many experimental models of PKD [91,92]. Many researchers have reasoned that increased cell proliferation is a primary event in the pathogenesis of ADPKD [11,91,92,94,123,124]. Grantham et al., in 1987 provided calculations showing that epithelial cell hyperplasia was a key element in the progressive increased surface area of the tubule [11]. He has shown that the cell size does not change appreciably in ADPKD, as assessed in 387 cysts obtained from 10 adult patients, but cell proliferation must be a requirement for progressive cyst growth [11]. Using human tissues from ADPKD patients, Lanoix et al., provided evidence that both epithelial cell proliferation and apoptosis were deregulated in ADPKD, and accompanied by abnormal expression of proto-oncogenes, which are regulators of these processes [92]. In addition to this study, Nadasdy et al., have revealed using three forms of cystic kidney diseases, that the non-cystic segments of the nephron from which the cysts were thought to originate had a high proliferative index, which was comparable to that of the cystic epithelium [91].

Cultured epithelial cells from ADPKD cysts displayed abnormally high levels of cell proliferation and genes associated with increased proliferation, such as c-myc, have been found to be overexpressed in cystic epithelium [92,99]. C-myc is a transcription factor with a role as a regulator of cell growth, proliferation, differentiation and apoptosis [125]. C-myc mRNA was also shown to be overexpressed in an autosomal recessive mouse model of PKD, namely the C57BL/6J (cpk/cpk) mouse model [126]. To determine whether c-myc mRNA expression contributed to PKD development, C57BL/6J-*cpk/cpk* mice were treated with a c-myc antisense oligomer (ASO) (AVI-4126, AVI Biopharma) [127]. The ASO treatment reduced the cystic renal enlargement and delayed the development of renal failure as assessed by kidney weight as a proportion to body weight and blood urea

Panayiota Koupepidou

nitrogen (BUN) concentrations [127]. Effects of the ASO treatment on cell proliferation were ambiguous, however, since Western blot data showed reduced levels of the PCNA marker, but Northern blot data for renal histone H4 mRNA were not altered [127]. This c-myc antisense oligomer (AVI-4126), was being tested in Phase II clinical trials for different types of cancer, cardiovascular disease and polycystic kidney disease [128].

Other proto-oncogenes, such as *c-fos* and *c-Ki-ras* have also been found to be elevated in the C57BL/6J-*cpk/cpk* mouse model of ARPKD [129]. Studies by Harding et al., have shown that the *c-fos* and *c-myc* proto-oncogenes were transcribed at higher rates in cystic kidneys and thus increased transcription partly accounted for the increased mRNA levels [130]. This group has also shown that *c-myc* mRNA was overexpressed in epithelia from both cystic and normal tubules [130].

The creation of a transgenic mouse model of polycystic kidney disease, that resulted from the overexpression of c-myc in the tubular epithelium was an indicator that c-myc is a sufficient event to directly or indirectly trigger the development of renal cysts [131]. Overexpression of c-myc resulted in a phenotype that closely resembled ADPKD, with increased rates of cell proliferation and apoptosis, renal enlargement, and cysts affecting all segments of the nephron [119]. The SBM transgene was completely penetrant and all transgenic mice died of renal failure. This demonstrated that overexpression of c-myc is sufficient for cyst formation. The epithelial cells of SBM kidney tissues displayed an increased rate of proliferation as measured by antibody staining to Ki67 of formalin fixed paraffin embedded tissues [132]. The proliferation index was increased not only in cystic tubular epithelium, but also in the noncystic tubules, as compared with age-matched controls [119].

The development of renal cystic disease in transgenic mice expressing proliferation-related genes, including the human H-ras [133], c-myc [131], SV40 T antigen [134], Erb-B2 [135], TGFα [136], and HGF [137] confirms the important role that enhanced proliferation plays in the development of renal cysts.

Polycystic kidneys are characterized by increased levels of cAMP [138,139]. The cAMP pathway is responsible for both augmented proliferation and fluid secretion in cystic epithelia [140]. In normal renal epithelial cells, cAMP mediated proliferation is blocked

Panayota Koupepidou

through Akt-mediated inhibition of the Ras/Raf/MEK/ERK pathway [138]. In contrast, in ADPKD-derived cystic cells, inhibition of Akt by a reduction in $[Ca^{2+}]_I$ allows cAMP-induced proliferation through activation of the B-Raf/MEK/ERK pathway [141].

Both PC-1 and PC-2 have been directly implicated in cell cycle regulation. PC-1 has been associated with a variety of pathways tied to proliferation including the G protein signaling, Wnt, AP-1 and JAK/STAT [142-145]. Bhunia et al. showed that overexpression of wild type PC-1 in MDCK cells induces cell cycle arrest in G0/G1 through the activation of the JAK/STAT pathway. It was shown that PC-1 associates with JAK2, in a process that requires PC-2, and induces activation (phosphorylation) of STAT-1, which in turn induces transcription of $p21^{waf1}$. Subsequently, p21 inhibits cdk2 activity, which arrests cells in G0/G1 [143]. An independent study showed that depletion of PKD1 by antisense oligonucleotides resulted in an increase in cell proliferation, and supported the idea that PC-1 participates in regulating the progression of the cell cycle [146].

Studies have recently shown that PC-2 directly regulates the cell cycle by physically interacting with Id2 – an inhibitor of Helix-Loop-Helix (HLH) transcription factors – and sequesters Id2 to the cytoplasm. Li et al. showed that PC-2 overexpression in HEK293T cells inhibits the transition of the cell cycle from G0/G1 to S phase through the Id2-p21-Cdk2 pathway [147]. These data predict that loss-of-function mutation in either PKD1 or PKD2, or disruption of their functional interaction, will cause Id2 to enter the nucleus and turn-off growth-suppressive genes. Such a mechanism might be involved in the pathogenesis of ADPKD. Grimm et al. also provided direct evidence that PC-2 expression acts as a negative regulator of cell growth and suggested that the regulation might be partially dependent on the calcium channel activity of the protein [148].

Additionally, an independent study demonstrated a reduction in the levels of p21 in tissues from ADPKD patients as well as tissues from the Han:SPRD/(cy/+) rat model. Park et al., have also demonstrated that an attenuation of the levels of p21 in the MDCK cell line resulted in increased cell proliferation [149].

Very recently, a gene expression profile study of early and progression phases of ADPKD, from the first to the third postnatal week in a mouse model, identified a possible gene network involved in the pathogenesis of ADPKD. The differentially expressed genes were

Panayota Koupepidou

involved in several pathways, including cell proliferation, suggesting that it has a potential role in cystogenesis [150]. Collectively, these results supported the hypothesis that deregulation of cellular proliferation plays an important role in cystogenesis.

However, recent reports have supported the idea that proliferation might not be connected to cystogenesis. Piontek et al. used an inducible *Pkd1* mouse model and identified an important developmental switch that defines the kinetics of cyst formation after loss of *Pkd1*. They reported a dramatically different response to *Pkd1* inactivation, whereby inactivation before postnatal day 13 resulted in severely cystic kidneys within 3 weeks, whereas inactivation at day 14 and later resulted in cysts after 5 months. They suggested that different pathways may be altered in the two groups, which would have important implications for clinical understanding of the disease and of potential therapies. Piontek et al. showed that inactivation of *Pkd1* did not result in higher proliferation in cystic specimens compared to age-matched controls. Based on their results, they suggest that abnormal growth is probably not a primary defect resulting from loss of Pkd1 and that the relationship between cellular proliferation and cyst formation may be indirect [151].

1.8 Animal models of PKD

The availability of numerous animal models has aided the clarification of the mechanism of pathogenesis of PKD. These include both mouse and rat models that arose by spontaneous mutation, random mutagenesis, transgenic technologies and gene-specific targeting (a selected list of available animal models are shown in **Table 1**) [reviewed in [152]]. Homozygous knockout of *Pkd1* or *Pkd2* in mice resulted in embryonic lethality and therefore efforts to generate animal models have been concentrated on other strategies [153].

Panayiota Kouppoudou

Model	Type	Gene	Protein	Ref
Mouse				
cpk	Spontaneous	Cys1	Cystin	[154]
bpk	Spontaneous	Bicc1	Bicaudal C	[155]
jcpk	Chemically induced	Bicc1	Bicaudal C	[156]
orpk	Transgenic	TgN737	Polaris	[157]
inv	Spontaneous	Invs	Inversin	[158,159]
pcy	Spontaneous	Nphp3	Nephrocystin-3	[160]
jck	Spontaneous	Nek8	Nek8	[161]
kat, kat ^{2J}	Spontaneous	Nek1	Nek1	[162]
SBM	Transgenic	c-myc	C-myc	[131]
kif3a	Ksp knockout	Kif3a	Kinesin-II 3a subunit	[6]
Pkd1	transgenic	Pkd1	Polycystin-1	[43]
Rat				
cy	Spontaneous	Pkdr1	SamCystin	[163]
wpk	Spontaneous	Mks3	Meckelin	[164]
pck	Spontaneous	Pkhd1	Fibrocystin	[118]
*TGR(CMV-hPKD2/1-703**	Transgenic	PKD2	Polycystin-2	[45]

Table 1: List of selected rodent models of polycystic kidney disease.
Ksp: kidney specific. *: the PKD2 transgenic rat model to be used in this study

The PKD2 transgenic rat model to be used in this study was generated by introducing a plasmid encoding a hemaglutinin (HA)-epitope tagged truncated human polycystin-2 protein extending from amino acids 1-703, to Sprague-Dawley (SD) rats [abbreviated in this text as *PKD2* (1-703)] [45]. The plasmid used contains a CMV promoter upstream of the cloning site and the intron and polyadenylation signal of SV40 downstream of the cloning site. The transgenic line used carried approximately 5 copies of the transgene according to Southern blot analysis. The PKD2 (1-703) rats present with proteinuria and renal cysts that predominantly originate from the proximal tubule. No other pathologic alterations were recognised in organs tested, apart from retinal degeneration, which supports the involvement of cilia in disease pathogenesis. Experimental data have shown no obvious difference in the proliferation rate between proximal tubular cells of transgenic rats and

Panayiota Kouneli

those of control rats, with the exception of cysts in fibrotic areas. Also, there was no evidence of a reversed epithelial polarity that contributed to cyst formation in the transgenic rats [45].

1.9 Treatment strategies for polycystic kidney disease

An effective therapy for the treatment of polycystic kidney disease does not yet exist. To date, treatment has been limited to transplantation in combination with the management of hypertension. Heamodialysis can also be used as a replacement method of therapy in chronic renal failure patients. Therefore, understanding the molecular cues that contribute to the pathogenesis of the disease would help develop effective treatments that slow down the progression of the disease and prevent end stage renal failure.

Therapeutic interventions have been developed through findings on the pathways deregulated in PKD; some have already been tested on animal models, others have advanced to clinical trials. Much attention has been given to the role of epithelial cell proliferation in cyst formation, and many of the therapeutic strategies include antiproliferative substances. Other approaches include targeting fluid secretion by exploiting ion transport inhibitors, targeting apoptosis, or targeting increased cAMP as it is believed to contribute to cell proliferation and fluid secretion. Therapeutic interventions include: epidermal growth factor receptor (EGFR) specific tyrosine kinase inhibitors [165,166], and the vasopressin V2 receptor antagonists Tolvaptan and OPC-31260, which decrease cAMP production, were effective in reducing cyst and kidney volume [167,168], small molecule inhibitors of the basolateral KCa3.1 K^+ channel [169], antagonists of the Cl^- channel cystic fibrosis transmembrane conductance regulator [170,171], angiotensin converting enzyme inhibitors [172], the somatostatin analogue octreotide [173], c-myc antisense oligonucleotide [127], the caspase inhibitor IDN-8050, which reduced the number of apoptotic tubular cells, renal enlargement, and cyst volume density [174], and inhibitors of the inflammatory mediator TNF-α [175]. Also, the cyclin dependent kinase inhibitor, roscovitine effectively arrested cystic disease in the *jck* and *cpk* mouse models of PKD [123], and the mTOR inhibitor and antiproliferative substance Rapamycin was found to reduce kidney volume and cyst volume density, decreased proliferation in cystic and non-cystic tubules and prevented the loss of renal function in the Han:SPRD rat [176]. Most of these therapeutic interventions were efficient in reducing cystic and kidney volume, thereby delaying disease progression, but

Paraskeva Koupepidou

development of cysts still occurred. Importantly, the observed effects on PKD depend on the model investigated, with some substances having a beneficial outcome in one animal model but a deteriorating effect in another.

Panayiota Koupepidou

2 SCIENTIFIC HYPOTHESIS AND SPECIFIC AIMS

ADPKD is characterised by formation of bilateral fluid-filled cysts that expand and eventually destroy the renal parenchyma. Although the genes causing the disease are known, the mechanism of cyst formation still remains incompletely understood. Consequently, an effective therapy for ADPKD has not yet been established. The process of cyst formation can be divided in different stages. These include (a) the out-pocketing of the tubule wall, (b) cyst separation from the nephron (cyst initiation), and (c) continued cell growth, fluid secretion and progressive expansion of cysts (cyst expansion). One of the pathogenic features of ADPKD has been proposed to be abnormal tubular epithelial cell proliferation and research has focused on identifying the pathways involved in this process. Previous studies have identified factors that regulate proliferation at stages where cysts are already visible in the kidneys of humans and animal models of PKD and therefore at later stages of disease development. Therefore, many therapeutic interventions have focused on cysts that are in the continued growth and expansion phase.

The aim of this study was to investigate the role of polycystin-2 in Polycystic Kidney Disease in cellular and animal models. It was hypothesized that mutant polycystin-2 induces cyst formation by promoting epithelial cell proliferation.

The specific aims of the study were:

1. Generation of a 'PKD microenvironment' in cell culture and examination of the proliferation profile.
2. Isolation and culture of primary tubular epithelial cells from transgenic rat overexpressing mutated polycystin-2 and assessment of proliferation.
3. Phenotype analysis of differently aged transgenic rats overexpressing mutant polycystin-2 and evaluation of proliferation-related genes in the early stages of disease pathogenesis.

Panayiota Koupepidou

3 MATERIALS AND METHODS

3.1 Cell culture

The following cell lines were used: HEK (Human embryonic kidney) 293 (ATCC, U.S.A.) cell line, NRK52E (ATCC, U.S.A.) cell line from normal rat kidney epithelial cells, and rat primary Tubular kidney Epithelial Cells (TECs) (see below for method of isolation). All cell cultures were maintained in a 37^{o}C, 5% CO_2 incubator. The HEK293 cell line was maintained in Dulbecco's Modified Eagle Medium (D-MEM) with GlutaMAX^{TM} I, 4500mg/L D-Glucose (GIBCO, Scotland, U.K.) and addition of 10% Fetal Bovine Serum (FBS) (GIBCO, Scotland, U.K.) plus 100units/ml Penicillin and 100μg/ml Streptomycin. The NRK52E cell line was maintained in D-MEM with addition of 5% FBS and 100units/ml Penicillin and 100μg/ml Streptomycin. The primary TECs were maintained in the Endothelial Cell Growth Medium MV (PROMOCELL, Heidelberg, Germany) supplemented with 5% Fetal Calf Serum (FCS), 0.4% Endothelial Cell Growth Supplement/ Heparin (ECGS), 10ng/ml Epidermal Growth Factor (EGF), 1μg/ml Hydrocortisone, 50μg/ml Gentamycin (PROMOCELL, Heidelberg, Germany) and 50ng/ml Amphotericin (PROMOCELL, Heidelberg, Germany).

3.2 Constructs- Expression plasmids

HEK293 and NRK52E cells were transfected with plasmids obtained from Dr Leonidas Tsiokas (The University of Oklahoma Health Sciences Centre, U.S.A.). The full length of PKD2 was cloned into the pcDNA3 vector (INVITROGEN, Scotland, U.K.) and a hemagglutinin (HA) tag was introduced at the N-terminus [described in [78]]. The HA-PKD2/ 1-702 mutant was constructed by addition of a stop linker in the PKD2 sequence. The HA-PKD2/ 1-742 mutant was created by site directed mutagenesis of the wild type PKD2 sequence.

3.3 Antibodies

Primary antibodies used include: mouse monoclonal antibody against c-myc (9E10) (sc-40), mouse monoclonal antibody against PCNA (sc-56), mouse monoclonal antibody against HA-probe (sc-7392), rabbit polyclonal antibody against p57 (sc-8298), goat

Panayiota Kouppidou

polyclonal antibody against p21 (sc-397-G), goat polyclonal antibody against cdk2 (sc-163-G), rabbit polyclonal antibody against megalin (sc-25470), goat polyclonal antibody against Vimentin (sc-7557) (all from SANTA CRUZ BIOTECHNOLOGY, INC., Heidelberg, Germany), mouse monoclonal anti-β- tubulin (T4026) (SIGMA, Taufkirchen, Germany), mouse monoclonal antibody against β-actin (A1978) (SIGMA, Taufkirchen, Germany), rabbit polyclonal antibody against Pan-cadherin (#4086) (CELL SIGNALING TECHNOLOGY®, Massachusetts, U.S.A.), rabbit polyclonal antibody against phosphor-Stat1 (Tyr701) (#9171) (CELL SIGNALING TECHNOLOGY®, Massachusetts, U.S.A.). A rabbit polyclonal antibody was also used that was raised against the amino acid sequence 679-745 of the carboxyl terminus of human PKD2 [kind gift from L. Tsiokas- previously described [177]].

Secondary antibodies used include: goat anti-mouse IgG-HRP (sc-2005), goat anti-rabbit IgG-HRP (sc-2004) and donkey anti-goat IgG-HRP (sc-2020) (SANTA CRUZ BIOTECHNOLOGY, INC., Heidelberg, Germany).

3.4 Transient transfection/ Generation of stable clones

Plasmids were transfected into HEK293 or NRK52E cells using the Lipofectamine™ 2000 reagent (INVITROGEN, Scotland, U.K.). Cells were grown in 6-well plates to 90% confluency and 4μg of each DNA was transfected to each well, according to the manufacturer's instructions. For transient transfections, cells were harvested 48 hours (unless otherwise stated) after transfection.

For the stable clones, transfected cells were selected using 600μg/ml G418 (GIBCO, Scotland, UK). Cells were cultured to obtain single isolated colonies. Individual clones were picked using 3mm cloning discs (SIGMA, Taufkirchen, Germany) and transferred to 24-well plates. 10-12 colonies were picked, whole cell lysates isolated and screened for the expression of the transgene. Out of the positive ones, three stable clones from each condition with good expression of the transfectants were selected to be used for further experimentation.

Panayiota Koupepidou

3.5 Animals and isolation of primary tubular epithelial cells

PKD2 mutant transgenic Sprague Dawley (SD) rats (TGR (CMV-h*PKD2*/1-703)) were used in this study [abbreviated in this text as *PKD2* (1-703)] [45]. Wild type (WT) SD rats were used as controls. The animals used in these experiments were kept under standard laboratory conditions (12h light cycles, 55% humidity, 20±2^{o}C) in an animal care facility in Mannheim, Germany. The animals had free access to tab water and received standard rat pellet feed (containing 19% protein).

3.5.1 Isolation of primary kidney tubular epithelial cells

PKD2 (1-703) and WT rats were sacrificed using standard procedures and their kidneys excised. For the isolation of primary Tubular kidney Epithelial Cells (TEC's), the kidneys were placed in sterile Phosphate Buffered Saline (PBS) (GIBCO, Scotland, UK) and the procedure was carried out in a sterile environment to avoid contamination. The kidneys were minced in a cell culture dish, transferred onto a metal 180μm sieve (RETSCH, Haan, Germany) and passed through the sieve by applying pressure with the back of a sterile syringe. The filtrate was collected in a clean tissue culture plate, and slowly transferred with a syringe on a disposable 40μm cell strainer (BD FALCON^{TM}, Massachusetts, U.S.A.). The cells that passed through were collected in a 50ml Falcon tube and discarded. The 40μm cell strainer was inverted and retained cells were transferred on a disposable 100μm cell strainer (BD FALCON^{TM}, Massachusetts, U.S.A.) placed in a 50ml Falcon tube. The cells that pass through this cell strainer are the tubular epithelial cells. The cells were then spun down for 10 minutes at 1000rpm at room temperature. The supernatant was discarded and the cells were resuspended in the Endothelial Cell Growth Medium MV (PROMOCELL, Heidelberg, Germany), transferred on laminin-coated tissue culture plates (BECTON DICKINSON, New Jersey, U.S.A.) and incubated at 37^{o}C, 5% CO_2 (**Figure 3**).

Panayiota Koupepidou

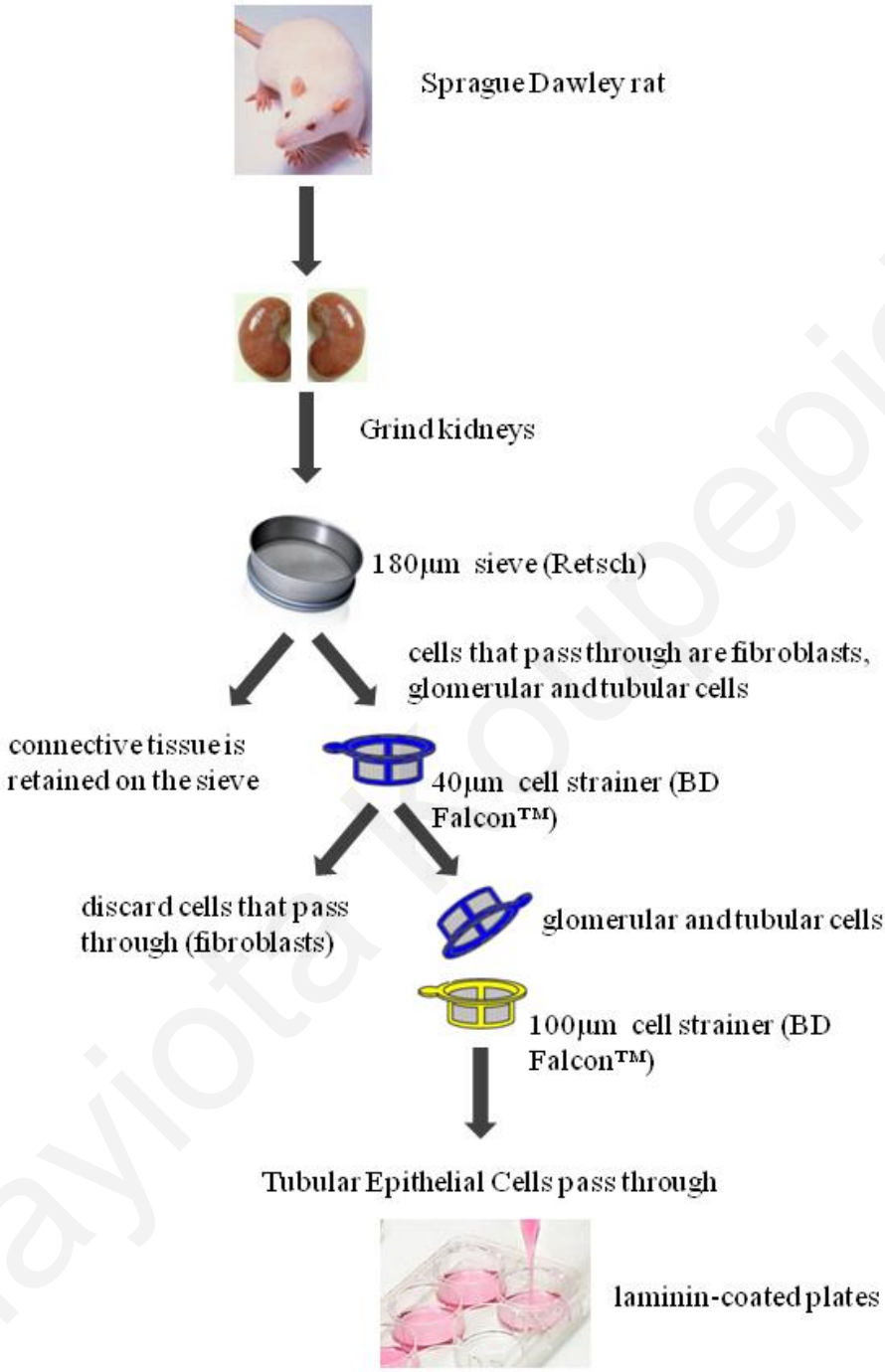

Figure 3: Schematic representation of the isolation of primary tubular epithelial cells from rat kidneys.

Panayiota Loupepidou

3.5.2 Kidney tissues obtained from rats

Three WT and three *PKD2* (1-703) rats from each age of 0, 6, 12, 24, 36, 48 and 60 days (**Table 2**) (will be referred to as the rat time course) were weighed and sacrificed following standard procedures and their kidneys excised (the whole procedure was performed in Mannheim, Germany, where the animal facility is). Both kidneys were weighed and divided in three parts. The middle part of the right kidney was fixed in 2% paraformaldehyde (PFA) for 24h, 1% PFA for 24h followed by 4% formalin. These parts were then embedded in paraffin to be used for cyst grading (see below). The middle part of the left kidney was submerged in 2% PFA for 24 hours, then submerged in 18% sucrose for 6 hours, frozen in liquid nitrogen and stored at -80^{o}C. All other parts were frozen immediately in liquid nitrogen and then stored at -80^{o}C. Blood from all the animals (apart from the animals of 0 days) was obtained by retro-orbital bleeding and used to measure several biochemical parameters.

	Group	**0 days**	**6 days**	**12 days**	**24 days**	**36 days**	**48 days**	**60 days**
1	PKD-2 mut rats, male	3	3	3	3	3	3	3
2	SD rats, male	3	3	3	3	3	3	3
		42						

Table 2: Experimental protocol for rat time course analysis.

3.5.3 Cyst grading

Cyst grading was performed at the animal facility in Mannheim, Germany. The extent of cyst formation was assessed using a previously described scoring system [178,179]. Cyst grading was performed on hematoxylin-eosin (HE)-stained sections.

Panayiota Kouppepou

For the area of the cortex:

Grade 1 **Occasionally small, medium- sized and large cysts** and sometimes small accumulations of predominantly small cysts in up to 4 localisations per slide

Grade 2 Few regularly distributed small, medium-sized and large cysts (**up to 5 medium-sized cysts per visual field**)

Grade 3 Several small, medium-sized and large cysts (**up to 10 medium-sized cysts per visual field**)

Grade 4 A great number of small, medium-sized and large cysts **with two or more large cysts in nearly any visual field; occurrence at least of 3 "network like structures"** consisting of many cysts of different size linked together

Grade 5 **Practically no normal kidney tissue is visible and histology exhibits only large cysts and "network like structures"** similar to that seen in homozygous Han: SPRD (cy/cy) rats. Cysts occurring even in the outer cortex area

Small-sized cysts are cysts of the size of 1 glomerulus.
Medium-sized cysts are cysts of the size of 2 glomeruli.
Large-sized cysts are cysts of the size of more than 2 glomeruli.

3.5.4 Assessment of fibrosis

The analysis of fibrosis on sections of the kidneys was also performed at Mannheim, Germany. Sections for the analysis of fibrosis were Azan-stained. Fibrosis score was assigned according to the following:

For the area of the cortex:

Grade 1 only a few fibroblasts and fibrocytes, diffuse, **occasionally small scars**

Grade 2 several fibroblasts and fibrocytes, diffuse, **a few small fibrotic foci**

Grade 3 a great number of fibroblasts and fibrocytes, diffuse, **a few small fibrotic foci and up to 3 large fibrotic foci**

Grade 4 many fibroblasts and fibrocytes, diffuse, **and more than 3 large fibrotic foci getting into contact with each other**

Panayiota Koupepidou

3.6 Biochemical analysis of blood

Blood was collected on ice in Li-heparin containing microfuge tubes and was centrifuged at 3000g for 15min at 4^{o}C. The plasma fraction was collected in a 1.5ml microfuge tube and frozen at -20^{o}C until further processing. Biochemical parameters were determined by standard laboratory methods at Mannheim, Germany using a Hitachi 911 Autoanalyzer (ROCHE, Mannheim, Germany). Biochemical parameters including urea, creatinine, cholesterol, triglycerides, glucose, PO_4^{3-}, K^+, Na^+, Ca^{2+} and total protein were determined.

3.7 RNA isolation

Total RNA from cultured cells was extracted using the QIAGEN RNeasy® Mini Kit according to the manufacturer's instructions. 15-50mg from kidney tissues were used to extract total RNA from the WT and PKD2(1-703) rats using the RNeasy® Mini or Midi (QIAGEN, West Sussex, U.K.) kit depending on the weight of the tissue obtained. Tissues were grinded in 1.5ml eppendorf tubes using a pestle. Total RNA was extracted according to the manufacturer's instructions. The quality of the RNA was assessed by agarose gel electrophoresis and the sample concentration was determined spectrophotometrically.

3.8 Quantitative real-time polymerase chain reaction (PCR)

Reverse transcription was performed in a total volume of 20μl using the ProtoScript™ First Strand cDNA Synthesis Kit (NEW ENGLAND BIOLABS) as recommended by the manufacturer. In brief, 1μg of total RNA was reverse transcribed, with 5μM oligo-dT (dT23VN) primer, 10 units of RNase Inhibitor, 25 units of M-MuLV Reverse Transcriptase, dNTPs, and RT buffer. For the standard curve of the RNA samples obtained from cell lines, 1μg of RNA of all the test samples were pooled together and reverse transcribed as described above ("Standard"). For the standard curve of the rat time course, 1μg of RNA from 4 different samples, selected randomly, were pooled and reverse transcribed as mentioned above ("Standard"). Reverse transcription was performed for 1h at 42^{o}C and the enzyme was heat inactivated for 5min at 95^{o}C. cDNA was stored at -20^{o}C until further processing.

Panayiota Koupepidou

The relative quantitative real-time PCR (qRT-PCR) amplifications were performed on the LightCycler® system (ROCHE, Mannheim, Germany) using the LightCycler® FastStart DNA Master SYBR Green I kit (ROCHE, Mannheim, Germany) in a reaction volume of 20μl. The primers are obtained from MWG (Ebersberg, Germany) used are shown in **Table 3**. The SYBR Green fluorescent dye binds to double stranded DNA and therefore fluorescent data were acquired at the end of each extension step of the PCR cycle. To generate the standard curve the "Standard" sample was used in serial dilutions and the logarithms of the initial concentrations of the dilution samples were plotted against the crossing points of the samples (the cycle at which the fluorescence of a sample rises above the background fluorescence- Cp). From the standard curve, the efficiency of the PCR reaction is calculated by the software. The same amount of a "Calibrator" sample was run in each amplification, to which each unknown sample was normalized against. The relative amount of target was calculated by the software after normalization to the reference gene (GAPDH and HPRT) and to the "Calibrator" (equation shown below). Relative quantification analysis was carried out on the LightCycler® Software 4.1.

Gene	**Species**	**Primers**	**Amplicon size**
HPRT	rat	5'-CTCATGGACTGATTATGGACAGGAC-3' 5'-GCAGGTCAGCAAAGAACTTATAGCC-3'	123bp
GAPDH	rat	5'-GTATTGGGCGCCTGGTCACC-3' 5'-CGCTCCTGGAAGATGGTGATGG-3'	202bp
p57	rat	5'-TGATGAGCTGGGAGCTGAG-3' 5'-TGGCGAAGAAGTCAGAGATG-3'	299bp
Cdk2	rat	5'-TGTGGCGCTTAAGAAAATCC-3' 5'-CCAGCAGCTTGACGATGTTA-3'	194bp
c-myc	rat	5'-AGCGACTCTGAAGAAGAACA-3' 5'-ACATGGCACCTCTTGAGGAC-3'	158bp
PCNA	rat	5'-TGAAGCACCAAATCAAGAGAAA-3' 5'-TTTGCACAGGAGATCACCAC-3'	183bp

Table 3: List of all the oligonucleotides used for quantitative real-time PCR analysis of the genes listed.

Panayiota Koupepidou

3.8.1 Quantification using the efficiency correction method

The expression of all genes tested in the rat time course was normalized against two reference genes. The relative expression ratio of a gene of interest (GOI) relative to a reference gene (RG) was calculated by the method of efficiency correction using the equation shown. The efficiency of the reaction was deduced from the slope of the standard curve, which was created by plotting the concentrations of the samples against the crossing points of the samples.

$$\text{Ratio} = \frac{(E_{RG})^{\text{Cp sample}}}{(E_{GOI})^{\text{Cp sample}}} \div \frac{(E_{RG})^{\text{Cp calibrator}}}{(E_{GOI})^{\text{Cp sample}}}$$

3.9 Protein preparation and Western blot analysis

Cells were lysed in a lysis buffer containing 1% Nonidet® P40 (NP-40), 15% glycerol, 50mM TrisCl (pH 7.4), 200mM NaCl, 5mM $MgCl_2$ and a cocktail of protease inhibitors (ROCHE, Mannheim, Germany) and centrifuged at 12,000 rpm for 5min at 4ºC to obtain whole cell lysates.

With reference to the frozen kidneys obtained from the rats, 10-50mg from each of the left kidneys were cut with a scalpel, and homogenized in NP40 buffer [1% NP40, 15% glycerol, 50mM TrisCl (pH 7.4), 200mM NaCl, 5mM $MgCl_2$ and a cocktail of protease inhibitors (ROCHE, Mannheim, Germany)]. The homogenates were centrifuged 3 times at 12,000rpm for 10min at 4ºC and the supernatants collected.

Protein concentrations were determined by the Bicinchoninic acid (BCA) assay (PIERCE) using Bovine Serum Albumin (BSA) as a standard. Protein lysates were diluted in equal volume of 2x Sodium Dodecyl Sulphate (SDS) loading buffer (125mM 4xTris-Cl pH6.8, 20% Glycerol, 2% SDS, 2% β-mercaptoethanol and bromophenol blue) and denatured at 50ºC for 15 min (Polycystin-2 tends to form aggregates when heated at 95ºC).

Equal amounts of protein were separated by SDS-Polyacrylamide Gel Electrophoresis (SDS-PAGE) and transferred onto a Hybond Polyvinylidene fluoride (PVDF) membrane

Panayota Koupepidou

(AMERSHAM BIOSCIENCES, Buckinghampshire, U.K.). Membranes were blocked after the transfer with 5% nonfat dry milk in PBS/0.1%Tween20 overnight at 4^{o}C. The next day the primary antibody dissolved in the milk was added to the membrane for an hour, the membrane was washed 3 times with PBS/0.01% Tween20 and the secondary antibody conjugated with Horseradish Peroxidase (HRP) was added to the membrane. The membrane was washed again 3 times with PBS/ 0.01% Tween20 and detection of the proteins was carried out by the Enhanced ChemiLuminescence (ECL) Plus Blotting Detection (AMERSHAM BIOSCIENCES, Buckinghamshire, U.K.) system and visualized by autoradiography (KODAK- X-OMAT, New York, USA). Autoradiographs were scanned and the relative amounts of the proteins were derived using the Scion Image Software (SCION) and normalized against the autoradiographs of β-actin or β-tubulin (where applicable).

3.10 CDK2 kinase assay

Cdk2 kinase assay was conducted as previously described [180]. Total cellular protein (250-500μg) was immunoprecipitated with 1μg of Cdk2 antibody for 2 hours at 4^{o}C. After extensive washes, the precipitate was subjected to the kinase assay in the presence of 50mM HEPES, 7.5mM $MgCl_2$, 0.5mM EDTA, 20mM β-glycerophosphate, 1mM NaF, 5mM dithiothreitol, 100μM ATP and 10μCi of [γ-^{32}P]ATP in a total volume of 30μl. As a substrate, 2μg of histone H1 (CALBIOCHEM, San Diego, U.S.A.) were added to the reaction. The reaction was carried pit at 30^{o}C for 30min. After elution, the supernatant was fractionated by SDS-PAGE, transferred onto a PVDF membrane and autoradiographed.

3.11 Electrophysiology

All electrophysiology experiments were performed at Dr L. Tsiokas laboratory. A conventional whole-cell voltage-clamp configuration was performed to measure transmembrane currents in single cells, as previously described [177]. Patch clamp recordings were obtained from single cells at room temperature using a Warner PC-505B amplifier (WARNER INSTRUMENT CORP., Hamden, U.S.A.) and pClamp8 software (AXON INSTRUMENT). Glass pipettes (plain, FISCHER SCIENTIFIC) with resistances of 5-8MΩ were prepared with pipette puller and polisher (PP-830 and MF-830, respectively, NARISHIGE, Japan). After the whole cell configuration was achieved, cell capacitance

Panayiota Koupepidou

and series resistance were compensated (~70%) before each recording period. From a holding potential of -60mV, voltage steps were applied from -100 to 100mV in 20mV increments with 200ms duration at 3s intervals. Current traces were filtered at 1 kHz and analyzed off-line with pClamp8. The pipette solution contained: 100mM K-aspartate, 30mM KCl, 0.3mM Mg-ATP, 10mM HEPES, 10mM EGTA, and 0.03mM GTP (pH 7.2). The extracellular solution contained: 135mM NaCl, 5.4mM KCl, 0.33mM NaH_2PO_4, 1mM $MgCl_2$, 1.8mM $CaCl_2$, 5 mM HEPES, 5.5mM glucose (pH 7.4) or 130mM KCl, 1mM $MgCl_2$, 10mM HEPES, 0.1mM $CaCl_2$ and 5mM glucose (pH 7.4).

3.12 Cell cycle analysis by flow cytometry

The same number of cells (250,000) was plated in each well of a 6-well plate. Each condition to be analysed was done in triplicate. After 24 hours cells were arrested in G0/G1, by addition of serum-free medium and 24h after that, medium with the appropriate amount of serum was added. The cells were trypsinised and washed once with PBS, 1ml of ice-cold 80% ethanol was added and samples were kept at 4ºC until they were going to be analysed on the FACSCAN flow cytometer (BECKTON DICKINSON, New Jersey, USA). Right before running the samples on the flow cytometer, cells were washed twice with PBS and resuspended in 1ml PBS containing 25μg RNAase A and 50μg Propidium Iodide (SIGMA, Taufkirchen, Germany). Samples were incubated for 30min at 37ºC and then run on the flow cytometer (BECKTON DICKINSON, New Jersey, USA).

3.13 Gene expression profiling by microarrays

The whole procedure of gene expression profiling using microarrays was performed at Prof. N. Gretz's laboratory. Gene expression profiling was performed using the primary tubular kidney epithelial cells (TECs) isolated from WT SD rats and compared to TECs isolated form PKD2 (1-703) rats. The RNA for this case was sent to Mannheim, Germany in dry ice. The whole procedure (including RNA extraction) for the gene expression profiling of transgenic rats sacrificed at three different ages (0, 6 and 24 days) was performed in Mannheim, Germany. Fresh kidney tissues were used and RNA was extracted using the Trizol® method, its concentration measured spectrophotometrically and its integrity checked with a RNA 6000 Nano LabChip® Kit on an Agilent Bioanalyzer (AGILENT TECHNOLOGIES, Boblingen, Germany). For both microarray analyses, RNA

Panayiota Koupepidou

was reverse transcribed, cRNA synthesized followed by labeling and hybridization performed according to the recommendations of Affymetrix (AFFYMETRIX, Santa Clara, U.S.A.). In the gene expression profiling of the isolated TECs, the Affymetrix GeneChip® Rat Expression Array Rae230A was used which displays 12,012 probe sets corresponding to approximately 6,328 known genes. In the experiments of 0, 6 and 24 day old rats, the Affymetrix GeneChip® Rat Expression Array Rae230_2 (AFFYMETRIX, Santa Clara, U.S.A.) was used, which displays 31,000 probe sets, corresponding to approximately 28,000 rat genes. All microarrays were scanned on the Affymetrix GeneArray Scanner3000. The data for the gene expression profiling in primary TECs were submitted to NCBI GEO (http://www.ncbi.nlm.nih.gov/geo/query), sample number [GSE11500].

3.14 Statistical analysis

Statistical analysis, where applicable, was performed using the statistical software SPSS (SPSS Inc., Chicago, U.S.A.). Comparisons between multiple groups were performed using single-factor ANOVA, and secondary comparisons were performed using the Tukey test. Data are reported as means ± SEM.

For the electrophysiology experiments statistical analysis was performed at Dr Tsiokas laboratory, using the SigmaStat software (SyStat software Inc, Chicago, U.S.A.). Data were reported as means ± SEM. Due to high variability in the cells transfected with wild type PKD2, statistical significance was determined with the Mann-Whitey Rank Sum test. Differences were considered significant at a p value < 0.05 if not stated otherwise.

Statistical analyses for the microarrays were performed at Prof. Gretz laborarory. A Custom CDF Version 11 with Entrez based gene definitions was used to annotate the microarrays. The raw fluorescence intensity values were normalized applying quantile normalization. Statistical analysis for the gene expression profiling was performed using a commercial software package SAS JMP7 Genomics, version 3.1, from SAS (SAS INSTITUTE, Cary, NC, USA) and was analysed based on loglinear mixed model ANOVA [181,182]. A false positive rate of a=0.05 with Holm correction was taken as the level of significance. The overrepresentation analysis (ORA) is a microarray data analysis that uses predefined gene sets to identify a significant overrepresentation of genes in data sets [183,184]. Pathways belonging to various cell functions such as cell cycle were obtained from public external databases (KEGG, http://www.genome.jp/kegg/). A Fisher's exact test was performed to detect the significantly regulated pathways.

4 RESULTS

4.1 Generation of stably or transiently transfected cell lines overexpressing wild type or mutant PC-2 to create a cellular model of PKD

4.1.1 Stable overexpression of wild-type or mutant PC-2 does not alter levels of proliferation-related genes in HEK293 cells

It has been proposed that PC-1 and PC-2 control cellular programs directing differentiation, cell cycle progression and apoptosis in the tubular epithelial cells from which cysts originate. Consistent with this, several proto-oncogenes, have been found to be abnormally regulated in cyst cells derived from ADPKD patients and animal models of cystic kidney disease [92,129]. The c-myc proto-oncogene, in particular, has received much attention concerning its role in the pathogenesis of PKD. Its overexpression in transgenic mice generates a PKD phenotype resembling ADPKD [131]. The role of c-myc in cyst formation, however, still remains elusive. Other proliferation-related genes, such as PCNA, Ki-67 and EGFR have been found to be upregulated as assessed by *in situ* hybridisation on kidney tissues or primary cultured epithelial cells from ADPKD patients or animal models of PKD [91,123,124,185].

In cell culture systems, overexpression of wild type PC-1 in Madin Darby Canine Kidney (MDCK) and HEK293 cells induced growth arrest by activating JAK2, which in turn phosphorylates STAT1. This resulted in the upregulation of $p21^{waf1}$ which inhibited the activity of Cdk2 [143]. This process requires PC-2 as an essential cofactor. Similarly, inducible overexpression of wild type PC-2 in HEK293T cells was shown to induce growth arrest in G0/G1 by directly interacting with Id2. This, in turn, regulates the cell cycle by induction of p21 and a subsequent reduction in Cdk2 activity [147]. These results lead to the hypothesis that PC-1 and PC-2 probably regulate the cell cycle together in a common signaling pathway.

The HEK293 cell line was used to examine the role of wild type and mutant PC-2 in cell proliferation by observing the expression of proliferation-related proteins. The HEK293 cell line has been extensively used as an expression tool for studying the function of the polycystins. To create a 'PKD microenvironment' and test the expression of the above

Panayota Koupepidou

mentioned proliferation-related genes, a series of stable clones were generated in HEK293 cells with stable expression of a haemagglutinin (HA)-tagged wild-type (WT) human PC-2 or an HA-tagged mutant PC-2 (*PKD2* R742X). As controls, stable clones with the empty vector (pcDNA3) were created. The R742X *PKD2* mutant encodes for a truncated PC-2, which lacks a part of the carboxy terminus, and consequently lacks the EF-hand, the ER retention signal and the coiled-coil domain through which PC-2 is thought to interact with the carboxy terminus of PC-1. The *PKD2* R742X mutant was found to be forwarded to the plasma membrane and display channel activity in sympathetic cells and Xenopus leavis oocytes [87,186]. Three stable clones from each condition with good expression of the transfectants as assessed by Western blotting with anti-HA antibody were selected for further experiments (**Figure 4**).

Western blots using whole cell lysates from the HEK293 clones were performed, using antibodies against different cell cycle-related proteins that have been previously shown to be involved in the pathogenesis of PKD. Cells were serum-starved for 6 hours, 24 hours before harvesting. Membranes were blotted with antibodies against c-myc, p21, and proliferating cell nuclear antigen (PCNA) that detect the expression levels of each protein and anti-phospho-STAT-1 antibody, which detects the levels of phosphorylated STAT-1 at Tyr701. An antibody against HA was used to detect the transfected PC-2 and an antibody against PC-2 (epitope corresponds to amino acids 679-742) was used to detect both endogenous and exogenous expression of PC-2.

Western blots indicate that the endogenous levels of c-myc, p21 and pSTAT-1 remain unaffected by stable overexpression of wild-type or mutant PC-2 in HEK293 cells (**Figure 4**). Additionally, the levels of PCNA were equal among the different clones. Equal loading of proteins was assessed by immunoblotting with anti-β-tubulin. Overexpression of PC-2 in the stable clones was confirmed by immunoblotting with PC-2 antibody.

Panayiota Koupepidou

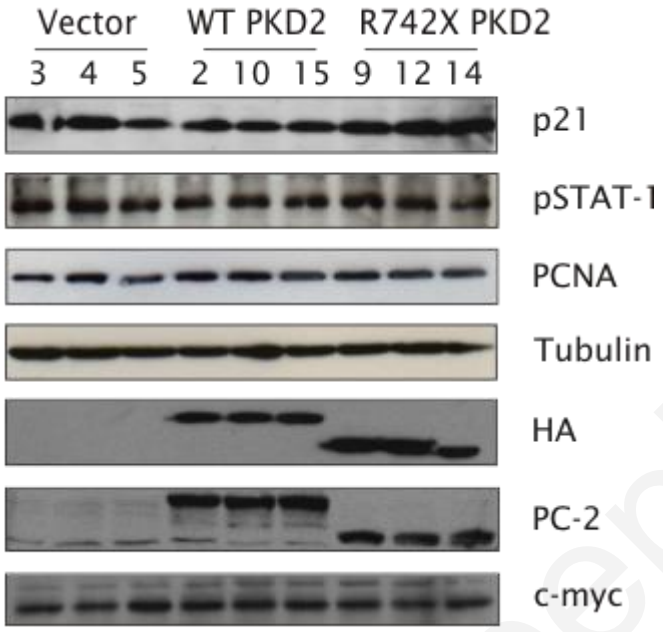

Figure 4: Immunoblot analyses of different cell cycle related proteins in whole cell lysates of stable clones of HEK293 cells overexpressing wild type (WT PKD2) or mutant (R742X) PKD2.
Empty vector stable clones (Vector) were used as controls. The result of a single experiment performed in triplicate is presented. Equal amount of protein was loaded as assessed by blotting with β-tubulin antibody. Stable HEK293 clones were analysed by Western blotting for expression of p21, phosphorylated STAT-1, PCNA, HA, PC-2 and c-myc.

Additionally, the Cdk2 activity was equal in selected clones from each condition, as assessed by the kinase assay performed on Cdk2 immunoprecipitates. Western blot analysis demonstrated that similar amount of cdk2 was precipitated from each clone (**Figure 5**).

Panayiota Koupepidou

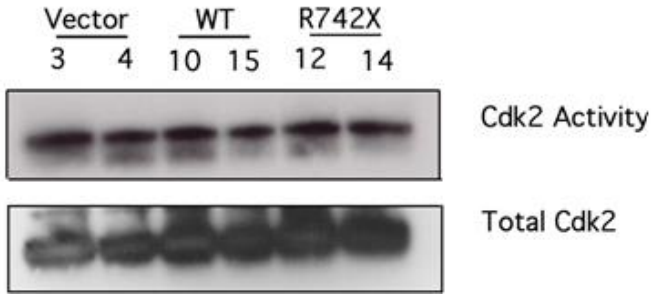

Figure 5: Cdk2 immunoprecipitates from two clones of each transfectant (Vector, Wild type PKD2 and mutant R742X PKD2) of an *in vitro* Cdk2 kinase assay using Histone 1A as substrate.
Equal amounts of Cdk2 were confirmed by immunoblotting the precipitates with anti-Cdk2 antibody. Data are representative of three independent experiments.

4.1.2 Overexpression of WT or mutant PC-2 in HEK293 cells does not alter the cell-cycle profile

The cell cycle profile of the stable clones of HEK293 cells was assessed by flow cytometry to identify whether overexpression of wild type or truncated PKD2 alters proliferation in these cells. Consistent with the Western blot data on the cell-cycle related proteins, cell cycle analysis with propidium iodide (PI) staining did not show any statistically significant alteration in the cell cycle profile of the HEK293 stable clones overexpressing wild type or mutant PC-2 (R742X) (**Figure 6**).

Panayiota Koupepidou

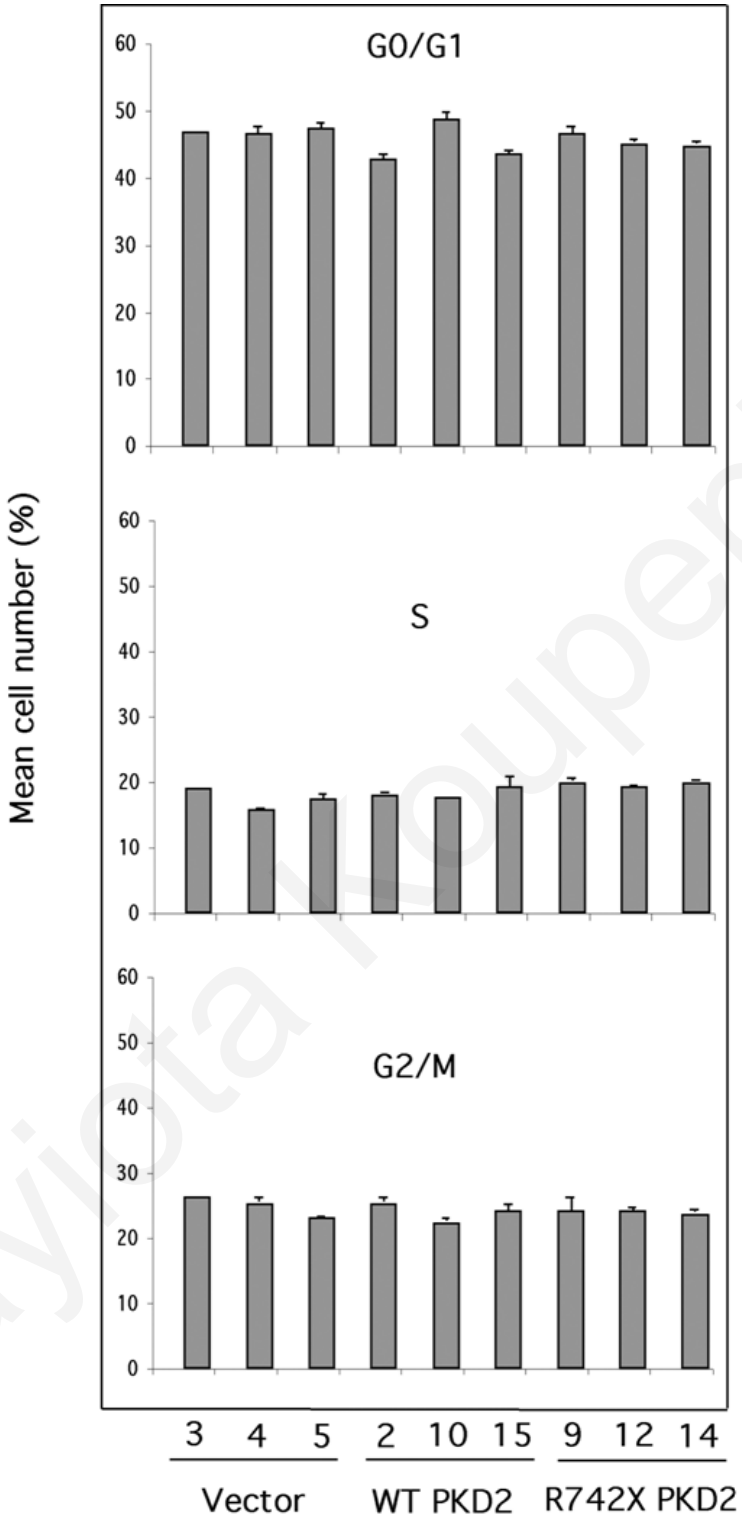

Figure 6: Cell cycle profile of the stable clones of HEK293 cells.

Each bar represents a mean value of triplicates for each clone. The percentage of cells in each phase of the cell cycle was determined. Three different clones from each condition of vector only (vector), wild type *PKD2* (WT PKD2) and mutant R742X *PKD2* were used.

Panayiota Koupepidou

Collectively, the results of the Western blot and the cell cycle profile of the clones suggest that stable overexpression of wild type or mutant PC-2 does not affect the proliferation of HEK293 cells.

4.1.3 Overexpression of WT PC-2 in HEK293 results in a functional plasma membrane channel

ER-localised PC-2 is known to function as a Ca^{2+}-activated intracellular Ca^{2+} release channel while plasma membrane-associated PC-2 is believed to function as a nonselective cation channel [56,71,75]. Ma et al., have demonstrated that *PKD2* overexpression augmented the amplitude of whole cell currents in renal epithelial cells [177]. To test the effectiveness of the expressed *PKD2* in HEK293 cells, whole cell current measurements in vector only, WT *PKD2* and R742X *PKD2* were performed (all electrophysiology experiments were performed at Dr Tsiokas laboratory in the USA).

The results shown in **Figure 7** depict that stable expression of WT *PKD2* in HEK293 cells results in a significant increase in the current amplitude of whole cell inward currents recorded either in normal extracellular tyrode solution (B) or symmetrical K^+ (G). Outward currents were larger in the WT PKD2 stable clones compared to mock-transfected or mutant *PKD2* (R742X) transfected cells in symmetrical K^+. Overexpression of mutant R742X *PKD2* did not have a significant effect on whole cell inward or outward currents in HEK293 cells. These data demonstrate that the transfected WT *PKD2* is functional in HEK293 cells. The lack of inward or outward currents in the *PKD2* (R742X) mutant is not surprising as previous reports on the channel activity of this mutant are controversial, and depend on the system being utilised. This means that R742X *PKD2* is either not transported to the plasma membrane or is unable to form a channel in the plasma membrane.

Panayiota Koupepidou

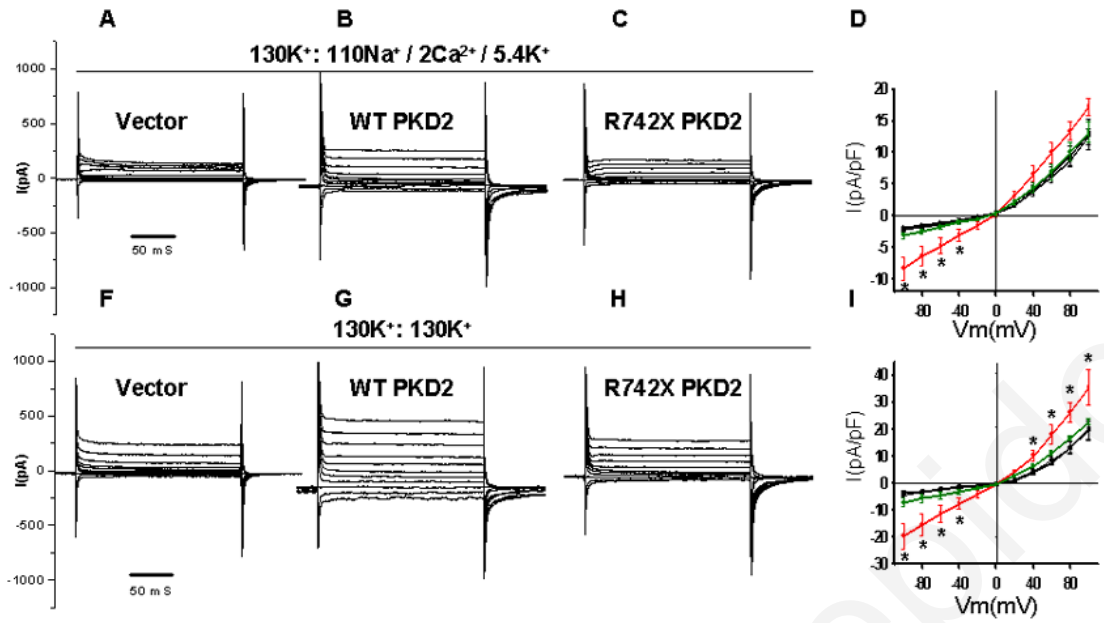

Figure 7: Electrophysiology experiments for functional expression of PC-2 in HEK293 cells.
Whole cell step currents in vector-only (A and F), wild-type PKD2 (B and G) and the mutant R742X –PKD2 (C and H) stable transfectants of the HEK293 cells in normal extracellular tyrode solution ($130K^+$:$135Na^+$/$2Ca^{2+}$/$5.4K^+$) (A-C) or symmetrical K^+ ($130K^+$:$130K^+$) (F-H). Current voltage (I-V) curves derived from step protocol in untransfected (black squares), vector-only (black circles), WT PKD2 (red circles), or mutant PKD2 (R742X) (green circles) stable transfected HEK293 cells in normal extracellular tyrode solution (D) or symmetrical K^+ (I). '*': $p< 0.05$.

The electrophysiology analysis demonstrated that although transfected wild type PC-2 appeared to be functional in the HEK293 stable clones, it did not affect cellular proliferation.

4.1.4 Transient overexpression of WT or mutant PC-2 does not affect the levels of proliferation-related genes in NRK52E cells

The HEK293 cell line is a widely used expression tool. The results from the HEK293 stable clones indicated that a reconsideration of the choice of cell line should be made. It was recently demonstrated that HEK293 cells are not typical kidney cells and display some properties associated to neuronal cells and therefore may not be the optimal cell line to use as kidney controls or to study any normal kidney-related function [187]. As a result, the NRK52E cell line, which is a cell line derived from normal rat kidney epithelial cells, that more closely resembles mature kidney epithelial cells was chosen to perform the same line of experiments.

Panayiota Kouneli

The NRK52E cell line was transiently transfected with the WT *PKD2* and two different *PKD2* mutants (R742X *PKD2* and 1-702 *PKD2*) to test the effect of PC-2 on proliferation-related proteins in this system. The PKD2 (1-702) mutant lacks almost the entire region of the C-terminus of PC-2 (including the EF hand, the ER retention motif and the coiled-coil domain). Transient transfection of an empty vector served as control. To test the efficiency of transfection, a pcDNA3 vector with the EGFP coding sequence was transfected. Twenty-four hours before cells were harvested, they were synchronised for 6 hours by serum starvation. Whole cell lysates were immunoblotted with p21, phosphorylated STAT-1, PCNA, β-tubulin, HA, PC-2 and c-myc.

The Western blots depicted that the levels of the proliferation-related proteins c-myc, p21 and pSTAT-1 remained unaffected in the different conditions of the transiently transfected NRK52E cells. Proliferation of the NRK52E cells appeared to remain unaffected as assessed by immunoblotting with PCNA antibody. Good expression of the transfectants was observed as judged by the immunoblots of HA and PC-2 antibodies (**Figure 8**). Equal loading of proteins was assessed by immunoblotting with anti-β-tubulin.

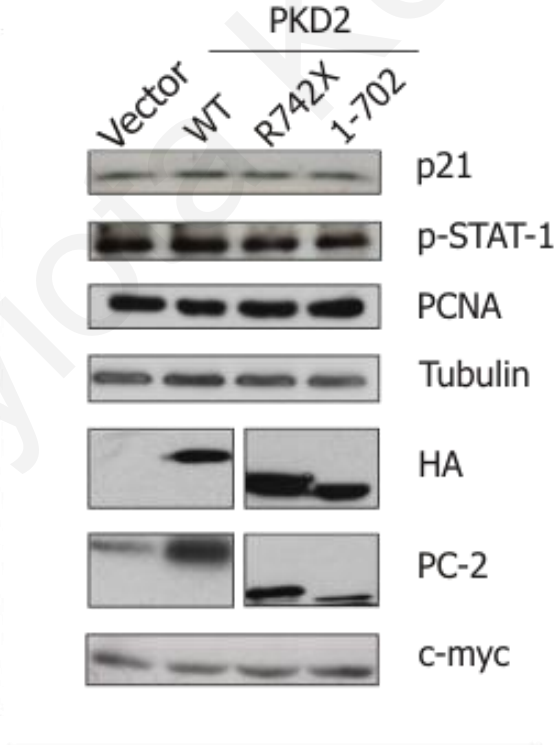

Figure 8: Western blot analyses of whole cell lysates from NRK52E cells transiently transfected with vector only, WT PKD2, and two mutants of *PKD2* (R742X and 1-702).
Samples were analysed for expression of p21, phosphorylated STAT-1, PCNA, HA, PC-2 and c-myc. Equal loading of proteins was assessed by immunoblotting with tubulin antibody.

Additionally, the levels of endogenous active Cdk2 were comparable among the four transfectants as judged by Cdk2 kinase assay (**Figure 9**).

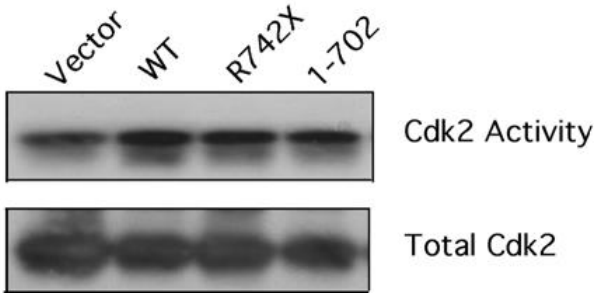

Figure 9: Cdk2 immunoprecipates from each transient transfectant of NRK52E cells for an *in vitro* Cdk2 kinase assay using Histone 1A as substrate.
Equal amount of Cdk2 loading was confirmed by immunoblotting the precipitates with anti-Cdk2 antibody. Data are representative of three independent experiments performed.

Viewed collectively, results using the HEK293 and NRK52E cells demonstrate that overexpression of wild type or mutant PKD2 in these cell lines did not result in c-myc overexpression, did not alter the cell cycle profile of these cells nor expression of proliferation-related genes and did not alter the expression or activity of any components of the JAK2/ STAT-1/ p21/ Cdk2 pathway.

Panayiota Koupepidou

4.2 Isolation of primary tubular kidney epithelial cells from WT SD and PKD2 (1-703) rats

Two transgenic rat lines (line 111 and 247), overexpressing an HA-tagged truncated (1-703) human PC-2 cDNA, were previously generated and described [45]. The truncated protein product lacks almost the entire C-terminal region of PC-2 (the 6th transmembrane domain ends at amino acid 679), therefore lacks the EF hand, the ER retention motif and the coiled coil domain. Both transgenic lines present with polycystic kidney disease with renal cysts predominantly arising at the proximal tubules (renal cortex). Similar to what is observed in ADPKD, the transgenic rats develop fibrosis and focal cyst formation [45].

4.2.1 Renal tubular epithelial cells from 7.5 week old PKD2 (1-703) rats display augmented proliferation independent of the JAK2/STAT-1 pathway

Due to the results obtained from the stable and transient transfections of established cell lines, the system being utilised was reconsidered. Animals from line 247 were sent to our laboratory in order to isolate primary tubular epithelial cells (TECs) from PKD2 (1-703) and wild type rats. TECs were isolated by a sequential filtration method described in the Materials and Methods section, and cultured for up to three passages without any detectable differentiation.

In contrast to the cell-line systems, an increase in cellular proliferation was demonstrated as assessed by Western blot analyses, which revealed augmented levels of PCNA in the primary tubular epithelial cells isolated from the PKD2 (1-703) transgenic rats as compared to their normal counterparts. This increase in the levels of PCNA was also accompanied by an increase in c-myc protein levels, as assessed by immunoblotting (**Figure 10**). However, the levels of p21 and phosphorylated STAT-1 remained unaffected. The epithelial phenotype of the primary cells was confirmed by immunoblotting with cadherin antibody, while a vimentin-specific antibody was also used to rule out the presence of any contaminating fibroblasts in the primary cultures (**Figure 10**). The truncated protein was tagged with an HA- epitope and therefore could easily be discriminated from the endogenous WT protein. As cysts in the PKD2 (1-703) transgenic rat originate predominantly from the proximal tubule segment of the nephron, the possibility that proximal tubules were overrepresented in the isolated cultures was

Panayota Koupepidou

excluded by immunoblotting with megalin antibody (proximal tubule marker). The western blot demonstrates that there is an equal percentage of proximal tubular epithelial cells in isolated cultures in both TECs isolated from WT and PKD2 (1-703) rats.

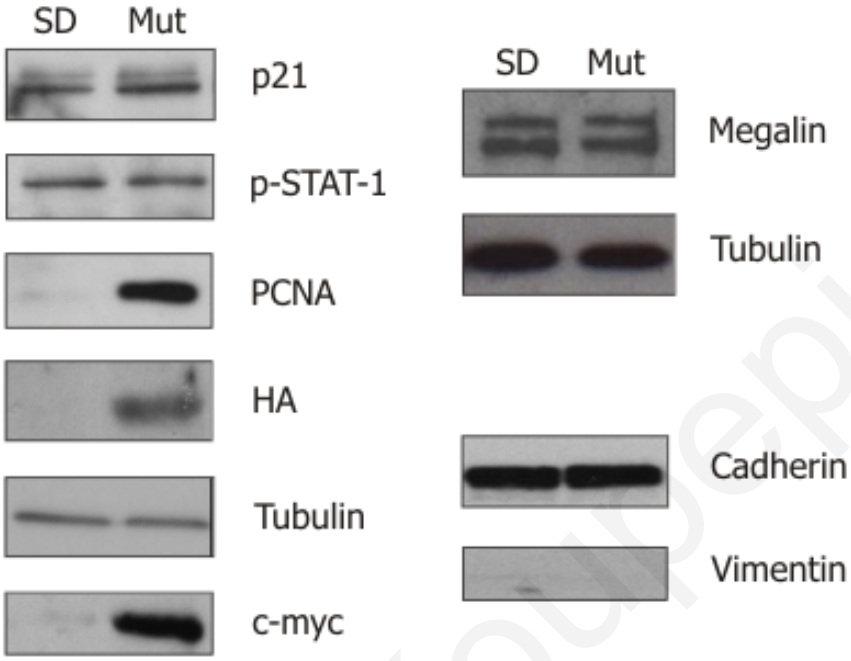

Figure 10: Western blot analysis of whole cell lysates from Tubular Epithelial Cells (TECs) isolated from Wild Type Sprague Dawley (SD) rats and PKD2 (1-703) transgenic rats (Mut).
Samples were analysed for expression of p21, phosphorylated STAT-1, PCNA, HA, PC-2 and c-myc. Equal loading of proteins was assessed by immunoblotting with tubulin antibody. Megalin is a proximal tubular epithelial cell marker, cadherin is an epithelial cell marker and vimentin a fibroblast marker.

Consistent with the increased levels in PCNA, primary tubular epithelial cells isolated from PKD2 (1-703) rats display higher proliferative activity compared to their normal counterparts as assessed by flow cytometry (**Figure 11**). Specifically, the fraction of cells in the G0/G1 phase of the cell cycle was lower in the cells isolated from PKD2 (1-703) rats than in their normal counterparts (84.1 ± 1.28 as opposed to 90.6 ± 0.93). Consequently, the percentage of cells in the G2/M phase of the cell cycle was higher in the cells isolated from the PKD2 (1-703) rats compared to cells isolated from normal Sprague Dawley rats (12.9 ± 1.37 as opposed to 5.06 ± 0.31).

Panayiota Koupepidou

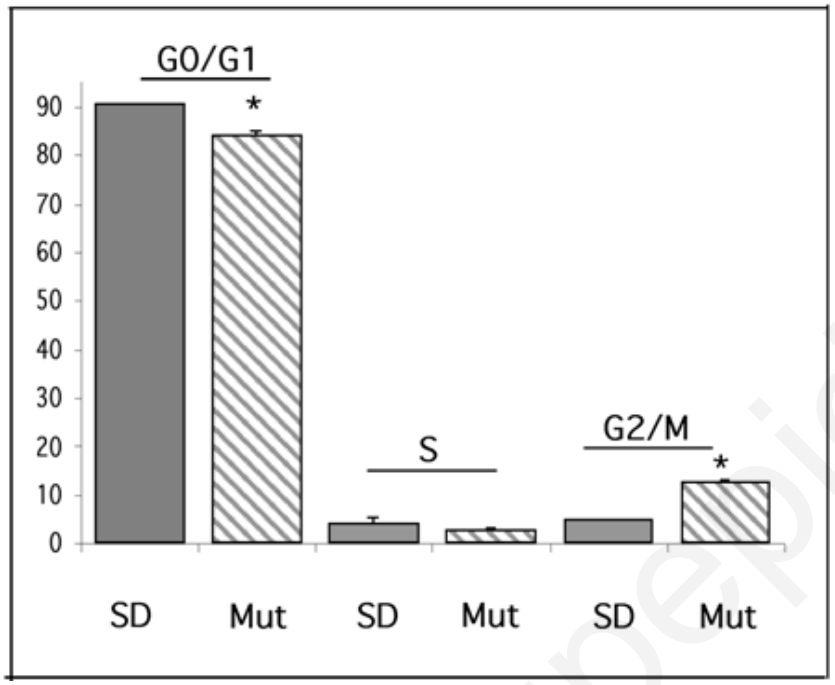

Figure 11: Graphical representation of the cell cycle profile of cells isolated from wild type Sprague Dawley (SD) rats or PKD2 (1-703) rats (Mut).

The results are represented in percentages, as a mean of triplicate counts using three independent cultures for each animal. '*': $p<0.05$ statistically significant. The results are representative of three different measurements and the mean value is represented.

4.2.2 Gene expression profiling of primary tubular kidney epithelial cells reveals that PC-2 induced proliferation is STAT1/p21-independent, and instead is accompanied by alterations in expression of p57 and Cdk2

Since augmented proliferation was independent of the JAK2/STAT1/p21 pathway, gene expression profiling to examine the cell cycle related genes of the primary TECs was performed using RNA isolated from TECs of two wild type (WT) SD and three PKD2 (1-703) rats. The microarray analysis revealed that there are about 700 significantly differentially expressed genes using a p-value of less than 10^{-3}. With a focus on the cell cycle genes, the analysis revealed p57 to be significantly down-regulated and Cdk2 significantly up-regulated in the TECs isolated from PKD2 (1-703) rats as compared to their normal counterparts. The list of the negative log of p-values and the fold change of cell cycle genes analysed on the chip are presented in **Table 4**. p21 (Cdkn1a), previously shown by other studies to be involved in the abnormal proliferation phenotype of PKD cell

Panayiota Koupepidou

lines, was not found to be among the differentially expressed genes in the mutant TECs compared to WT TECs.

Gene Symbol	Gene title	Neg log of p (Mut/SD)	Log2 fold change (Mut/SD)
APAF1	apoptotic peptidase activating factor 1	0.1043	0.06935
BRCA1	Breast cancer 1	0.0936	-0.02977
CCNA1	cyclin A1	0.1690	-0.05265
CCNB1	cyclin B1	0.0312	0.03944
CCND1	cyclin D1	0.3380	-0.34452
CCNH	cyclin H	2.1093	-0.38506
CDC16	CDC16 cell division cycle 16 homolog (S. cerevisiae)	0.1462	-0.06494
CDC20	cell division cycle 20 homolog (S. cerevisiae)	0.0282	-0.01929
CDC25A	Cell division cycle 25 homolog A (S. cerevisiae)	0.6886	0.20664
CDC37	cell division cycle 37 homolog (S. cerevisiae)-like 1	0.1065	0.23135
CDK2	cyclin dependent kinase 2	**5.4836**	0.23011 *****
CDKN1A	cyclin-dependent kinase inhibitor 1A(p21)	1.3781	0.40840
CDKN1B	cyclin-dependent kinase inhibitor 1B (p27)	0.4489	0.06993
CDKN1C	cyclin-dependent kinase inhibitor 1C (p57)	**9.5262**	-0.83724 *****
FOXM1	forkhead box M1	0.2379	-0.05692
MCM7	minichromosome maintenance deficient 7 (S. cerevisiae)	0.5931	-0.29236
MRE11A	meiotic recombination 11 homolog A (S. cerevisiae)	0.2538	-0.03134
NBN	nibrin	1.3961	-0.50471
NEDD8	neural precursor cell expressed, developmentally down-regulated gene 8	2.5638	-0.10046
RAD17	RAD17 homolog (S. pombe)	1.8372	-0.24432
RAD50	RAD50 homolog (S. cerevisiae)	0.1157	-0.01911
RB1	retinoblastoma 1	0.2440	-0.04238
RBL2	Retinoblastoma-like 2	1.0302	0.26708
RBX1	ring-box 1	1.7562	-0.35810
RIT2	Ras-like without CAAX 2	0.1803	-0.04616
SKP1A	S-phase kinase-associated protein 1A	0.1875	0.21280
TIMP3	tissue inhibitor of metalloproteinase 3 (Sorsby fundus dystrophy, pseudoinflammatory)	1.0674	-0.49676
TRP63	transformation related protein 63	2.1536	0.59233
YWHAE	Tyrosine 3-monooxygenase/tryptophan 5-monooxygenase activation protein, epsilon polypeptide	0.0255	-0.00476

Table 4: List of cell cycle genes and the results obtained after statistical evaluation of the genome-wide expression analysis in TECs isolated from transgenic rats PKD2 (1-703) (Mut) compared to TECs isolated from SD rats (SD).

Data were considered significant if the negative log of the p-value of Mut/SD was greater than 3. '*' denotes statistical significance after Bonferroni correction.

Panagiota Koupenioti

The volcano plot of the results of the cell cycle genes of the microarray experiment is presented in **Figure 12**, which is the plot of the values of the negative log of the p-value in relation to the log2 of the fold change in mutant versus WT TECs.

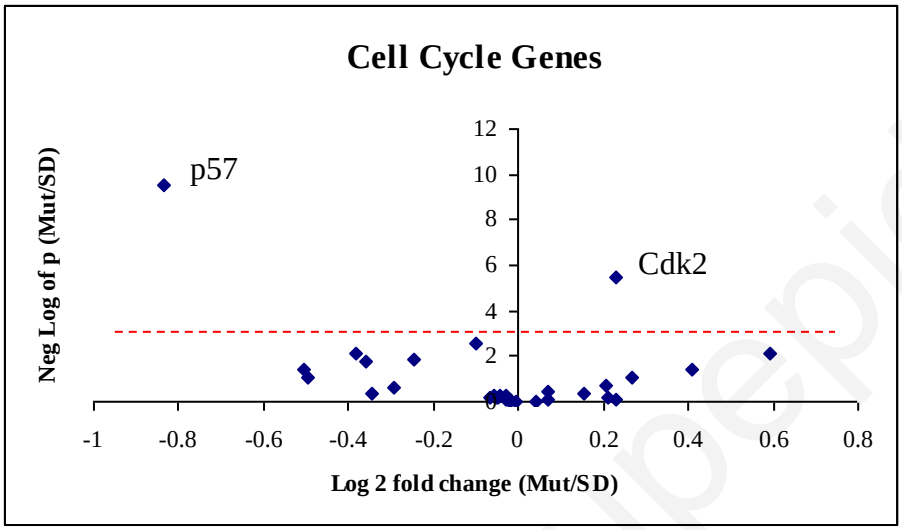

Figure 12: Volcano plot of all cell cycle genes analysed in the genome wide expression analysis.
Each data point represents a different gene. Data points to the right of the Y-axis denote up-regulation of the certain gene, whereas data points to the left of the Y-axis denote down-regulation of the gene in question. Only significantly deregulated genes' names are shown. The dotted red line represents the threshold of the p-value: 10^{-3} (Bonferroni correction). Mut: PKD2 (1-703) rats, SD: SD WT rats

To verify the microarray data, real-time quantitative PCR was performed for p57 and Cdk2. The data were normalised against two reference genes, namely HPRT and GAPDH. In accordance with the microarray data, p57 mRNA levels were lower (normalized fold change 4.7 ± 0.19) and Cdk2 levels were higher (normalized fold change 1.2 ± 0.015) in the TECs from the PKD2 (1-703) rats as compared to the TECs from wild type SD rats (**Figure 13A**). Immunoblots of whole cell lysates of TECs isolated from wild type and mutant rats were also performed using antibodies against p57 and Cdk2. Consistent with the microarray data, as well as the quantitative real-time PCR results, p57 protein levels were significantly downregulated (normalized fold change 1.9 ± 0.2) and Cdk2 protein levels were significantly elevated (normalized fold change 2.2 ± 0.06) in the TECs of the PKD2 (1-703) rats compared to TECs of WT rats (**Figure 13B**).

Panayota Koupepidou

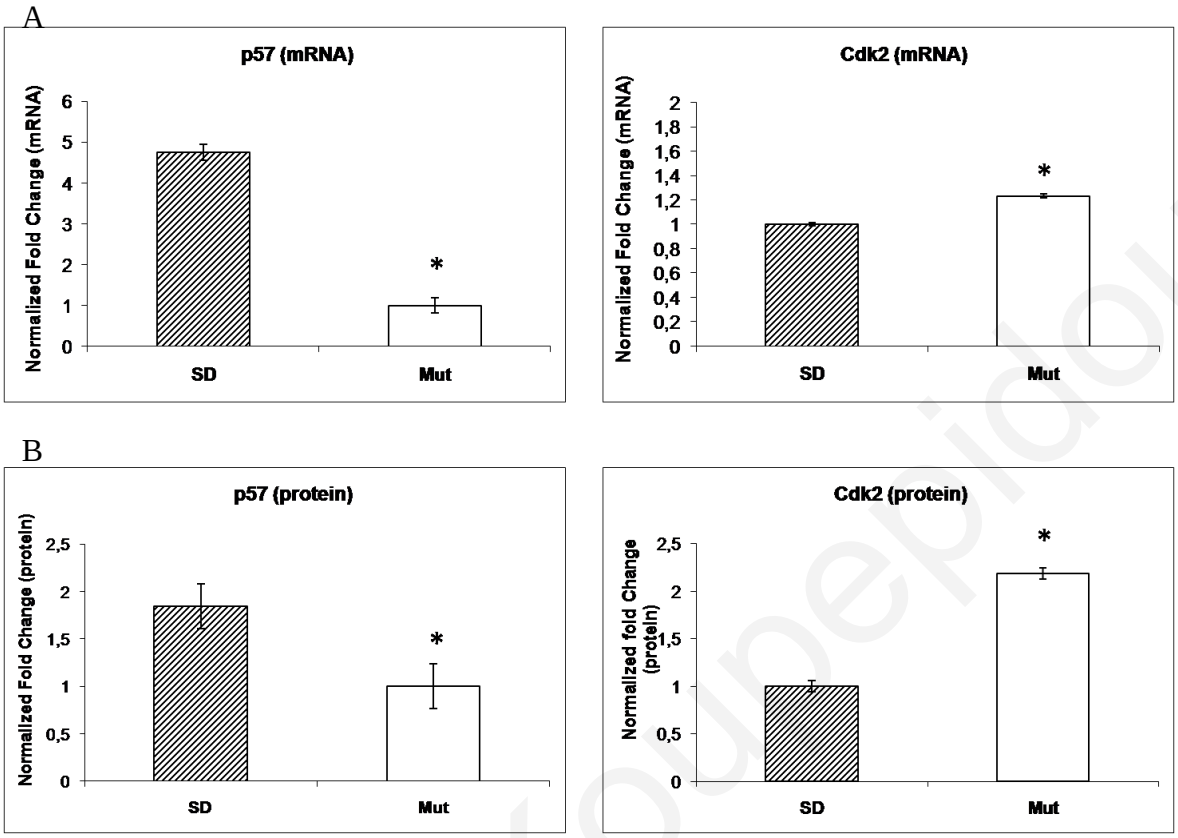

Figure 13: A: Quantitative PCR analysis of p57 and Cdk2 in isolated primary TECs. B: Western blotting analysis of p57 and Cdk2 in the isolated primary TECs.

A: Data represent the mean of normalised fold change from three independent samples ± SEM ($p < 0.01$, *: significant difference). Data were normalised against two different reference genes, namely HPRT and GAPDH.

B: Protein levels of p57 and Cdk2 are represented as the mean of normalised fold change of two independent Western blotting experiments ± SEM ($p < 0.05$, *: significant difference). Data were normalised against β-tubulin expression. SD: wild type Sprague Dawley rat, Mut: transgenic PKD2 (1-703) rat

Since p57 and Cdk2 were found to be involved in PC-2-induced augmentation of proliferation in the isolated TECs, the levels of these two proteins were not expected to be altered in the cell line systems of HEK293 and NRK52E. Western blotting analysis of p57 and Cdk2 was performed in the HEK293 stable clones and NRK52E transient transfectants and, as expected, the protein levels in these cell lines remained unaffected. It should be noted, however, that p57 in the cell lines examined is expressed at very low levels and was barely detectable by Western blotting (**Figure 14**).

Panayiota Koupepidou

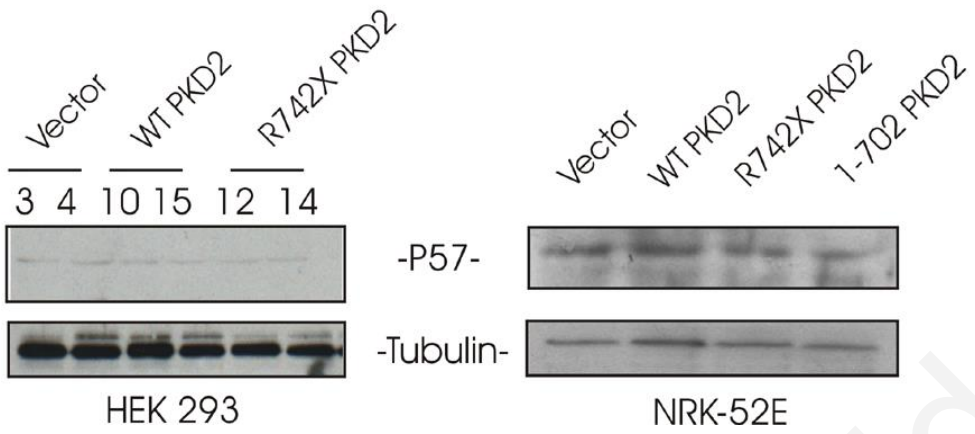

Figure 14: Western blot analyses of p57 of whole cell lysates of HEK293 stable clones and NRK52E transient transfectants.
Equal loading of proteins was assessed by immunoblotting with tubulin antibody.

Taken together, the results using the isolated primary TECs suggested a new mechanism for mutant PC-2 induced proliferation, which involves the downregulation of $p57^{kip2}$ and the upregulation of Cdk2.

Panayiota Koupepidou

4.3 Isolation of kidneys from WT and PKD2 (1-703) rats of different ages

Much of the research of PKD has focused on the reasoning that abnormal cell proliferation is a primary defect in the progression of PKD. Most studies of human and rodent PKD, however, have unavoidably utilised kidneys obtained at a later stage of the disease, at a stage where chronic or end-stage renal failure had already began. This may give rise to a false representation of the factors affecting the progression of the disease, since chronic secondary effects of renal failure may superimpose the primary defects in the initiation of PKD. Therefore, false results as regards to abnormal levels of proliferation in tissues could have been obtained. Also, consistent with the results obtained with the cellular models of this study, abnormal cell proliferation is probably not a primary defect in the pathogenesis of PKD, but is instead a secondary effect, produced by deregulation of other cellular processes.

To examine the regulation of the proliferation-related genes at the early stages of the disease, PKD2 (1-703) rats and WT rats at the ages of 0, 6, 12, 24, 36, 48 and 60 days were sacrificed and their kidneys excised. Blood from the animals was collected by retro-orbital bleeding before they were sacrifised to examine biochemical parameters (the procedure of sacrification, cyst and fibrosis grading, the measurement of biochemical parameters and the gene expression analysis by microarrays were performed at Prof. Gretz laboratory).

4.3.1 Body weight, kidney weight and kidney mass index

The body weight of all rats was measured at all time points and the graph of body weight measurements of mutant and WT rats is depicted in **Figure 15**. No apparent difference between the body weight of the WT and the PKD2 (1-703) rats was observed, although mutant rats tended to be slightly lighter. Kidney weight differences and kidney to body weight ratio (in percentage) between WT and PKD2 (1-703) rats are depicted in **Figure 16**. There was no statistically significant difference in kidney weight between WT and PKD2 (1-703) animals of the same age, whereas a marked difference in the kidney to body weight ratio was observed (**Figure 16**).

Panayiota Koupepidou

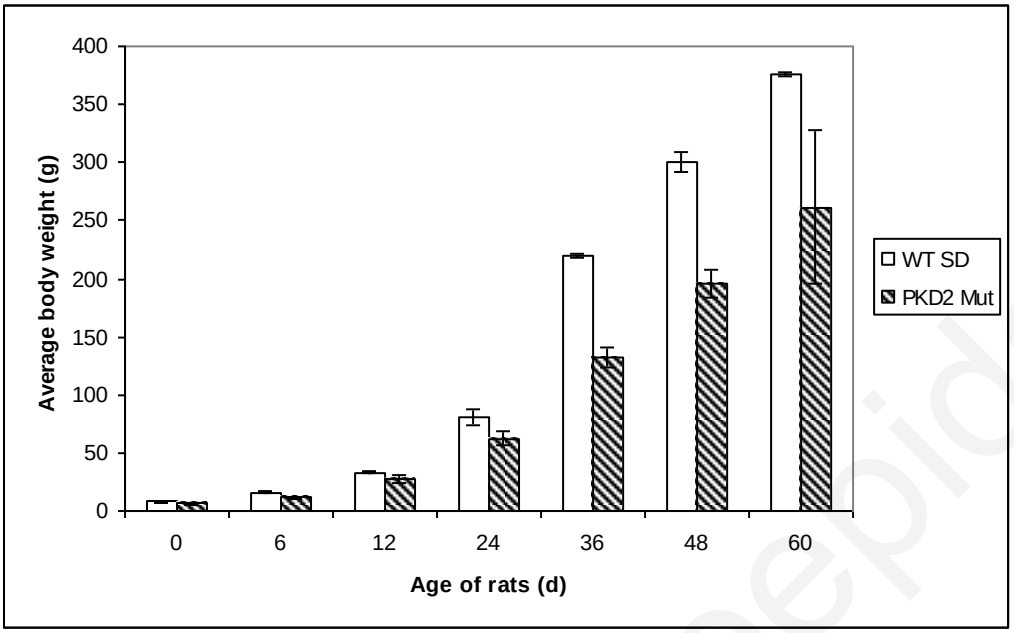

Figure 15: Graphical representation of the mean body weight (g) of WT SD and PKD2 mut : PKD2 (1-703) rats.

Error bars indicate standard deviation (s.d.). Each bar represents the mean body weight of three animals.

Panayiota Koupepidou

A

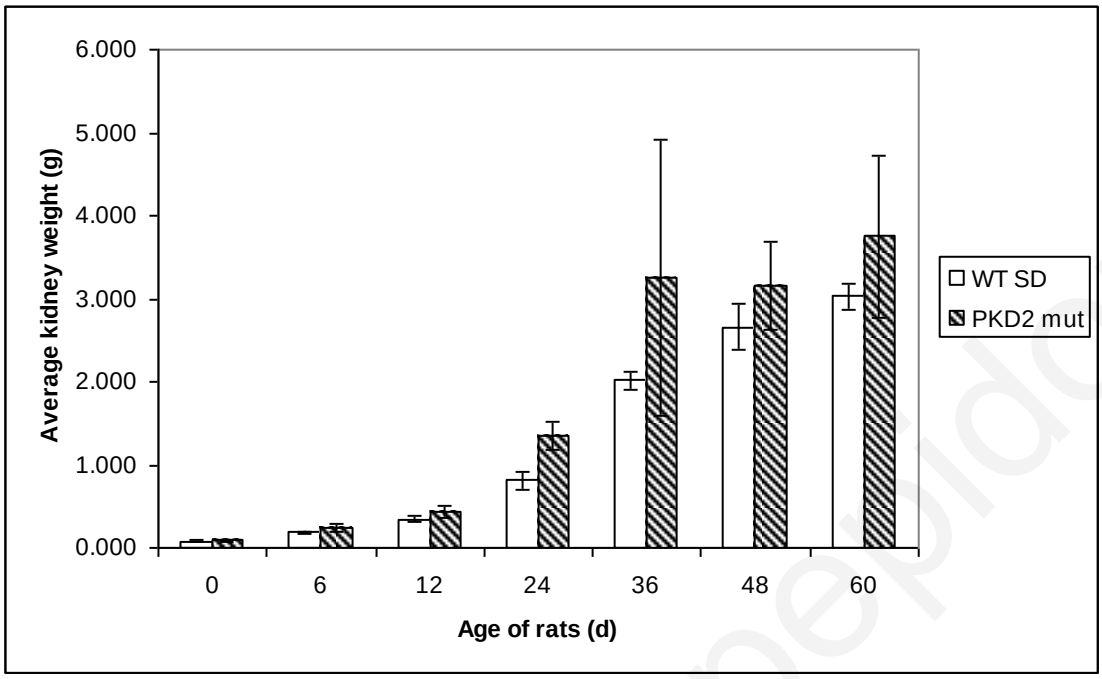

B

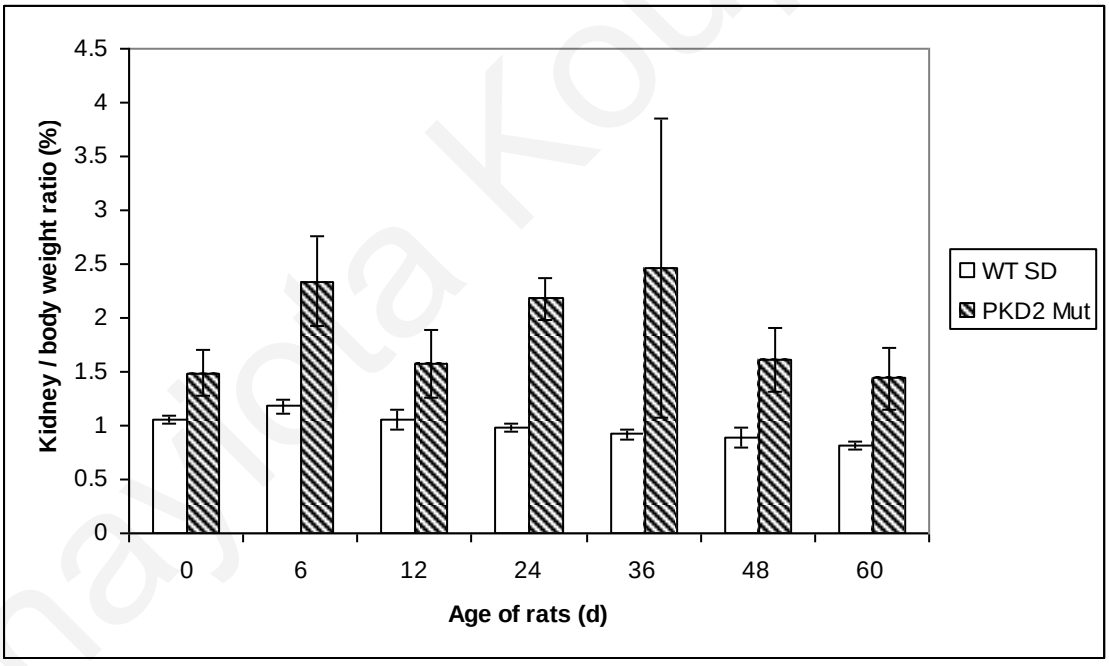

Figure 16: The graphical representation of (A) the mean kidney weight of WT SD and PKD2 (1-703) mutant rats and (B) the kidney to body weight ratio (as a percentage) of SD WT and PKD2 mut rats.
The error bars represent the s.d. Each bar represents the mean of the kidney weight or the kidney/ body weight ratio of three animals.

Panajna Koupepidou

4.3.2 Renal function

Blood from all the animals of the time course (apart from those of 0 days that was not possible) was obtained by retro-orbital bleeding, before the animal was sacrificed, to be used for analysis of several biochemical parameters. Parameters reflecting renal function are shown in **Figure 17**. A marked difference in plasma creatinine and urea levels was observed between PKD2 (1-703) and WT rats at the age of 60 days although the difference was not statistically significant. This was not surprising, however, as the PKD2 (1-703) rats display a marked difference in markers of renal function at much later stages of the disease. Renal insufficiency becomes apparent at 15 months of age [45].

Panayiota Koupepidou

A

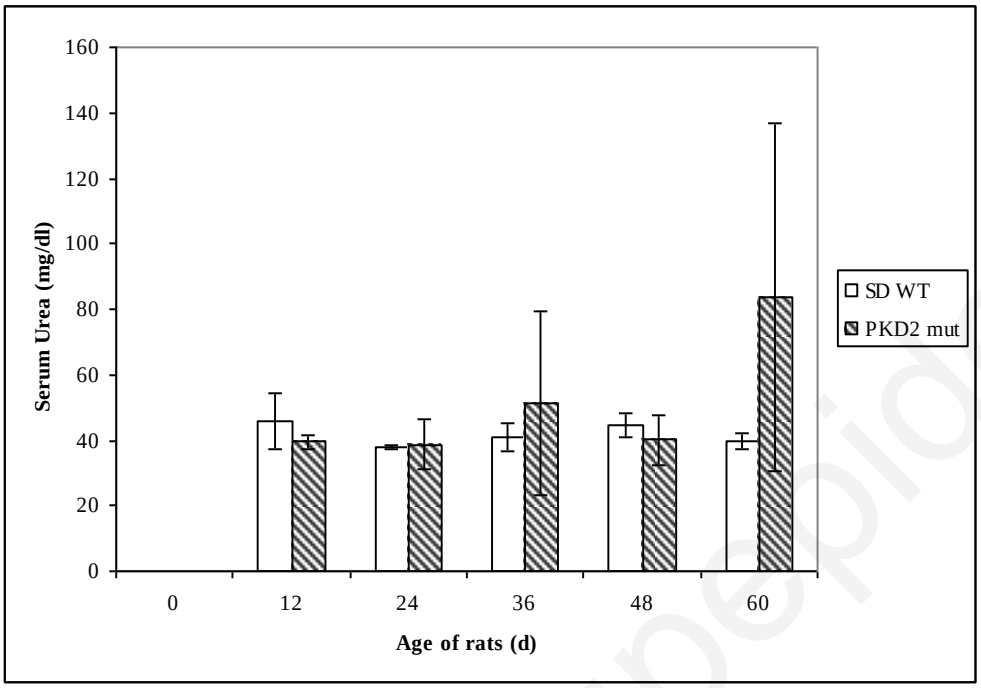

B

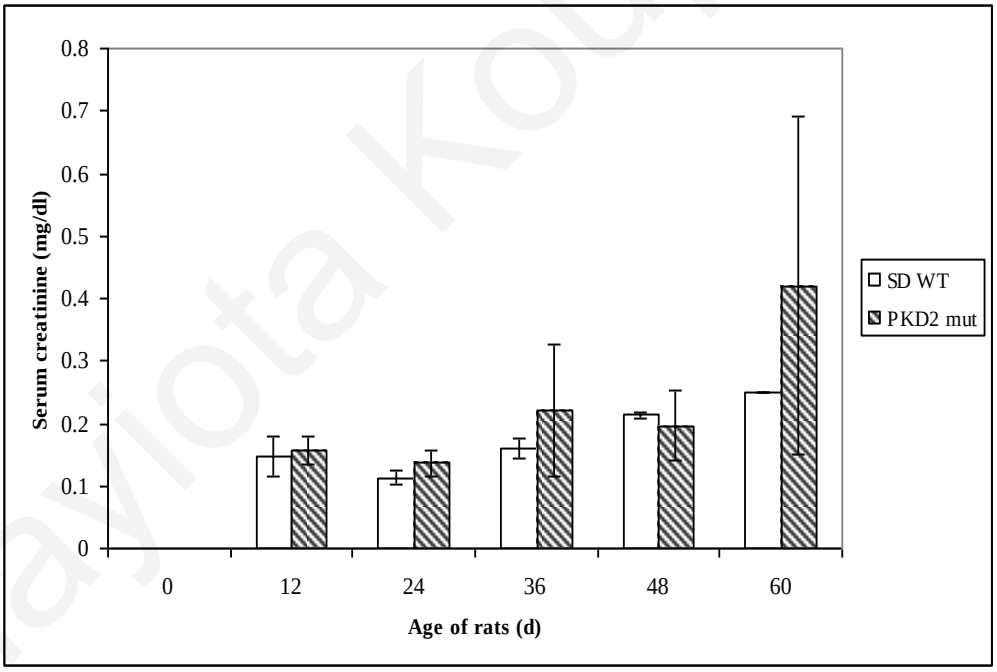

Figure 17: Graphical representation of the plasma values of urea (A) and creatinine (B) of WT SD and PKD2 (1-703) rats as a measure of the renal function of the rats.

Error bars represent the s.d. Each bar represents the mean of urea or creatinine values of three animals. Blood was not obtained from the rats of 0 days.

Panayiota Koupepidou

4.3.3 Cyst and fibrosis grading of kidneys

After the kidneys were excised they were both fragmented in three parts. The middle part of the left kidney was fixed in paraformaldehyde for 24h, submerged in formalin for 24h and then placed in paraffin to be used for cyst grading. Sections from this part of the kidney were obtained and stained with haematoxylin and eosin (H & E). Cysts were graded in three animals from each age according to the scoring system described in the Materials and Methods section.

No cysts were observed in the wild type SD rats at any time point (data not shown). In the kidney sections of the PKD2 (1-703) rats cysts were visible as early as 0 days in the cortex of the kidneys which indicates that cystogenesis begins *in utero* (**Figure 18**). Cysts seem to form and grow from day 0 to day 24, where grading seems to plateau.

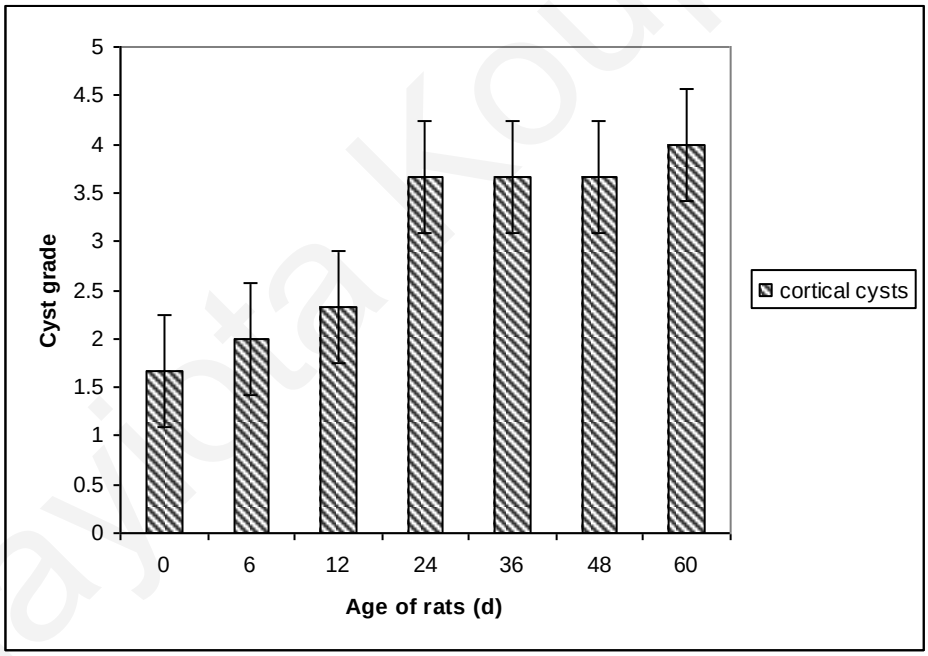

Figure 18: Graphical overview of cyst grading at the different ages of the rat time course.
Mean values from three different PKD2 (1-703) rats at each age are represented. Error bars represent the s.d. Each bar represents the mean of cyst grading of three animals.

Sections from the kidneys of all the rats in the time course were also Azan stained to assess the grade of fibrosis in each animal (fibrosis grading was not possible in tissues from 0 day old animals). A graphical overview of the fibrosis grading is given in **Figure 19**. Fibrosis in the cortex clearly increases with increasing age.

Panayota Koupepidou

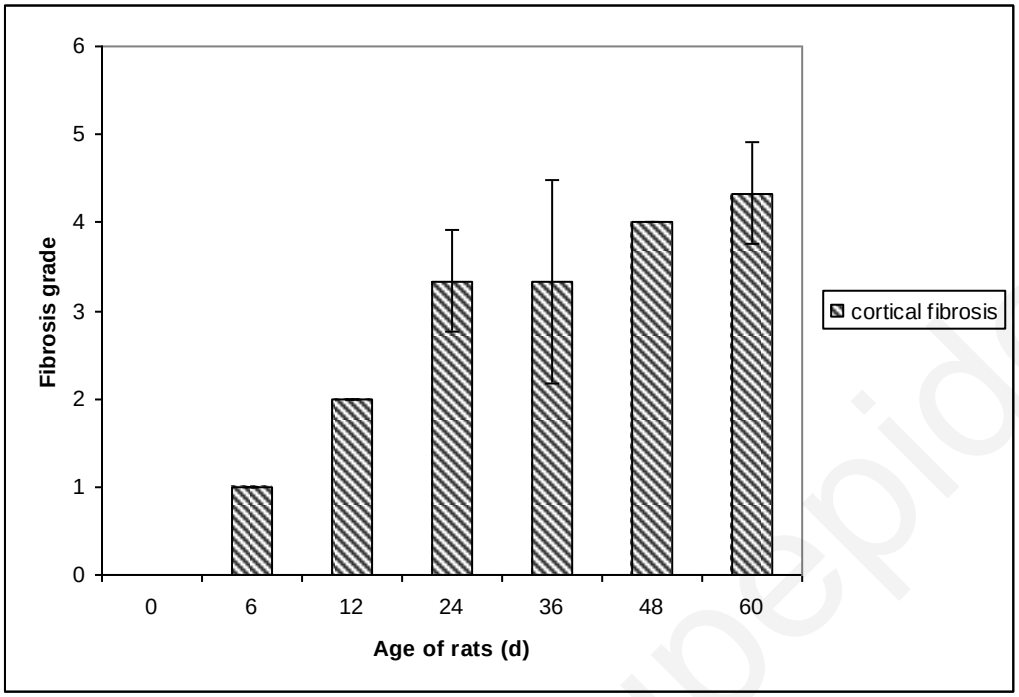

Figure 19: Graphical overview of the fibrosis grading of the rat time course.
Mean values from three different PKD2 (1-703) rats at each age are represented. The fibrosis grading was not possible for the kidneys of rats at age 0 days. Error bars represent the s.d. Each bar represents the mean of fibrosis grading of three animals.

4.3.4 Gene expression profiling at 0, 6 and 24 day-old rats

Cysts were demonstrated to appear at birth (0-day old rats), and therefore the question arose as to which genetic factors were involved at these initial stages of cyst formation. Consequently, our investigation included gene expression profiling of whole kidney homogenates, performed at early stages of the disease in PKD2 (1-703) rats at 0, 6 and 24 days. Hence, three WT SD and three PKD2 (1-703) male rats at the age of 0, 6 and 24 days were sacrificed, their kidneys excised and RNA was isolated from whole kidney homogenate. The quality of the RNA samples was assessed by the Agilent Bioanalyzer and the concentration measured spectrophotometrically. Differentially expressed genes were identified by microarray analysis using the Affymetrix GeneChip® Rat Expression Array Rae230_2 (the whole procedure including the statistical analysis of the results of gene expression profiling was performed at Prof Gretz laboratory in Mannheim, Germany).

Panayiota Kouppepidou

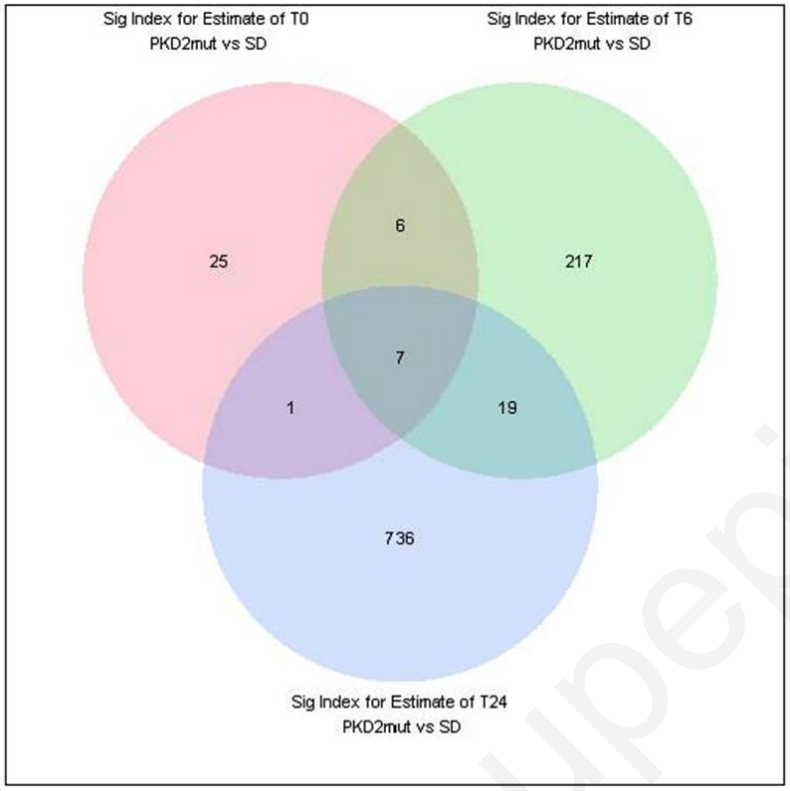

Figure 20: Venn diagram displaying the number of significant genes that are deregulated in PKD2 (1-703) mutant rats compared to wild type SD rats analysed by microarrays in each of the three time points of 0, 6, and 24 days.
At 0 days, 39 genes were significantly differentially expressed, at 6 days, 249 genes and at 24 days, 763 genes. The overlaps of the circles display the common genes differentially expressed at these three time points.

The microarray data of the PKD2 (1-703) rats compared to their normal counterparts, revealed a total of 1011 statistically significant differentially expressed genes at all three time points (p-value$\leq 10^{-5.83}$) (**Figure 20**). Comparison of the data of the PKD2 (1-703) rats to their normal counterparts at day 0, revealed 39 statistically significant differentially expressed genes (**Table 5**– only 18 genes are shown, the rest were predicted sequences). Interestingly, from the list of the 18 genes, not one of them is known to be involved either directly in cell cycle regulation.

Panayiota Koupepidou

	Gene symbol	Gene name	-log10(p-value)	Reg
1	Zfp180	zinc finger protein 180	9.056438	+
2	Myo5a	myosin Va	10.06866	+
3	Lip1	lysosomal acid lipase 1	7.977989	+
4	Vps52	vacuolar protein sorting 52 (yeast)	7.379136	-
5	Dyrk1a	dual-specificity tyrosine phosphorylation regulated kinase 1	6.036715	+
6	Myo1e	myosin IE	11.97402	-
7	Cma1	chymase 1, mast cell	7.142448	-
8	Mfap3	microfibrillar-associated protein 3	27.18254	-
9	Psen1	presenilin 1	7.301317	+
10	Dync1h1	dynein cytoplasmic 1 heavy chain 1	10.76819	+
11	Pmm1	phosphomannomutase 1	7.285327	+
12	Snapc2	small nuclear RNA activating protein complex, polypeptide 2	9.201842	-
13	Tor1b	torsin family 1, member B	10.75092	+
14	Igfbp4	insulin-like growth factor binding protein	7.690679	-
15	Galnt3	UDP-N-acetyl-alpha-D-galactosamine:polypeptide n-acetylgalactosaminyltransferase 3	10.21628	+
16	Ihpk2	inositol hexaphosphate kinase 2	10.16789	-
17	Fntb	farnesyltransferase, CAAX box, beta	6.598515	+
18	Cirbp	cold inducible RNA binding protein	8.588284	-

Table 5: List of the 18 known genes that are significantly regulated in PKD2 (1-703) rats compared to wild type rats.
The negative log of p-value of Mut/ SD is listed. Reg: regulation, +: upregulated, -: downregulated.

At 6 days, 249 genes and at 24 days, 763 genes were found to be statistically significant differentially expressed.

The volcano plots of the results of the proliferation-related genes of the gene expression profiling are represented in **Figure 21**, which are the plots of the values of the negative log of p-value in relation to the log2 of fold change. The volcano plots of cell cycle genes demonstrate that at 0 days no proliferation-related or cell cycle genes become significantly deregulated, at 6 days only two become significantly deregulated and at 24 days that number was markedly increased. This suggests that proliferation and cell cycle do not become deregulated at the early stages of cyst formation but instead contribute to PKD pathogenesis at later stages of the disease.

Panayiota Poulpeiou

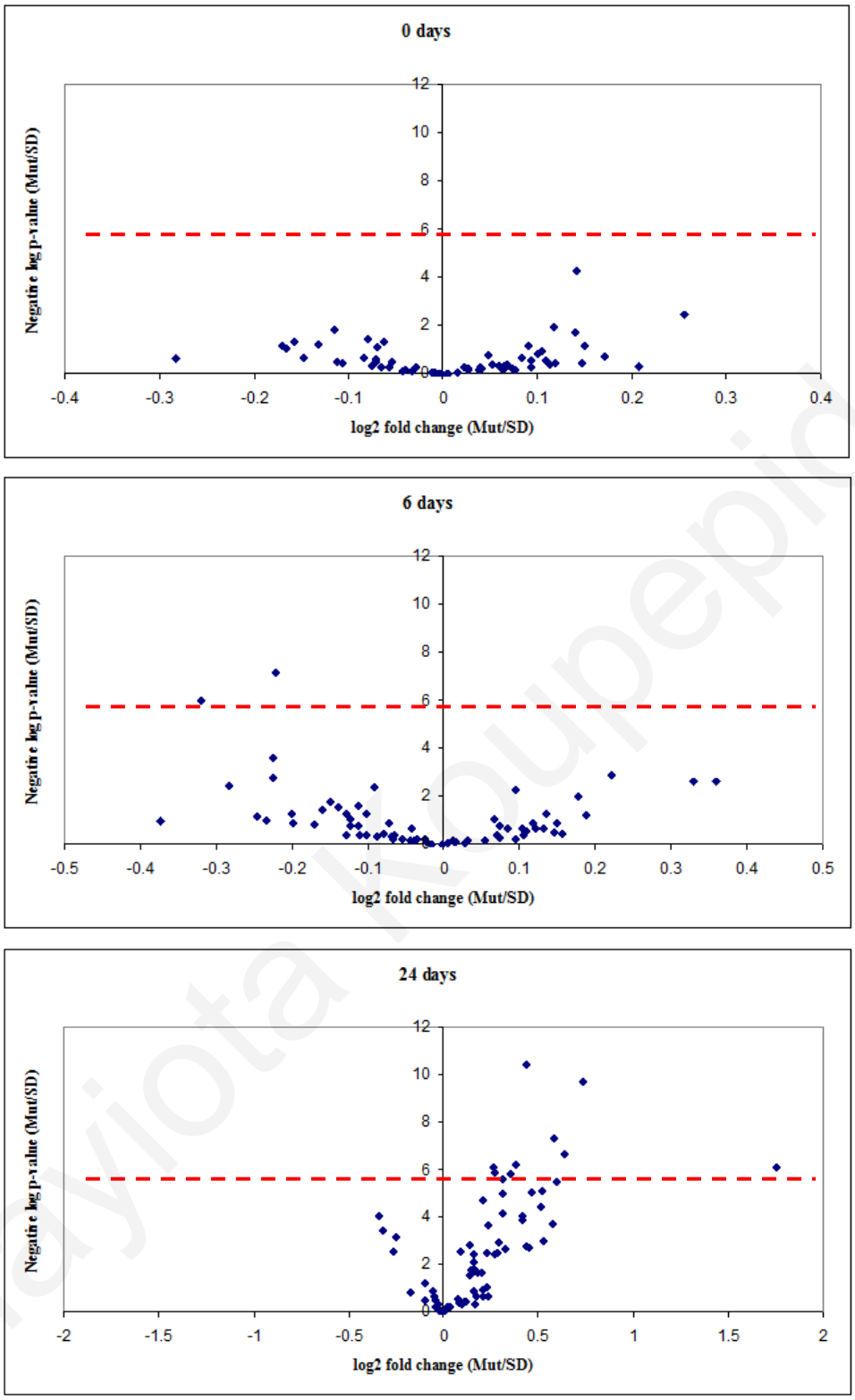

Figure 21: Volcano plots of cell cycle and proliferation-related genes analysed by microarray experiments of whole kidney homogenates of PKD2 (1-703) rats (Mut) compared to Wild type SD rats (SD) in the time points of 0, 6 and 24 days.

Each data point represents a different gene. Data points to the right of the Y-axis denote up-regulation of the gene, whereas data points to the left of the Y-axis denote down-regulation. Some of the significantly deregulated genes' names are shown. The dotted red line represents the threshold of the p-value: $10^{-5.83}$ (Bonferroni correction).

Panagiota Koupepidou

Further analysis of the pathways that are significantly deregulated in the 3 time points in PKD2 (1-703) rats, showed a total of 42 pathways, to be significantly deregulated at all three time points, out of which only one (the renin-angiotensin system – **Appendix Table 6**) was deregulated at 0 days, 6 pathways become deregulated at 6 days and 35 pathways become deregulated at 24 days. The 6 pathways deregulated at the time point of 6 days are the focal adhesion pathway (**Appendix Table 7**), the Wnt pathway (**Appendix Table 8**), glutathione metabolism (**Appendix Table 9**), basal transcription factors (**Appendix Table 10**), chronic myeloid leukemia (**Appendix Table 11**) and metabolism of xenobiotics by cytochrome P450 (**Appendix Table 12**). Interestingly, the cell cycle pathway, which is represented by 63 genes on the Affymetrix chip is not significantly deregulated in any of the three time points examined (p-values: 1, 0.472204, 0.22454 at 0, 6 and 24 days respectively). Other proliferation-related pathways including the JAK-STAT pathway and the MAPK pathway become deregulated at the time point of 24 days (p-values: 0.009 and $1.7x10^{-5}$ respectively). **Figure 22** summarizes the significantly regulated pathways found after analysis with Fischer's exact test. Displayed are 42 (out of a total of 180) pathways found to be significantly deregulated in the 3 time points.

Panayiota Kouloumpou

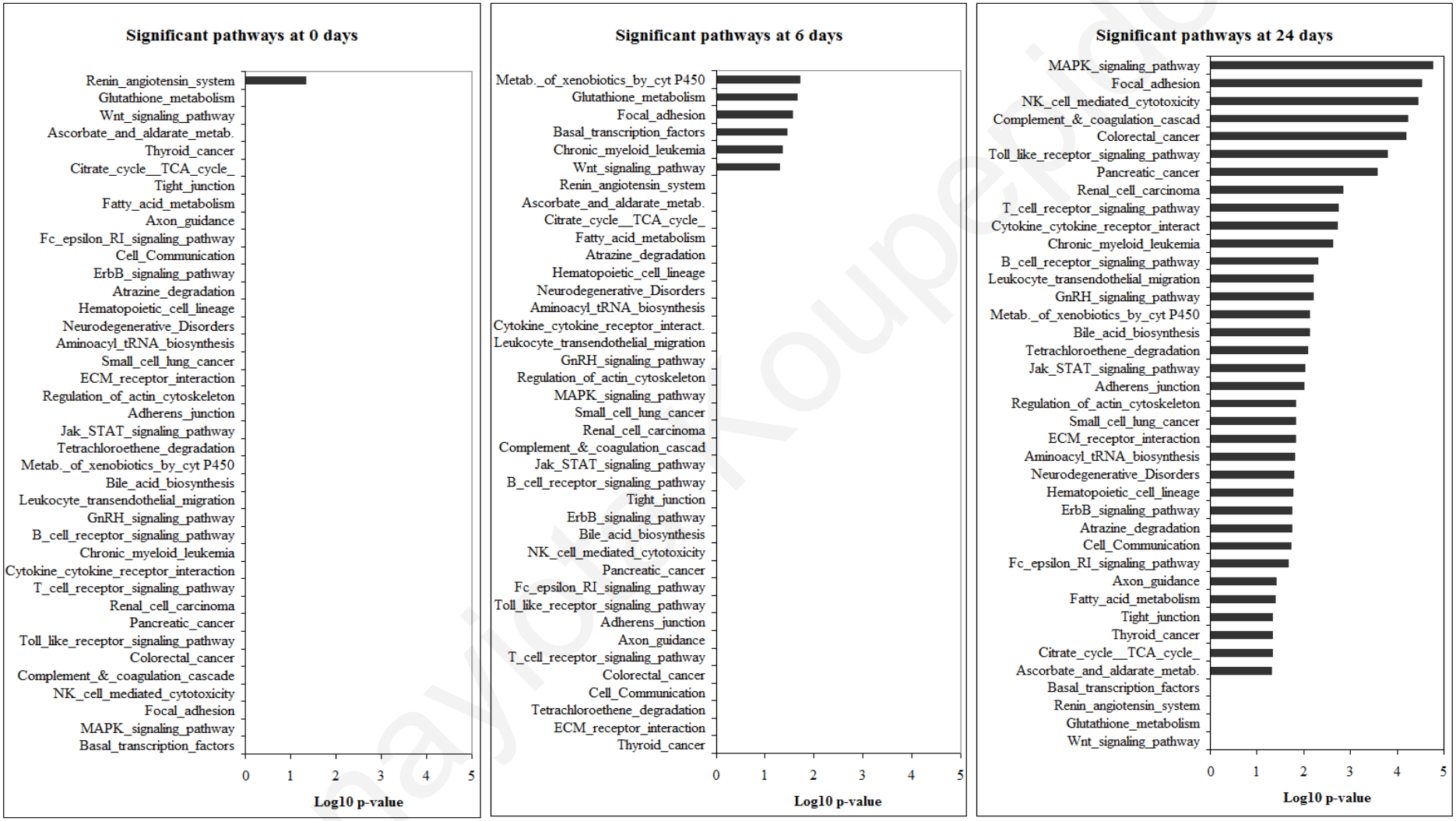

Figure 22: Graphical overview of the significantly regulated pathways analysed by Fischer's exact test (log10 of the p-value is represented) in the gene expression profiling of whole kidney homogenates of PKD2 (1-703) rats at the ages of 0, 6 and 24 days.

The genome-wide expression analysis in the PKD2 (1-703) rat showed that deregulation of proliferation-related genes occurred after the 24 days. More importantly, pathway analysis revealed that the cell-cycle pathway was not altered in any of the time points and proliferation-related pathways became significantly deregulated after 24 days. This suggested that deregulation of proliferation is probably not a causative event for cyst initiation but instead becomes deregulated at a later stage in the progression of the disease, in the expansion of cysts. It appeared from the pathway analysis that other pathways are affected at early stages of the disease.

4.3.5 Verification by quantitative real-time PCR and Western blotting of the proliferation-related genes of interest

Interestingly, the results from the gene expression profiling revealed that the cell cycle and proliferation-related genes did not become deregulated until later stages of disease development. In order to verify the results from the gene expression profile and check the expression of the proliferation-related genes, quantitative real-time PCR and Western blotting analyses were performed for c-myc and PCNA. RNA and protein were isolated from whole kidney homogenates of WT SD and PKD2 (1-703) rats.

Panayiota Koupepidou

A

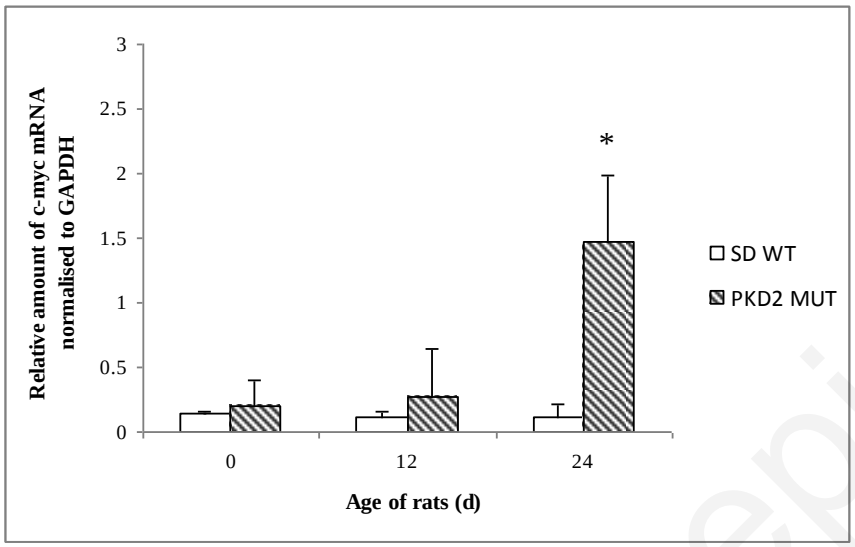

B

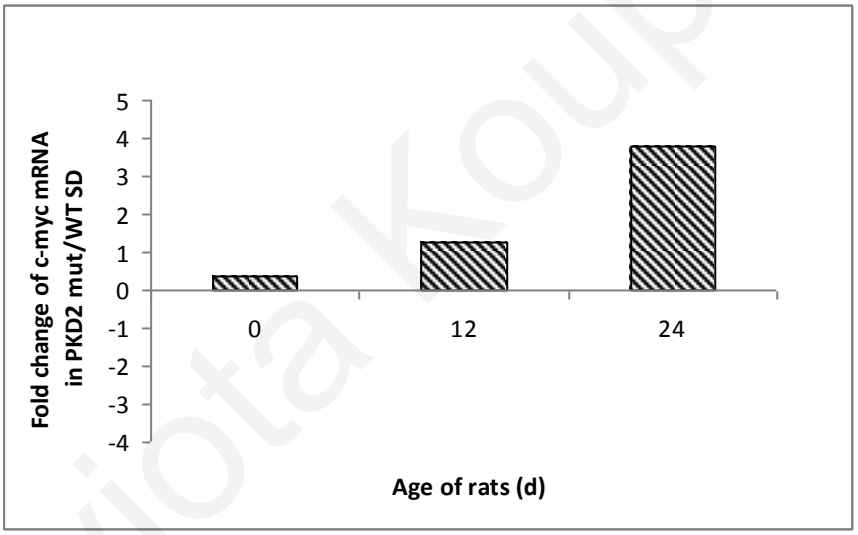

Figure 23: Quantitative real-time PCR analysis of c-myc mRNA in PKD2 (1-703) and WT SD rats.
The graphs represent the mean of normalised relative amount (A) and normalised fold change of PKD2 mut over WT SD (B) from three independent samples. Data were normalised against GAPDH. *: denotes statistical significance

In agreement with the chip data, the relative amount of c-myc mRNA is augmented at the age of 24 days in PKD2 (1-703) rats as compared to WT SD rats, whereas at previous time points the difference was not statistically significantly altered (**Figure 23**).

Panayiota Koupepidou

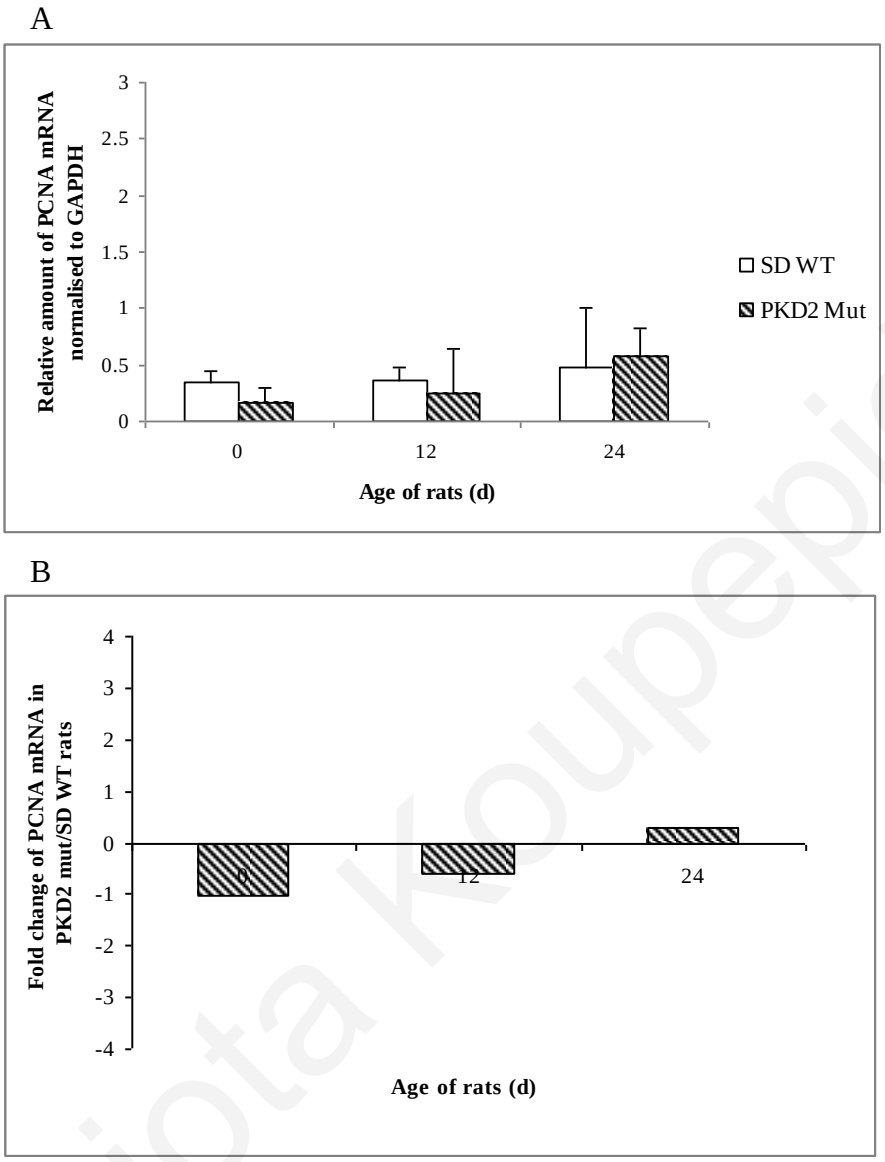

Figure 24: Quantitative real-time PCR analysis of PCNA mRNA in PKD2 (1-703) and WT SD rats.
The graphs represent mean of normalised relative amount (A) and normalised fold change of PKD2 mut over WT SD (B) from three independent samples. Data were normalised against GAPDH.

However, the relative levels of PCNA mRNA were not significantly altered between PKD2 (1-703) and WT SD rats. These results were also in accordance with the microarray data (**Figure 24**).

Immunoblot analysis of c-myc and PCNA proteins revealed that that there was no statistical difference between the PKD2 (1-703) and the WT SD rats. Data were normalised against β-actin and are represented as a graph (**Figure 25**).

Panayiota Koupepidou

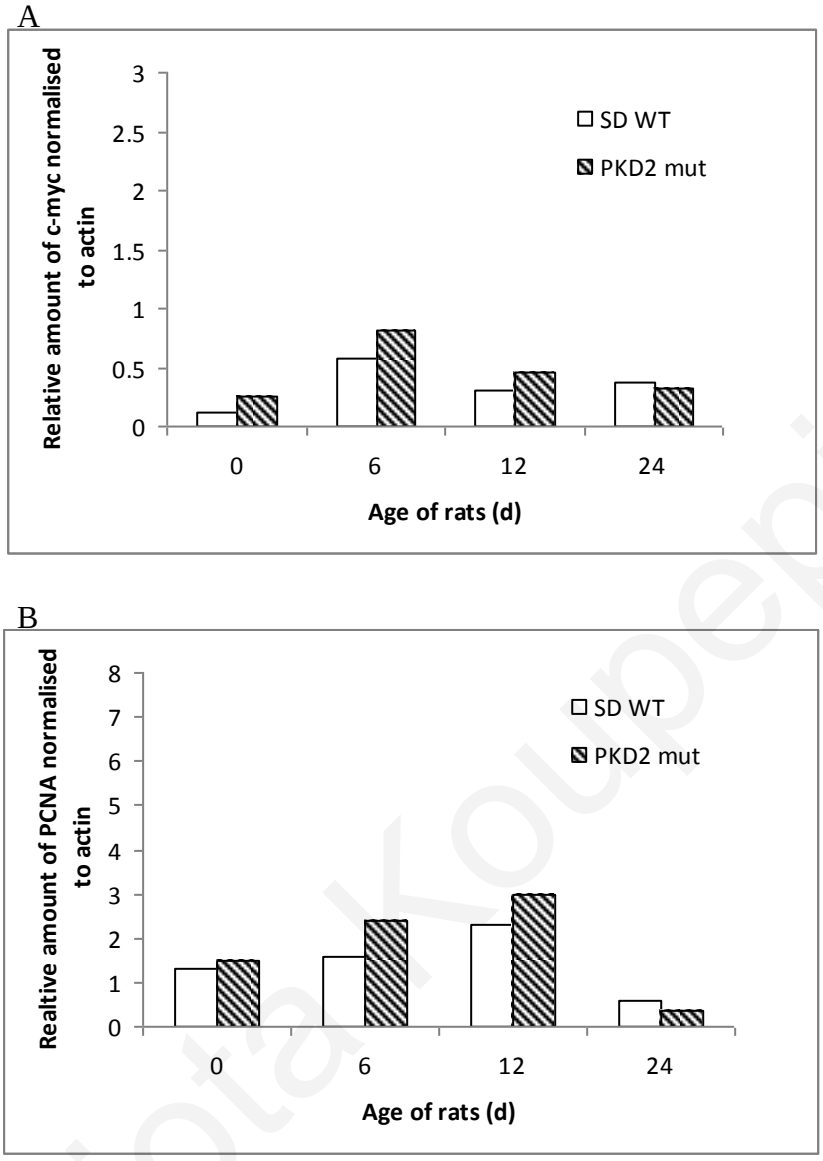

Figure 25: Protein levels of c-myc (A) and PCNA (B) represented as the mean of normalised fold change of two independent Western blot experiments. Data were normalised against β-actin.

Collectively, these results demonstrated that cell proliferation was not a prerequisite of cyst initiation in PKD but instead was involved in later stages of the disease, as in cyst expansion. It was also suggested that other pathways are involved in the initial stages of cyst formation, which need further characterisation.

Panayiota Koupepidou

5 DISCUSSION

The genes mutated in ADPKD, were identified in the mid 1990s, and since then research has focused on understanding the normal biochemical functions of their products, the polycystins. Although it took several years of research, it is now well documented that PC-2 acts as a Ca^{2+} -permeable non selective cation channel, but the function of PC-1 is less clear. It appears to be associated with the extracellular matrix and cell-cell contacts, but also it regulates PC-2 activity. The polycystins have been found to interact forming a heteromeric complex, with a channel activity [56]. Both polycystins have been found to be involved in a confounding plethora of signaling pathways. Nonetheless, the discovery of the normal cellular and biological functions of the polycystins remains elusive and, consequently, the clarification of the molecular cues occurring in cystogenesis has not yet been achieved. Cystogenesis is thought to initiate *in utero*, but it is unknown whether it is an ongoing process throughout the lifetime of patients. Cyst formation and growth is considered to occur from the deregulation of cellular functions, including cell proliferation, apoptosis, epithelial cell polarity and differentiation.

It is believed that one of the early events in the pathogenesis of ADPKD is abnormal epithelial cell proliferation. The increased cell proliferation observed as a central feature of PKD led Grantham to describe it as 'neoplasia in disguise' [188]. This is supported by microdissection studies of cystic kidneys, showing that cyst size is due to an increase in the number of epithelial cells lining the cysts and not to the stretching of the cyst wall [11]. Moreover, transgenic overexpression of proliferation-related genes, results in renal cystic disease [reviewed in [153]]. Cultured epithelial cells from ADPKD cysts display abnormally high levels of cell proliferation and genes associated with proliferation, such as c-myc, have been found to be overexpressed in cystic epithelium [92,99]. The c-myc proto-oncogene, in particular, has received much attention concerning its role in the pathogenesis of PKD, as transgenic overexpression in mice generates a PKD phenotype resembling ADPKD (the SBM model) [131]. The role of c-myc in cyst formation, however, and specifically whether it drives epithelial cells to proliferation or apoptosis still remains elusive.

Additionally, the involvement of Cyclin dependent kinase 2 (Cdk2) coupled to alterations in cell cycle, has also been addressed in the process of cystogenesis. Bhunia et al. demonstrated that overexpression of PC-1 leads to activation of the JAK2/STAT-1 pathway in a process

Panayiota Kouppidou

that requires PC-2, which results in the upregulation of the cyclin-dependent kinase inhibitor cdkn1a ($p21^{waf1}$). This in turn leads to the inhibition of Cdk2 and cell cycle arrest [143]. The involvement of the polycystins in JAK2/STAT-1 signaling might explain why mutations in either of the genes result in abnormal growth and hence, cystogenesis. A recent report demonstrated a reduction in the levels of p21 in tissues from ADPKD patients as well as tissues from the Han:SPRD/(cy/+) rat model, which supports the role of CKIs in cystogenesis [149]. In another study, PC-2 was directly linked to cell cycle regulation. Specifically, it was demonstrated that PC-2 could directly interact with Id2, a member of the helix-loop-helix family of transcription factors that promote cellular growth and inhibit differentiation. The direct interaction of PC-2 and Id2 was shown to regulate the nuclear translocation of Id2, causing an induction of the cyclin-dependent kinase inhibitor p21. Increased p21 could inhibit Cdk2 activity and arrest the cells at the G0/G1 phase of the cell cycle [147].

5.1 Proliferation is not affected in a constructed 'PKD microenvironment'

In this study the HEK293 cell line was used as an expression tool to study the role of polycystin-2 in proliferation and specifically the expression of different proliferation-related proteins. In this cell line, it was demonstrated, however, that overexpression of wild type or mutant polycystin-2 does not affect cellular proliferation, nor does it affect the levels of proliferation-related proteins previously shown to be differentially expressed in PKD. Specifically, cell cycle profile, expression levels of PCNA, p21, c-myc, phosphorylated STAT-1 and activity of Cdk2 were not affected in transfectants of this cell line. This can be explained by different reasons. To start with, the alteration of the basal proliferation rate is one of the unwanted side effects of cellular immortalisation, and can be disadvantageous in proliferation studies. Although cultured cells are a very good expression tool, they cannot represent the complexity and organisation that accompanies a whole organ or organism. Additionally, these cell lines may differ from renal cystic cells in the efficiency of delivering the expressed protein to its appropriate location whether that is the plasma membrane, the ER or the primary cilium. Or, they might differ in the type and degree of post-translational processing as well as the occurrence of appropriate intracellular signaling pathways, and therefore it could be difficult to reproduce the effects that a mutant polycystin protein has on the renal epithelial cells. One surprising observation as far as the HEK293 cell line is concerned was the demonstration that the cells have an unexpected relationship to neurons [187]. And thus it can be argued that they are not typical kidney cells.

Panayiota Koupepidou

In order to eliminate the possibility that the exogenously expressed wild type or mutant PC-2 was not functional in the HEK293 stable transfectants, electrophysiology experiments were performed. Overexpression of wild type *PKD2* displayed an increase in the current amplitude of whole cell inward and outward currents recorded either in normal extracellular tyrode solution or symmetrical K^+. Overexpression of mutant R742X *PKD2* had no effect on the whole cell currents. Although, the *PKD2* R742X mutant was found to be forwarded to the plasma membrane and display channel activity in sympathetic cells and *Xenopus leavis* oocytes [87,186], this mutant did not display channel activity in Chinese Hamster Ovary (CHO) cells [56]. Therefore, it is possible that in the HEK293 stable transfectants, the R742X *PKD2* mutant is either not efficiently transported to the plasma membrane or is unable to form a channel therein. Although overexpression of wild type PC-2 is functional in HEK293 cells, it is possible that expression in the plasma membrane is not sufficient for function and perhaps interactions with other molecules are necessary.

As the balance between proliferation and apoptosis is disturbed in PKD, apoptosis was also examined by flow cytometry using Annexin-V-FLUOS staining kit in the stable clones of HEK293 cells. No statistical significance between the stable clones overexpressing mutated PC-2 as compared to controls was observed (data not shown). These results further supported the hypothesis that the 'PKD microenvironment' could not be easily reproduced *in vitro*.

It was decided from the above-mentioned experiments that the HEK293 cells were not the appropriate cell line to use and the same line of experimentation was followed using another cell line, the NRK52E cells, which are derived from normal rat kidney epithelial cells. The expression of proliferation-related genes in transient transfectants of these cells overexpressing wild type or two different mutants of *PKD2* remained unaltered. Specifically, c-myc, p21, p-STAT-1, PCNA and the activity of Cdk2 were unaffected by overexpression of wild type or mutant PC-2. This supports the idea that the pathologic conditions in animal models or the human disease cannot directly be extrapolated in cell culture and transfection studies.

Recently, much attention has been accumulated in the involvement of the primary cilium in PKD pathogenesis and that of other cystic diseases of the kidney, as it has been demonstrated that most of the cystogenic proteins reside to the cilium or the basal body. The cilium is

Panayiota Koupepidou

thought to act as a mechanosensor in tubular epithelial cells. Stimulation of the cilium by bending in fluid flow results in a calcium influx through the polycystin1/2 complex, which resides in the cilium [7]. The downstream signaling pathways triggered by stimulation of the cilium and the role of the cilium in the pathogenesis of PKD still remain unknown. If the function of PC-1 and PC-2 as cilial chemo- or mechano-sensors proves to be an essential requirement for disease pathogenesis, it would be difficult to reproduce their function in cell culture systems. Ciliary expression *in vitro* depends on several factors, including the state of cell division, confluency and differentiation. The imitation of the ciliary system in cell culture is possible when cells are cultured under confluent conditions for several days and the experiments performed under flow and non-flow conditions. A limitation of this study was that the cell line systems were not cultured under confluent conditions as this would contradict results obtained from proliferation assays. Taken together, all these could explain why the stable or transient expression of PC-2 in these cell lines could not be sufficient to trigger the abnormal proliferation and/or differential expression of proliferation-related genes. These features are probably complicated and cannot be easily reproduced in *in vitro* systems. This is surprising, however, as the HEK293 cell line and similar experimental conditions were used in the studies previously mentioned [143,147]. Worth mentioning is the fact that the experiments in those studies were similarly not performed under confluent conditions to investigate cilium involvement in PKD.

5.2 Proliferation and proliferation-related genes are deregulated in isolated TECs from 7.5 week old PKD2 (1-703) rats

Taking into account the results using the HEK293 and NRK52E cell lines, the cellular model to be utilised was reconsidered and primary tubular epithelial cells (TECs) were isolated from the PKD2 (1-703) transgenic rat using a sequential filtration method. The transgenic line used carried approximately 5 copies of the transgene according to Southern blot analysis [45]. The sequential filtration method was selected in order to avoid any potential activation of surface receptors taking place during antibody-based isolation techniques. Purified TECs were cultured in low serum medium and on laminin-coated plates to avoid differentiation. Culturing on other substrates such as collagen or fibronectin resulted in the differentiation of TECs (Prof. Gretz, personal communication). As can be expected, the isolation protocol of the primary TECs from both wild type and transgenic rats would likely enrich all segments of the nephron. However, it is possible that proximal tubules in the TECs isolated from the PKD2

Παναγιώτα Κουρεμπού

(1-703) rats were over-represented, as the renal cysts in this model predominantly originate from the proximal tubule. In order to eliminate this possibility, the levels of a proximal tubule specific marker were analysed by immunoblotting with anti-Megalin antibody. The protein levels of Megalin were equivalent among TECs isolated from wild type and transgenic rats, suggesting that the proportion of proximal tubular cells among the different cultures was comparable and did not create a sampling bias.

Immunoblotting of samples showed augmented levels of PCNA and flow cytometry revealed a significant decrease in percentage of cells in the G0/G1 phase and an increase in percentage of cells in the G2/M phase of the cell cycle. ***These results indicated that PC-2 can alter cellular proliferation in renal epithelial cells, and also suggested that such process is complicated and possibly multifactorial and cannot be easily recapitulated in in vitro cell line systems.***

Analysis of the expression levels of c-myc and PCNA in the isolated TECs revealed that c-myc and PCNA levels were upregulated at the protein level in mutant as compared to wild type TECs. Interestingly, c-myc and PCNA expression at the mRNA level remained unaltered in mutant compared to wild type TECs, as assessed by quantitative real-time PCR and microarray analysis. Different reasons might account for this. It was suggested by Piontek et al. that proliferation occurs in bursts. It is possible that the cells used to isolate proteins were caught in a phase undergoing proliferation. Also, it is possible that the two proteins might become stabilised by post-translational modifications, and escape degradation by the proteasome. The relatively long half life of PCNA, which is 20 hours, could also be responsible for upregulation of the protein in isolated TECs, because cells that have recently left the cell cycle could still have residual non-degraded PCNA protein [189]. In the case of c-myc, a possible explanation of the increased protein levels in isolated TECs, could be that the protein was post-translationally stabilised by phosphorylation at Serine 62, while the subsequent phosphorylation at Threonine 58 that targets the protein for proteasomal degradation, was somehow inhibited.

Examination of the previously implicated STAT-1/p21/Cdk2 pathway in the PKD2 (1-703) primary TECs, indicated that abnormal cellular proliferation in these cells proceeds through a pathway other than STAT-1/p21. Specifically, expression levels of p21 and phosphorylated STAT-1 remained unaffected in the isolated TECs. PC-2-induced proliferation in these cells

Panayiota Koupepidou

may be regulated by abnormal expression of the cyclin-dependent kinase inhibitor 1C ($p57^{kip2}$) and Cyclin-dependent kinase 2 (Cdk2) as identified by gene expression profiling. The $p57^{kip2}$ belongs to the $p21^{waf/cip1}$ family of Cyclin-dependent kinase inhibitors (CKIs). A decrease in both the mRNA and protein level was observed for p57 in isolated TECs of PKD2 (1-703) rats as compared to their normal counterparts. In addition, there was an increase in the levels of Cdk2 both at the mRNA and the protein level. This is interesting as it appears that Cdk2 activity might be augmented simultaneously by two different ways (downregulation of the inhibitor and upregulation of the kinase). Thus, the simultaneous alteration in p57 and Cdk2 might result in a rapid increase in Cdk2 and subsequently to higher proliferation.

The role of p57 in the PC2-induced proliferation in renal epithelial cells is unclear. Future experiments will focus in identifying the regulatory signals leading to p57 reduction and whether this decrease is necessary for PC-2 induced proliferation in renal tubular epithelial cells. It is possible that expression of mutant PC-2 can result in reduction of p57 by augmenting Id2 nuclear import and subsequent inhibition of p57 transcription [147]. This hypothesis is in agreement with experiments in neural cells where it was shown that Id2 could regulate the cell cycle through p57 [190]. Other mechanisms of altered signal transduction or transcriptional or post-translational silencing could be involved in the reduction of p57. Hypermethylation of the p57 promoter has been shown to inactivate the p57 gene and TGF-β has been shown to cause p57 degradation in osteoblasts [191,192]. Also, insulin growth factor II (IGF-II) treatment in primary embryo fibroblasts and mice with increased levels of serum IGF-II have reduced expression of p57 [193]. These issues will be addressed in future experiments.

5.3 Identification of pathways deregulated in the cyst initiation process

As previously mentioned, one of the primary events of cyst formation in TECs is believed to be the increased cellular proliferation and much of the research in the field of PKD has focused on identifying the molecules that contribute to this. Consequently many of the therapeutic strategies in PKD target this abnormal cellular proliferation. Most studies of human and rodent PKD, however, have unavoidably utilised kidneys obtained at a later stage of the disease, at a stage where chronic or end-stage renal failure has already began. Research has focused on cysts that are in the continued growth and expansion phase rather than cyst initiation. This might have given rise to a false representation of the factors affecting the

Panayiota Koupepidou

progression of the disease, since chronic secondary effects of renal failure might have superimposed the primary defects in the initiation and progression of PKD. Therefore, the characterisation of the detailed molecular cues at the very early stages of initiation of cystogenesis remain unknown and in need of intensive investigation.

In this study, an attempt was made in identifying early events leading to cystogenesis by utilising the transgenic rat model overexpressing a truncated form of PC-2. As demonstrated in the gene expression profiling of the 0, 6, and 24 days old PKD2 (1-703) rats, proliferation-related pathways become deregulated at 24 days as compared to their normal counterparts. Interestingly, the cell cycle pathway represented by 63 genes on the microarray did not significantly change at any of the three time points examined. Cyst grading performed at these time points, showed that cysts are visible as early as 0 days and cyst formation proceeds up to and reaches a maximum at 24 days. Quantitative Real-Time PCR analysis correlated with the microarray data and showed that c-myc mRNA expression gradually increases from 0 to 24 days and PCNA mRNA levels practically remain unchanged, with no significant difference between the PKD2 (1-703) and the wild type rats. Western blot analysis demonstrated that the protein levels of c-myc and PCNA are not different in transgenic compared to normal rats. The protein levels of c-myc and PCNA, however, were shown to be augmented in isolated TECs from 7.5week old transgenic rats compared to their normal counterparts. These results demonstrated that proliferation-related genes remained unaffected at the early time points of disease initiation in the PKD2 (1-703) rat, but become deregulated later on in disease development. Supporting data for this were observed by Piontek et al. who have demonstrated that cellular proliferation was not appreciably higher in cystic specimens compared to age-matched controls in a mouse model with inactivation of the Pkd1. The authors suggested that defective growth regulation could not be the primary defect in the initiation of cysts, but rather the relationship between proliferation and cyst formation might be indirect. The authors also suggested that proliferation might occur in bursts, and implied that other studies that have implicated proliferation as a primary cause of polycystic kidney disease might have acquired proliferation data from cysts undergoing bursts of proliferation [151]. More supporting data were provided by a mouse model of kidney-specific inactivation of Kif3a which resulted in the loss of primary cilia, in which the rate of cell proliferation in pre-cystic tubules in mutant mice was similar to the rates in control littermates. These results demonstrated that the loss of primary cilia did not stimulate cell proliferation, but produced abnormalities in the orientation of cell division as a demonstration of abnormal planar cell polarity (PCP) [194]. ***It is therefore***

Παναγιώτα Κουρεπίδου

proposed that other mechanisms instead of cell proliferation are involved in renal cyst initiation.

Although cysts appear as early as 0 days in the renal cortex of the PKD2 (1-703) rats, deregulation of proliferation-related genes occurs after 24 days. In contrast, renin-angiotensin system (**Appendix Table 6**), focal adhesion pathways (**Appendix Table 7**), the Wnt signaling pathway (**Appendix Table 8**), glutathione metabolism (**Appendix Table 9**), basal transcription factors (**Appendix Table 10**), chronic myeloid leukemia pathway (**Appendix Table 11**) and the metabolism of xenobiotics by cytochrome P450 (**Appendix Table 12**) appear to be affected at very early time-points (0 and 6 days) correlating with the initial appearance of cysts. Future studies will focus on these pathways to unravel the complexities underlying cyst initiation in the kidney. The role of microRNAs at these early stages of cyst initiation will also be examined. As cysts were shown to begin *in utero*, factors shown to be deregulated at early stages of cyst formation will also be investigated in embryonic stages of the transgenic rats. Also, perhaps a better *in vitro* cellular model to study the mechanism of cyst initiation is needed for subsequent studies, and specifically one that imitates cyst formation, such as the system of MDCK cells that when grown on a collagen matrix form cysts [195].

It is known that the renin-angiotensin system controls the proper development of the kidney, although the exact mechanisms are poorly understood. The genes that contribute to the statistically significant deregulation of the renin-angiotensin system are chymase 1 (CMA1), carboxypeptidase A3 (CPA3) both of which are secreted by mast cells, and Leucyl/cystinyl aminopeptidase also known as insulin-regulated membrane aminopeptidase and angiotensin IV receptor (LNPEP-IRAP). All three of them were shown to be downregulated in PKD2 (1-703) compared to WT SD rats at the time point of 0 days. Future studies will focus on verifying these results and identifying the role of these genes in PC-2 induced cyst initiation.

Overexpression of different transcription factors in transgenic mouse models leads to renal cystic disease [reviewed in [153]]. Interestingly, mouse overexpression of β-catenin that can function both as a transcription factor and as a cell-cell adhesive protein also leads to development of cysts [196]. Cyst formation has been observed in models with knockout or inactivation of genes and proteins involved in cell-cell and cell-matrix interactions. These include laminin α5, the matrix receptor a3b1-integrin, the focal adhesion protein tensin, and

Panayota Koupepidou

the b-catenin complex protein APC [reviewed in [153]]. Also considering the localization of PC-1 and complexes formed at cell-matrix focal adhesion contacts and cell-cell adherens junctions of renal epithelia, these data suggest that normal renal tubule epithelial development is dependent upon these cell-cell and cell-matrix-related functions. Collectively, transgenic models of renal cystic disease suggest that a tight control of transcriptional activity and cell adhesive functions during development is critical for the differentiation of a kidney with normal tubular architecture and function [153]. This is consistent with the results of the gene expression profiling at 6 days where deregulated pathways include the basal transcription factors and focal adhesion pathway. Also, proteins such as presenilin1 (Psen1) and microfibrillar-associated protein 3 (Mfap3), which are involved in cell-cell contacts and extracellular matrix interactions are two of the 39 deregulated genes at 0 days. In support of this concept, it was recently reported that cell adhesion but not cell proliferation mediates cyst formation in polycystic liver disease [197]. In accordance with Patel et al. the deregulation of the Wnt pathway at 6 days in the gene expression profiling suggests that early development of cysts results from loss of primary cilia and consequently aberrant planar cell polarity which activates the noncanonical Wnt pathway [194].

It is probable that different signal transduction pathways contribute to the different stages of cystogenesis. Cyst initiation probably involves the deregulation of planar cell polarity, which depends on the function of cilia, and focal adhesion mediated pathways. Cyst expansion is characterised by augmented cell proliferation, apoptosis, alterations in extracellular matrix and fluid secretion (**Figure 26**). The processes identified to be involved in cyst initiation will be the focus of future studies.

Panayiota Kouppoudou

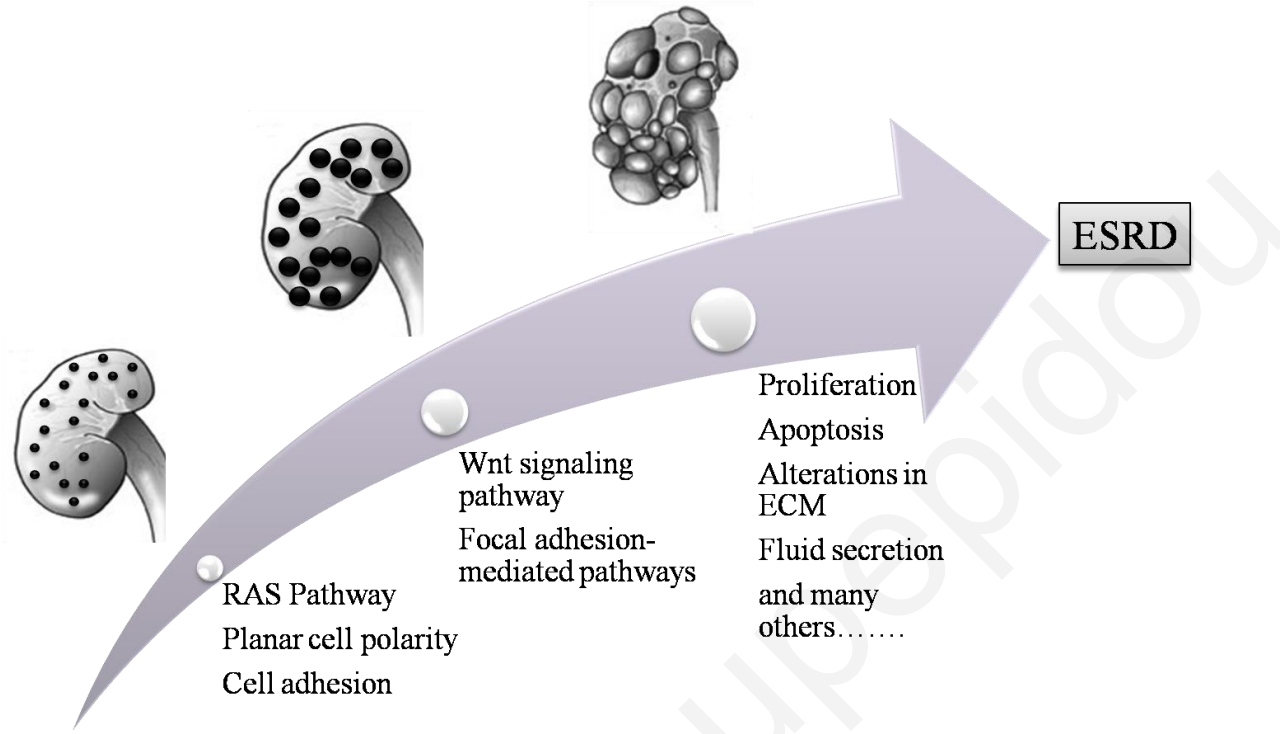

Figure 26: Graphical representation of the pathways suggested to be affected at different stages of cystogenesis, from cyst initiation to cyst expansion.

It is suggested that processes of planar cell polarity and cell adhesion are involved in the initial stages of cyst formation. Nonetheless, epithelial cell proliferation seems to be an important determinant of cyst expansion, although is probably not a primary cause of cyst initiation. As far as therapy is concerned, considering cyst formation as a multistep process, perhaps a dual strategy for therapeutic intervention could be employed. One branch could be to target cyst initiation, which would decrease the number of cysts formed at an early age and a second branch to target the process of cyst expansion, and specifically the mechanisms of proliferation and fluid secretion. As more is learned regarding the normal functions of polycystins, and how mutations in them disrupt normal cell biology and cellular physiology, the ability to design therapeutic interventions based on gene function and specific pathophysiological mechanisms may progress.

Panayiota Koupepidou

5.4 Conclusion

In this study the role of polycystin-2 (PC-2) in PKD cellular proliferation was addressed by using primary cultures of Tubular Epithelial Cells (TECs) from 7.5 week old transgenic rats overexpressing a mutated form of PC-2, the protein product of PKD2. These cultured cells displayed increased proliferation as assessed by increased levels of PCNA, c-myc, cdk2, decreased levels of $p57^{kip2}$ and abnormal cell cycle profile as compared to their normal counterparts.

However, the contribution of PC-2-induced abnormal proliferation in cyst initiation remained unclear. To further address this issue gene expression profiling of whole kidney homogenates from rats at an early stage of the disease, at 0, 6 and 24 days, was performed. Although cysts appear as early as 0 days, deregulation of proliferation-related genes occurs after 24 days. Instead, pathways including the renin-angiotensin system, the Wnt, focal adhesion, glutathione metabolism and basal transcription factors are altered at these early time points. This demonstrates that abnormal cell proliferation is probably not a primary event in the initiation and formation of cysts but is probably involved at later stages in disease pathogenesis.

Panayiota Koupepidou

BIBLIOGRAPHY

1. Martini, F. *Fundamentals of Anatomy and Physiology*, 1248 (Pearson, 2005).
2. Torres, V.E., Harris, P.C. & Pirson, Y. Autosomal dominant polycystic kidney disease. *The Lancet* **369**, 1287-1301 (2007).
3. Guay-Woodford, L. Renal cystic diseases: diverse phenotypes converge on the cilium/centrosome complex. *Pediatric Nephrology* **21**, 1369-1376 (2006).
4. Deltas, C. & Papagregoriou, G. Cystic Disease of the Kidney: Molecular Biology and Genetics. *Arch Pathol Lab Med.* **in press**.
5. Watnick, T. & Germino, G. From cilia to cyst. *Nat Genet* **34**, 355-6 (2003).
6. Lin, F. et al. Kidney-specific inactivation of the KIF3A subunit of kinesin-II inhibits renal ciliogenesis and produces polycystic kidney disease. *Proc Natl Acad Sci U S A* **100**, 5286-91 (2003).
7. Nauli, S.M. et al. Polycystins 1 and 2 mediate mechanosensation in the primary cilium of kidney cells. *Nat Genet* **33**, 129-137 (2003).
8. Simons, M. & Walz, G. Polycystic kidney disease: cell division without a c(l)ue? *Kidney Int* **70**, 854-64 (2006).
9. Cowley, B.D., Jr. Recent advances in understanding the pathogenesis of polycystic kidney disease: therapeutic implications. *Drugs* **64**, 1285-94 (2004).
10. Wilson, P.D. Polycystic Kidney Disease. *N Engl J Med* **350**, 151-164 (2004).
11. Grantham, J.J., Geiser, J.L. & Evan, A.P. Cyst formation and growth in autosomal dominant polycystic kidney disease. *Kidney Int* **31**, 1145-52 (1987).
12. Daoust, M.C., Reynolds, D.M., Bichet, D.G. & Somlo, S. Evidence for a third genetic locus for autosomal dominant polycystic kidney disease. *Genomics* **25**, 733-6 (1995).
13. Gabow, P.A. Autosomal Dominant Polycystic Kidney Disease. *N Engl J Med* **329**, 332-342 (1993).
14. Hateboer, N. et al. Comparison of phenotypes of polycystic kidney disease types 1 and 2. *The Lancet* **353**, 103-107 (1999).
15. Demetriou, K. et al. Autosomal dominant polycystic kidney disease--type 2. Ultrasound, genetic and clinical correlations. *Nephrol. Dial. Transplant.* **15**, 205-211 (2000).
16. Persu, A. et al. Comparison between siblings and twins supports a role for modifier genes in ADPKD. *Kidney Int* **66**, 2132-6 (2004).
17. Paterson, A.D. et al. Progressive Loss of Renal Function Is an Age-Dependent Heritable Trait in Type 1 Autosomal Dominant Polycystic Kidney Disease. *J Am Soc Nephrol* **16**, 755-762 (2005).
18. Magistroni, R. et al. Genotype-renal function correlation in type 2 autosomal dominant polycystic kidney disease. *J Am Soc Nephrol* **14**, 1164-74 (2003).
19. Ong, A.C.M. & Harris, P.C. Molecular pathogenesis of ADPKD: The polycystin complex gets complex. *Kidney Int* **67**, 1234-1247 (2005).
20. Tazon-Vega, B. et al. Study of candidate genes affecting the progression of renal disease in autosomal dominant polycystic kidney disease type 1. *Nephrol. Dial. Transplant.* **22**, 1567-1577 (2007).
21. Burn, T.C. et al. Analysis of the genomic sequence for the autosomal dominant polycystic kidney disease (PKD1) gene predicts the presence of a leucine-rich repeat: The AMERICAN PKD1 Consortium (APKD1 Consortium). *Hum. Mol. Genet.* **4**, 575-582 (1995).
22. The International Polycystic Kidney Disease, C. Polycystic kidney disease: The complete structure of the PKD1 gene and its protein. *Cell* **81**, 289-298 (1995).

Panagiota Kousepiou

23. Hughes, J. et al. The polycystic kidney disease 1 (PKD1) gene encodes a novel protein with multiple cell recognition domains. *Nat Genet* **10**, 151-160 (1995).
24. The European Polycystic Kidney Disease, C. The polycystic kidney disease 1 gene encodes a 14 kb transcript and lies within a duplicated region on chromosome 16. *Cell* **77**, 881-894 (1994).
25. Mochizuki, T. et al. PKD2, a gene for polycystic kidney disease that encodes an integral membrane protein. *Science* **272**, 1339-42 (1996).
26. Hayashi, T. et al. Characterization of the Exon Structure of the Polycystic Kidney Disease 2 Gene (PKD2). *Genomics* **44**, 131-136 (1997).
27. Koptides, M. & Deltas, C.C. Autosomal dominant polycystic kidney disease: molecular genetics and molecular pathogenesis. *Hum Genet* **107**, 115-26 (2000).
28. Bogdanova, N. et al. Homologues to the first gene for autosomal dominant polycystic kidney disease are pseudogenes. *Genomics* **74**, 333-41 (2001).
29. Rossetti, S. et al. The position of the polycystic kidney disease 1 (PKD1) gene mutation correlates with the severity of renal disease. *J Am Soc Nephrol* **13**, 1230-7 (2002).
30. Deltas, C.C. Mutations of the human polycystic kidney disease 2 (PKD2) gene. *Hum Mutat* **18**, 13-24 (2001).
31. Qian, F., Watnick, T.J., Onuchic, L.F. & Germino, G.G. The molecular basis of focal cyst formation in human autosomal dominant polycystic kidney disease type I. *Cell* **87**, 979-87 (1996).
32. Koptides, M. et al. Loss of heterozygosity in polycystic kidney disease with a missense mutation in the repeated region of PKD1. *Hum Genet* **103**, 709-717 (1998).
33. Koptides, M., Hadjimichael, C., Koupepidou, P., Pierides, A. & Constantinou Deltas, C. Germinal and somatic mutations in the PKD2 gene of renal cysts in autosomal dominant polycystic kidney disease. *Hum. Mol. Genet.* **8**, 509-513 (1999).
34. Pei, Y. et al. Somatic PKD2 Mutations in Individual Kidney and Liver Cysts Support a "Two-Hit" Model of Cystogenesis in Type 2 Autosomal Dominant Polycystic Kidney Disease. *J Am Soc Nephrol* **10**, 1524-1529 (1999).
35. Badenas, C. et al. Loss of heterozygosity in renal and hepatic epithelial cystic cells from ADPKD1 patients. *Eur J Hum Genet* **8**, 487-92 (2000).
36. Koptides, M., Mean, R., Demetriou, K., Pierides, A. & Deltas, C.C. Genetic evidence for a trans-heterozygous model for cystogenesis in autosomal dominant polycystic kidney disease. *Hum. Mol. Genet.* **9**, 447-452 (2000).
37. Watnick, T. et al. Mutations of PKD1 in ADPKD2 cysts suggest a pathogenic effect of trans-heterozygous mutations. *Nat Genet* **25**, 143-4 (2000).
38. Wu, G. et al. Trans-heterozygous Pkd1 and Pkd2 mutations modify expression of polycystic kidney disease. *Hum Mol Genet* **11**, 1845-54 (2002).
39. Gallagher, A.R., Hidaka, S., Gretz, N. & Witzgall, R. Molecular basis of autosomal-dominant polycystic kidney disease. *Cell Mol Life Sci* **59**, 682-93 (2002).
40. Leeuwen, I.S.L.-v. et al. Lowering of Pkd1 expression is sufficient to cause polycystic kidney disease. *Hum. Mol. Genet.* **13**, 3069-3077 (2004).
41. Jiang, S.T. et al. Defining a link with autosomal-dominant polycystic kidney disease in mice with congenitally low expression of Pkd1. *Am J Pathol* **168**, 205-20 (2006).
42. Thivierge, C. et al. Overexpression of PKD1 Causes Polycystic Kidney Disease. *Mol. Cell. Biol.* **26**, 1538-1548 (2006).
43. Pritchard, L. et al. A human PKD1 transgene generates functional polycystin-1 in mice and is associated with a cystic phenotype. *Hum. Mol. Genet.* **9**, 2617-2627 (2000).
44. Rossetti, S. et al. Incompletely penetrant PKD1 alleles suggest a role for gene dosage in cyst initiation in polycystic kidney disease. *Kidney Int* (2009).

45. Gallagher, A.R. et al. A Truncated Polycystin-2 Protein Causes Polycystic Kidney Disease and Retinal Degeneration in Transgenic Rats. *J Am Soc Nephrol* **17**, 2719-2730 (2006).
46. Ong, A.C.M. & Harris, P.C. Molecular basis of renal cyst formation--one hit or two? *The Lancet* **349**, 1039-1040 (1997).
47. Bycroft, M. et al. The structure of a PKD domain from polycystin-1: implications for polycystic kidney disease. *EMBO J* **18**, 297-305 (1999).
48. Weston, B.S., Malhas, A.N. & Price, R.G. Structure-function relationships of the extracellular domain of the autosomal dominant polycystic kidney disease-associated protein, polycystin-1. *FEBS Lett* **538**, 8-13 (2003).
49. Malhas, A.N., Abuknesha, R.A. & Price, R.G. Interaction of the leucine-rich repeats of polycystin-1 with extracellular matrix proteins: possible role in cell proliferation. *J Am Soc Nephrol* **13**, 19-26 (2002).
50. Weston, B.S., Bagneris, C., Price, R.G. & Stirling, J.L. The polycystin-1 C-type lectin domain binds carbohydrate in a calcium-dependent manner, and interacts with extracellular matrix proteins in vitro. *Biochim Biophys Acta* **1536**, 161-76 (2001).
51. Qian, F. et al. Cleavage of polycystin-1 requires the receptor for egg jelly domain and is disrupted by human autosomal-dominant polycystic kidney disease 1-associated mutations. *Proc Natl Acad Sci U S A* **99**, 16981-6 (2002).
52. Ibraghimov-Beskrovnaya, O. & Bukanov, N. Polycystic kidney diseases: From molecular discoveries to targeted therapeutic strategies. *Cellular and Molecular Life Sciences (CMLS)* **65**, 605-619 (2008).
53. Parnell, S.C. et al. The polycystic kidney disease-1 protein, polycystin-1, binds and activates heterotrimeric G-proteins in vitro. *Biochem Biophys Res Commun* **251**, 625-31 (1998).
54. Chauvet, V. et al. Mechanical stimuli induce cleavage and nuclear translocation of the polycystin-1 C terminus. *J Clin Invest* **114**, 1433-1443 (2004).
55. Yoder, B.K., Hou, X. & Guay-Woodford, L.M. The polycystic kidney disease proteins, polycystin-1, polycystin-2, polaris, and cystin, are co-localized in renal cilia. *J Am Soc Nephrol* **13**, 2508-16 (2002).
56. Hanaoka, K. et al. Co-assembly of polycystin-1 and -2 produces unique cation-permeable currents. *Nature* **408**, 990-994 (2000).
57. Boletta, A. et al. Biochemical characterization of bona fide polycystin-1 in vitro and in vivo. *Am J Kidney Dis* **38**, 1421-9 (2001).
58. Newby, L.J. et al. Identification, characterization, and localization of a novel kidney polycystin-1-polycystin-2 complex. *J Biol Chem* **277**, 20763-73 (2002).
59. Tsiokas, L., Kim, E., Arnould, T., Sukhatme, V.P. & Walz, G. Homo- and heterodimeric interactions between the gene products of PKD1 and PKD2. *Proc Natl Acad Sci U S A* **94**, 6965-70 (1997).
60. Kim, E. et al. Interaction between RGS7 and polycystin. *Proc Natl Acad Sci U S A* **96**, 6371-6 (1999).
61. Xu, G.M. et al. Polycystin-1 interacts with intermediate filaments. *J Biol Chem* **276**, 46544-52 (2001).
62. Huan, Y. & van Adelsberg, J. Polycystin-1, the PKD1 gene product, is in a complex containing E-cadherin and the catenins. *J Clin Invest* **104**, 1459-68 (1999).
63. Somlo, S. & Ehrlich, B. Human disease: Calcium signaling in polycystic kidney disease. *Current Biology* **11**, R356-R360 (2001).
64. Anyatonwu, G.I. & Ehrlich, B.E. Calcium signaling and polycystin-2. *Biochemical and Biophysical Research Communications* **322**, 1364-1373 (2004).
65. Cantiello, H.F. Regulation of calcium signaling by polycystin-2. *Am J Physiol Renal Physiol* **286**, F1012-29 (2004).

Pamięć Kobiecia

66. Geng, L. et al. Polycystin-2 traffics to cilia independently of polycystin-1 by using an N-terminal RVxP motif. *J Cell Sci* **119**, 1383-1395 (2006).
67. Scheffers, M.S. et al. Distinct subcellular expression of endogenous polycystin-2 in the plasma membrane and Golgi apparatus of MDCK cells. *Hum. Mol. Genet.* **11**, 59-67 (2002).
68. Luo, Y., Vassilev, P.M., Li, X., Kawanabe, Y. & Zhou, J. Native polycystin 2 functions as a plasma membrane Ca2+-permeable cation channel in renal epithelia. *Mol Cell Biol* **23**, 2600-7 (2003).
69. Foggensteiner, L. et al. Cellular and subcellular distribution of polycystin-2, the protein product of the PKD2 gene. *J Am Soc Nephrol* **11**, 814-27 (2000).
70. Cai, Y. et al. Identification and characterization of polycystin-2, the PKD2 gene product. *J Biol Chem* **274**, 28557-65 (1999).
71. Koulen, P. et al. Polycystin-2 is an intracellular calcium release channel. *Nat Cell Biol* **4**, 191-197 (2002).
72. Pazour, G.J., San Agustin, J.T., Follit, J.A., Rosenbaum, J.L. & Witman, G.B. Polycystin-2 localizes to kidney cilia and the ciliary level is elevated in orpk mice with polycystic kidney disease. *Curr Biol* **12**, R378-80 (2002).
73. Jurczyk, A. et al. Pericentrin forms a complex with intraflagellar transport proteins and polycystin-2 and is required for primary cilia assembly. *J. Cell Biol.* **166**, 637-643 (2004).
74. Rundle, D.R., Gorbsky, G. & Tsiokas, L. PKD2 Interacts and Co-localizes with mDia1 to Mitotic Spindles of Dividing Cells: ROLE OF mDia1 IN PKD2 LOCALIZATION TO MITOTIC SPINDLES. *J. Biol. Chem.* **279**, 29728-29739 (2004).
75. Gonzalez-Perrett, S. et al. Polycystin-2, the protein mutated in autosomal dominant polycystic kidney disease (ADPKD), is a Ca 2+ -permeable nonselective cation channel. *Proceedings of the National Academy of Sciences of the United States of America* **98**, 1182-1187 (2001).
76. Vassilev, P.M. et al. Polycystin-2 Is a Novel Cation Channel Implicated in Defective Intracellular Ca2+ Homeostasis in Polycystic Kidney Disease. *Biochemical and Biophysical Research Communications* **282**, 341-350 (2001).
77. Tsiokas, L., Kim, S. & Ong, E.C. Cell biology of polycystin-2. *Cell Signal* **19**, 444-53 (2007).
78. Tsiokas, L. et al. Specific association of the gene product of PKD2 with the TRPC1 channel. *Proceedings of the National Academy of Sciences* **96**, 3934-3939 (1999).
79. Lehtonen, S. et al. In vivo interaction of the adapter protein CD2-associated protein with the type 2 polycystic kidney disease protein, polycystin-2. *J Biol Chem* **275**, 32888-93 (2000).
80. Gallagher, A.R., Cedzich, A., Gretz, N., Somlo, S. & Witzgall, R. The polycystic kidney disease protein PKD2 interacts with Hax-1, a protein associated with the actin cytoskeleton. *Proc Natl Acad Sci U S A* **97**, 4017-22 (2000).
81. Li, Q. et al. Polycystin-2 associates with tropomyosin-1, an actin microfilament component. *J Mol Biol* **325**, 949-62 (2003).
82. Li, Q., Shen, P.Y., Wu, G. & Chen, X.Z. Polycystin-2 interacts with troponin I, an angiogenesis inhibitor. *Biochemistry* **42**, 450-7 (2003).
83. Li, Y., Wright, J.M., Qian, F., Germino, G.G. & Guggino, W.B. Polycystin 2 interacts with type I inositol 1,4,5-trisphosphate receptor to modulate intracellular Ca2+ signaling. *J Biol Chem* **280**, 41298-306 (2005).
84. Sohara, E. et al. Nek8 Regulates the Expression and Localization of Polycystin-1 and Polycystin-2. *J Am Soc Nephrol* **19**, 469-476 (2008).

85. Qian, F. et al. PKD1 interacts with PKD2 through a probable coiled-coil domain. *Nat Genet* **16**, 179-183 (1997).
86. Lakkis, M. & Zhou, J. Molecular complexes formed with polycystins. *Nephron Exp Nehrol* **93**, E3-E8 (2003).
87. Delmas, P. et al. Gating of the polycystin ion channel signaling complex in neurons and kidney cells. *FASEB J* **18**, 740-2 (2004).
88. Pelucchi, B. et al. Nonspecific cation current associated with native polycystin-2 in HEK-293 cells. *J Am Soc Nephrol* **17**, 388-97 (2006).
89. Grantham, J.J. 1992 Homer Smith Award. Fluid secretion, cellular proliferation, and the pathogenesis of renal epithelial cysts. *J Am Soc Nephrol* **3**, 1841-1857 (1993).
90. Murcia, N.S., Sweeney, J.W.E. & Avner, E.D. New insights into the molecular pathophysiology of polycystic kidney disease. *Kidney Int* **55**, 1187-1197 (1999).
91. Nadasdy, T. et al. Proliferative activity of cyst epithelium in human renal cystic diseases. *J Am Soc Nephrol* **5**, 1462-1468 (1995).
92. Lanoix, J., D'Agati, V., Szabolcs, M. & Trudel, M. Dysregulation of cellular proliferation and apoptosis mediates human autosomal dominant polycystic kidney disease (ADPKD). *Oncogene* **13**, 1153-60 (1996).
93. Boletta, A. et al. Polycystin-1, the gene product of PKD1, induces resistance to apoptosis and spontaneous tubulogenesis in MDCK cells. *Mol Cell* **6**, 1267-73 (2000).
94. Ramasubbu, K., Gretz, N. & Bachmann, S. Increased epithelial cell proliferation and abnormal extracellular matrix in rat polycystic kidney disease. *J Am Soc Nephrol* **9**, 937-945 (1998).
95. Wilson, P.D. Cell biology of human autosomal dominant polycystic kidney disease. *Semin Nephrol* **11**, 607-16 (1991).
96. Zhang, Q., Taulman, P.D. & Yoder, B.K. Cystic Kidney Diseases: All Roads Lead to the Cilium. *Physiology* **19**, 225-230 (2004).
97. Davenport, J.R. & Yoder, B.K. An incredible decade for the primary cilium: a look at a once-forgotten organelle. *Am J Physiol Renal Physiol* **289**, F1159-1169 (2005).
98. Torres, V.E. & Harris, P.C. Mechanisms of Disease: autosomal dominant and recessive polycystic kidney diseases. *Nat. Clin. Pract. Nephrol.* **2**, 40-55 (2006).
99. Du, J. & Wilson, P.D. Abnormal polarization of EGF receptors and autocrine stimulation of cyst epithelial growth in human ADPKD. *Am J Physiol* **269**, C487-95 (1995).
100. Avner, E.D. Epithelial polarity and differentiation in polycystic kidney disease. *J Cell Sci Suppl* **17**, 217-22 (1993).
101. Hanaoka, K., Devuyst, O., Schwiebert, E.M., Wilson, P.D. & Guggino, W.B. A role for CFTR in human autosomal dominant polycystic kidney disease. *Am J Physiol* **270**, C389-99 (1996).
102. Mangoo-Karim, R., Uchic, M., Lechene, C. & Grantham, J.J. Renal epithelial cyst formation and enlargement in vitro: dependence on cAMP. *Proc Natl Acad Sci U S A* **86**, 6007-11 (1989).
103. Germino, G.G. Linking cilia to Wnts. *Nat Genet* **37**, 455-7 (2005).
104. Simons, M. et al. Inversin, the gene product mutated in nephronophthisis type II, functions as a molecular switch between Wnt signaling pathways. *Nat Genet* **37**, 537-43 (2005).
105. Roitbak, T. et al. A polycystin-1 multiprotein complex is disrupted in polycystic kidney disease cells. *Mol Biol Cell* **15**, 1334-46 (2004).
106. Cuppage, F.E., Huseman, R.A., Chapman, A. & Grantham, J.J. Ultrastructure and function of cysts from human adult polycystic kidneys. *Kidney Int* **17**, 372-81 (1980).
107. Cowley, B.D., Jr. et al. Autosomal-dominant polycystic kidney disease in the rat. *Kidney Int* **43**, 522-34 (1993).

108. Obermuller, N., Morente, N., Kranzlin, B., Gretz, N. & Witzgall, R. A possible role for metalloproteinases in renal cyst development. *Am J Physiol Renal Physiol* **280**, F540-50 (2001).
109. Schaefer, L. et al. Tubular gelatinase A (MMP-2) and its tissue inhibitors in polycystic kidney disease in the Han:SPRD rat. *Kidney Int* **49**, 75-81 (1996).
110. Praetorius, H.A. & Spring, K.R. Bending the MDCK cell primary cilium increases intracellular calcium. *J Membr Biol* **184**, 71-9 (2001).
111. Praetorius, H.A., Frokiaer, J., Nielsen, S. & Spring, K.R. Bending the primary cilium opens Ca2+-sensitive intermediate-conductance K+ channels in MDCK cells. *J Membr Biol* **191**, 193-200 (2003).
112. Xu, C. et al. Human ADPKD primary cyst epithelial cells with a novel, single codon deletion in the PKD1 gene exhibit defective ciliary polycystin localization and loss of flow-induced Ca2+ signaling. *Am J Physiol Renal Physiol* **292**, F930-945 (2007).
113. Pazour, G.J. et al. Chlamydomonas IFT88 and its mouse homologue, polycystic kidney disease gene tg737, are required for assembly of cilia and flagella. *J Cell Biol* **151**, 709-18 (2000).
114. Hou, X. et al. Cystin, a novel cilia-associated protein, is disrupted in the cpk mouse model of polycystic kidney disease. *J Clin Invest* **109**, 533-40 (2002).
115. Otto, E.A. et al. Mutations in INVS encoding inversin cause nephronophthisis type 2, linking renal cystic disease to the function of primary cilia and left-right axis determination. *Nat Genet* **34**, 413 - 420 (2003).
116. Zhou, X.J. & Kukes, G. Pathogenesis of autosomal dominant polycystic kidney disease: role of apoptosis. *Diagn Mol Pathol* **7**, 65-8 (1998).
117. Woo, D. Apoptosis and loss of renal tissue in polycystic kidney diseases. *N Engl J Med* **333**, 18-25 (1995).
118. Lager, D.J., Qian, Q., Bengal, R.J., Ishibashi, M. & Torres, V.E. The pck rat: a new model that resembles human autosomal dominant polycystic kidney and liver disease. *Kidney Int* **59**, 126-36 (2001).
119. Trudel, M., Barisoni, L., Lanoix, J. & D'Agati, V. Polycystic kidney disease in SBM transgenic mice: role of c-myc in disease induction and progression. *Am J Pathol* **152**, 219-29 (1998).
120. Moser, M. et al. Enhanced apoptotic cell death of renal epithelial cells in mice lacking transcription factor AP-2beta. *Genes Dev* **11**, 1938-48 (1997).
121. Veis, D.J., Sorenson, C.M., Shutter, J.R. & Korsmeyer, S.J. Bcl-2-deficient mice demonstrate fulminant lymphoid apoptosis, polycystic kidneys, and hypopigmented hair. *Cell* **75**, 229-240 (1993).
122. Ecder, T. et al. Caspases, Bcl-2 proteins and apoptosis in autosomal-dominant polycystic kidney disease. *Kidney Int* **61**, 1220-30 (2002).
123. Bukanov, N.O., Smith, L.A., Klinger, K.W., Ledbetter, S.R. & Ibraghimov-Beskrovnaya, O. Long-lasting arrest of murine polycystic kidney disease with CDK inhibitor roscovitine. *Nature* **444**, 949-52 (2006).
124. Chang, M.Y. et al. Haploinsufficiency of Pkd2 is associated with increased tubular cell proliferation and interstitial fibrosis in two murine Pkd2 models. *Nephrol. Dial. Transplant.* **21**, 2078-2084 (2006).
125. Dang, C.V. et al. Function of the c-Myc Oncogenic Transcription Factor. *Experimental Cell Research* **253**, 63-77 (1999).
126. Cowley, B.D., Jr., Smardo, F.L., Jr., Grantham, J.J. & Calvet, J.P. Elevated c-myc protooncogene expression in autosomal recessive polycystic kidney disease. *Proc Natl Acad Sci U S A* **84**, 8394-8 (1987).

127. Ricker, J.L., Mata, J.E., Iversen, P.L. & Gattone, V.H., II. c-myc antisense oligonucleotide treatment ameliorates murine ARPKD. *Kidney Int* **61**, S125-S131 (2002).
128. Stephens, A.C. Technology evaluation: AVI-4126, AVI BioPharma. *Curr Opin Mol Ther* **6**, 551-8 (2004).
129. Cowley, B.D., Jr., Chadwick, L.J., Grantham, J.J. & Calvet, J.P. Elevated proto-oncogene expression in polycystic kidneys of the C57BL/6J (cpk) mouse. *J Am Soc Nephrol* **1**, 1048-1053 (1991).
130. Harding, M.A., Gattone, V.H., 2nd, Grantham, J.J. & Calvet, J.P. Localization of overexpressed c-myc mRNA in polycystic kidneys of the cpk mouse. *Kidney Int* **41**, 317-25 (1992).
131. Trudel, M., D'Agati, V. & Costantini, F. C-myc as an inducer of polycystic kidney disease in transgenic mice. *Kidney Int* **39**, 665-71 (1991).
132. Trudel, M. et al. C-myc-induced apoptosis in polycystic kidney disease is Bcl-2 and p53 independent. *J Exp Med* **186**, 1873-84 (1997).
133. Schaffner, D.L. et al. Targeting of the rasT24 oncogene to the proximal convoluted tubules in transgenic mice results in hyperplasia and polycystic kidneys. *Am J Pathol* **142**, 1051-60 (1993).
134. Kelley, K.A., Agarwal, N., Reeders, S. & Herrup, K. Renal cyst formation and multifocal neoplasia in transgenic mice carrying the simian virus 40 early region. *J Am Soc Nephrol* **2**, 84-97 (1991).
135. Stocklin, E., Botteri, F. & Groner, B. An activated allele of the c-erbB-2 oncogene impairs kidney and lung function and causes early death of transgenic mice. *J Cell Biol* **122**, 199-208 (1993).
136. Lowden, D.A. et al. Renal cysts in transgenic mice expressing transforming growth factor-alpha. *J Lab Clin Med* **124**, 386-94 (1994).
137. Takayama, H., LaRochelle, W.J., Sabnis, S.G., Otsuka, T. & Merlino, G. Renal tubular hyperplasia, polycystic disease, and glomerulosclerosis in transgenic mice overexpressing hepatocyte growth factor/scatter factor. *Lab Invest* **77**, 131-8 (1997).
138. Yamaguchi, T. et al. Cyclic AMP activates B-Raf and ERK in cyst epithelial cells from autosomal-dominant polycystic kidneys. *Kidney Int* **63**, 1983-94 (2003).
139. Torres, V.E. & Harris, P.C. Polycystic kidney disease: genes, proteins, animal models, disease mechanisms and therapeutic opportunities. *J Intern Med* **261**, 17-31 (2007).
140. Cowley B D, Jr. Calcium, cyclic AMP, and MAP kinases: Dysregulation in polycystic kidney disease. *Kidney Int* **73**, 251-253 (2008).
141. Yamaguchi, T. et al. Calcium Restriction Allows cAMP Activation of the B-Raf/ERK Pathway, Switching Cells to a cAMP-dependent Growth-stimulated Phenotype. *J. Biol. Chem.* **279**, 40419-40430 (2004).
142. Kim, E. et al. The polycystic kidney disease 1 gene product modulates Wnt signaling. *J Biol Chem* **274**, 4947-53 (1999).
143. Bhunia, A.K. et al. PKD1 induces p21(waf1) and regulation of the cell cycle via direct activation of the JAK-STAT signaling pathway in a process requiring PKD2. *Cell* **109**, 157-68 (2002).
144. Arnould, T. et al. The Polycystic Kidney Disease 1 Gene Product Mediates Protein Kinase C alpha -dependent and c-Jun N-terminal Kinase-dependent Activation of the Transcription Factor AP-1. *J. Biol. Chem.* **273**, 6013-6018 (1998).
145. Delmas, P. et al. Constitutive Activation of G-proteins by Polycystin-1 Is Antagonized by Polycystin-2. *J. Biol. Chem.* **277**, 11276-11283 (2002).
146. Kim, H., Bae, Y., Jeong, W., Ahn, C. & Kang, S. Depletion of PKD1 by an antisense oligodeoxynucleotide induces premature G1//S-phase transition. *Eur J Hum Genet* **12**, 433-440 (2004).

147. Li, X. et al. Polycystin-1 and polycystin-2 regulate the cell cycle through the helix-loop-helix inhibitor Id2. *Nat Cell Biol* **7**, 1202-12 (2005).
148. Grimm, D.H. et al. Polycystin-2 Regulates Proliferation and Branching Morphogenesis in Kidney Epithelial Cells. *J. Biol. Chem.* **281**, 137-144 (2006).
149. Park, J.-Y. et al. p21 is decreased in polycystic kidney disease and leads to increased epithelial cell cycle progression: roscovitine augments p21 levels. *BMC Nephrology* **8**, 12 (2007).
150. Chen, W.C., Tzeng, Y.S. & Li, H. Gene expression in early and progression phases of autosomal dominant polycystic kidney disease. *BMC Res Notes* **1**, 131 (2008).
151. Piontek, K., Menezes, L.F., Garcia-Gonzalez, M.A., Huso, D.L. & Germino, G.G. A critical developmental switch defines the kinetics of kidney cyst formation after loss of Pkd1. *Nat Med* **13**, 1490-1495 (2007).
152. Guay-Woodford, L.M. Murine models of polycystic kidney disease: molecular and therapeutic insights. *Am J Physiol Renal Physiol* **285**, F1034-49 (2003).
153. Wilson, P.D. Mouse models of polycystic kidney disease. *Curr Top Dev Biol* **84**, 311-50 (2008).
154. Preminger, G.M. et al. Murine congenital polycystic kidney disease: a model for studying development of cystic disease. *J Urol* **127**, 556-60 (1982).
155. Nauta, J., Ozawa, Y., Sweeney, W.E., Jr., Rutledge, J.C. & Avner, E.D. Renal and biliary abnormalities in a new murine model of autosomal recessive polycystic kidney disease. *Pediatr Nephrol* **7**, 163-72 (1993).
156. Flaherty, L., Bryda, E.C., Collins, D., Rudofsky, U. & Montogomery, J.C. New mouse model for polycystic kidney disease with both recessive and dominant gene effects. *Kidney Int* **47**, 552-8 (1995).
157. Yoder, B.K. et al. Differential rescue of the renal and hepatic disease in an autosomal recessive polycystic kidney disease mouse mutant. A new model to study the liver lesion. *Am J Pathol* **150**, 2231-41 (1997).
158. Mochizuki, T. et al. Cloning of inv, a gene that controls left/right asymmetry and kidney development. *Nature* **395**, 177-81 (1998).
159. Morgan, D. et al. Inversin, a novel gene in the vertebrate left-right axis pathway, is partially deleted in the inv mouse. *Nat Genet* **20**, 149-56 (1998).
160. Takahashi, H. et al. A new mouse model of genetically transmitted polycystic kidney disease. *J Urol* **135**, 1280-3 (1986).
161. Atala, A., Freeman, M.R., Mandell, J. & Beier, D.R. Juvenile cystic kidneys (jck): a new mouse mutation which causes polycystic kidneys. *Kidney Int* **43**, 1081-5 (1993).
162. Janaswami, P.M. et al. Identification and genetic mapping of a new polycystic kidney disease on mouse chromosome 8. *Genomics* **40**, 101-7 (1997).
163. Schafer, K. et al. Characterization of the Han:SPRD rat model for hereditary polycystic kidney disease. *Kidney Int* **46**, 134-52 (1994).
164. Nauta, J. et al. New Rat Model that Phenotypically Resembles Autosomal Recessive Polycystic Kidney Disease. *J Am Soc Nephrol* **11**, 2272-2284 (2000).
165. Sweeney, W.E., Chen, Y., Nakanishi, K., Frost, P. & Avner, E.D. Treatment of polycystic kidney disease with a novel tyrosine kinase inhibitor. *Kidney Int* **57**, 33-40 (2000).
166. Torres, V.E. et al. EGF receptor tyrosine kinase inhibition attenuates the development of PKD in Han:SPRD rats. *Kidney Int* **64**, 1573-9 (2003).
167. Gattone, V.H., 2nd, Wang, X., Harris, P.C. & Torres, V.E. Inhibition of renal cystic disease development and progression by a vasopressin V2 receptor antagonist. *Nat Med* **9**, 1323-6 (2003).

168. Wang, X., Gattone, V., 2nd, Harris, P.C. & Torres, V.E. Effectiveness of vasopressin V2 receptor antagonists OPC-31260 and OPC-41061 on polycystic kidney disease development in the PCK rat. *J Am Soc Nephrol* **16**, 846-51 (2005).
169. Albaqumi, M. et al. KCa3.1 potassium channels are critical for cAMP-dependent chloride secretion and cyst growth in autosomal-dominant polycystic kidney disease. *Kidney Int* (2008).
170. Yang, B., Sonawane, N.D., Zhao, D., Somlo, S. & Verkman, A.S. Small-molecule CFTR inhibitors slow cyst growth in polycystic kidney disease. *J Am Soc Nephrol* **19**, 1300-10 (2008).
171. Li, H., Findlay, I.A. & Sheppard, D.N. The relationship between cell proliferation, Cl- secretion, and renal cyst growth: a study using CFTR inhibitors. *Kidney Int* **66**, 1926-38 (2004).
172. Zafar, I. et al. Effect of statin and angiotensin-converting enzyme inhibition on structural and hemodynamic alterations in autosomal dominant polycystic kidney disease model. *Am J Physiol Renal Physiol* **293**, F854-9 (2007).
173. Ruggenenti, P. et al. Safety and efficacy of long-acting somatostatin treatment in autosomal-dominant polycystic kidney disease. *Kidney Int* **68**, 206-16 (2005).
174. Tao, Y. et al. Caspase inhibition reduces tubular apoptosis and proliferation and slows disease progression in polycystic kidney disease. *Proceedings of the National Academy of Sciences* **102**, 6954-6959 (2005).
175. Li, X. et al. A tumor necrosis factor-[alpha]-mediated pathway promoting autosomal dominant polycystic kidney disease. *Nat Med* **14**, 863-868 (2008).
176. Tao, Y., Kim, J., Schrier, R.W. & Edelstein, C.L. Rapamycin markedly slows disease progression in a rat model of polycystic kidney disease. *J Am Soc Nephrol* **16**, 46-51 (2005).
177. Ma, R. et al. PKD2 Functions as an Epidermal Growth Factor-Activated Plasma Membrane Channel. *Mol. Cell. Biol.* **25**, 8285-8298 (2005).
178. Bihoreau, M.T. et al. Characterization of a major modifier locus for polycystic kidney disease (Modpkdr1) in the Han:SPRD(cy/+) rat in a region conserved with a mouse modifier locus for Alport syndrome. *Hum Mol Genet* **11**, 2165-73 (2002).
179. Gretz, N. et al. Gender-dependent disease severity in autosomal polycystic kidney disease of rats. *Kidney Int* **48**, 496-500 (1995).
180. Ohkawa, K. et al. Hepatitis C virus core functions as a suppressor of cyclin-dependent kinase-activating kinase and impairs cell cycle progression. *J Biol Chem* **279**, 11719-26 (2004).
181. Hsieh, W.P., Chu, T.M., Wolfinger, R.D. & Gibson, G. Mixed-model reanalysis of primate data suggests tissue and species biases in oligonucleotide-based gene expression profiles. *Genetics* **165**, 747-57 (2003).
182. Roy, J. SAS for mixed models. *J Biopharm Stat* **17**, 363-65 (2007).
183. Subramanian, A. et al. Gene set enrichment analysis: a knowledge-based approach for interpreting genome-wide expression profiles. *Proc Natl Acad Sci U S A* **102**, 15545-50 (2005).
184. Manoli, T. et al. Group testing for pathway analysis improves comparability of different microarray datasets. *Bioinformatics* **22**, 2500-6 (2006).
185. Wilson, P.D., Du, J. & Norman, J.T. Autocrine, endocrine and paracrine regulation of growth abnormalities in autosomal dominant polycystic kidney disease. *Eur J Cell Biol* **61**, 131-8 (1993).
186. Chen, X.Z. et al. Transport function of the naturally occurring pathogenic polycystin-2 mutant, R742X. *Biochem Biophys Res Commun* **282**, 1251-6 (2001).

187. Shaw, G., Morse, S., Ararat, M. & Graham, F.L. Preferential transformation of human neuronal cells by human adenoviruses and the origin of HEK 293 cells. *FASEB J* **16**, 869-71 (2002).
188. Grantham, J.J. Polycystic kidney disease: neoplasia in disguise. *Am J Kidney Dis* **15**, 110-6 (1990).
189. Bravo, R. & Macdonald-Bravo, H. Existence of two populations of cyclin/proliferating cell nuclear antigen during the cell cycle: association with DNA replication sites. *J. Cell Biol.* **105**, 1549-1554 (1987).
190. Rothschild, G., Zhao, X., Iavarone, A. & Lasorella, A. E Proteins and Id2 converge on p57Kip2 to regulate cell cycle in neural cells. *Mol Cell Biol* **26**, 4351-61 (2006).
191. Shin, J.Y., Kim, H.S., Park, J., Park, J.B. & Lee, J.Y. Mechanism for inactivation of the KIP family cyclin-dependent kinase inhibitor genes in gastric cancer cells. *Cancer Res* **60**, 262-5 (2000).
192. Nishimori, S. et al. Smad-mediated transcription is required for transforming growth factor-beta 1-induced p57(Kip2) proteolysis in osteoblastic cells. *J Biol Chem* **276**, 10700-5 (2001).
193. Grandjean, V., Smith, J., Schofield, P.N. & Ferguson-Smith, A.C. Increased IGF-II protein affects p57kip2 expression in vivo and in vitro: implications for Beckwith-Wiedemann syndrome. *Proc Natl Acad Sci U S A* **97**, 5279-84 (2000).
194. Patel, V. et al. Acute kidney injury and aberrant planar cell polarity induce cyst formation in mice lacking renal cilia. *Hum Mol Genet* **17**, 1578-90 (2008).
195. McAteer, J.A., Evan, A.P. & Gardner, K.D. Morphogenetic clonal growth of kidney epithelial cell line MDCK. *Anat Rec* **217**, 229-39 (1987).
196. Saadi-Kheddouci, S. et al. Early development of polycystic kidney disease in transgenic mice expressing an activated mutant of the beta-catenin gene. *Oncogene* **20**, 5972-81 (2001).
197. Waanders, E., Van Krieken, J.H., Lameris, A.L. & Drenth, J.P. Disrupted cell adhesion but not proliferation mediates cyst formation in polycystic liver disease. *Mod Pathol* **21**, 1293-302 (2008).

Panayiota Kyriakidou

APPENDIX

	Gene		neglogp Mut/SD T0	fold Mut/SD		neglogp Mut/SD T6	fold Mut/SD		neglogp Mut/SD T24	fold Mut/SD
1	NLN		0,150885927	0,0464844		0,351251873	0,0942708		5,661345069	0,60664063
2	LNPEP		2,080108032	-0,0963697		0,106140746	0,0099981		0,14185505	0,01295883
3	AGT		0,175300125	-0,0406250		0,798090505	0,1336914		0,752973881	-0,12828776
4	AGTR1A		0,023601315	0,0104906		0,253698672	0,0927586		2,097692634	-0,42154948
5	ACE		0,784058668	0,1028646		2,026840743	0,1938657		4,620189321	0,32194010
6	MME		0,179076241	-0,0523593		1,417878439	-0,2496449		2,747416611	-0,37926136
7	REN1		0,258819913	0,2166667		0,32506807	-0,2608073		3,182477042	-1,26265811
8	MAS1		0,188126973	-0,0304806		0,241263737	0,0376125		0,968210232	-0,10795455
9	CMA1	*	7,142448361	-0,3340929		0,442158156	-0,0537109		0,962373816	-0,09458189
10	CPA3		1,790241126	-0,1924552		1,384705282	0,1629051		0,648129728	-0,09639034
11	THOP1		0,490948314	0,0558594		3,726512304	-0,2156250		0,357015914	0,04365234
12	AGTR1B		1,206995957	-0,3728693		0,101962201	-0,0527640		0,290275384	-0,13029711
13	ANPEP		0,359375763	0,1457741		0,245620915	-0,1070668	*	9,646845174	-1,26554451

Table 6: List of the renin angiotensin system genes and the results obtained after statistical evaluation of the genome-wide expression analysis of whole kidney homogenates from 0, 6 and 24 day old transgenic rats PKD2 (1-703) (Mut) compared to TECs isolated from SD rats (SD).

Data were considered significant if the negative log of the p-value of Mut/SD was greater than 5.83. '*' denotes statistical significance after Bonferroni correction.

	Gene		neglogp Mut/SD T0	fold Mut/SD		neglogp Mut/SD T6	fold Mut/SD		neglogp Mut/SD T24	fold Mut/SD
1	VEGFC		0,980765522	-0,1464844		0,252633319	-0,0525391		3,202353175	0,3132161
2	ITGA6		0,93532046	-0,1448161		0,401730571	0,0778402		3,914900634	0,3635254
3	ZYX		0,016892425	-0,0092330		0,025354181	-0,0137311		5,485452715	0,9296303
4	SHC3		0,510330843	-0,0944372		1,869587403	0,2313730		0,42551195	-0,0822121
5	MAPK8		3,28260558	-0,1062973		0,078972877	0,0064290		0,065863146	-0,0053859
6	MAPK1		0,278007726	0,0508174		2,879831529	0,2629485		3,354361086	0,2887370
7	VWF		0,35308883	-0,0686035		0,624815405	-0,1059977		1,404160503	0,1858317
8	PPP1R12A		1,323980387	0,1046730		0,49823191	-0,0527523		0,329640149	0,0381944

Panagiota Potsiou

9	LAMC1		0,198096363	0,0505332		0,068411	-0,0194994		3,056844192	0,3559253
10	MYLK2		0,19671721	-0,0347900		0,335145396	0,0540161		1,177078367	-0,1351929
11	LAMA5		0,128465027	0,0130329		0,460523646	0,0375916		0,107342943	0,0110918
12	MAP2K1		0,096443175	-0,0179332		0,300453402	0,0481066	*	6,691150146	0,3856037
13	PIK3CA		0,355668949	0,0412760		3,647181057	-0,1986793		2,896289983	-0,1733352
14	ILK		0,262663461	0,0263376		0,378457451	-0,0353338		4,447791332	0,1849550
15	ACTN3		0,14470194	-0,0230824		2,969706474	0,2112926		0,886369768	-0,0966205
16	RAP1B		0,028938618	0,0083333		0,366594328	0,0815104		5,430112608	0,5170573
17	LAMC2		0,090971228	0,0872758		0,013369879	0,0138708	*	6,709870166	1,9458966
18	AKT1		0,313378976	-0,0790654		0,307772515	-0,0780037		4,281601863	0,4729456
19	BCL2		0,125617809	-0,0165128		1,023150579	0,0864998		0,004619513	-0,0006894
20	ERBB2		0,498574245	-0,0712891		2,743076087	-0,2253196		3,170701456	-0,2461529
21	HGF		0,477304334	-0,0714337		1,113178668	0,1310402		0,603648513	0,0851418
22	IBSP		0,123832787	0,0207357		0,47644883	0,0634766		0,860440284	0,0976563
23	IGF1		0,119932149	-0,0400391		0,396177456	-0,1095434		1,761143654	-0,3130208
24	ITGB1		0,146638826	0,0461648		0,580726613	0,1412718	*	6,243567687	0,6528764
25	JUN		0,022732108	-0,0098544		0,284767832	-0,0993826	*	6,071685313	0,7673356
26	MET		0,168504381	0,0409831		2,192317789	0,2726237	*	9,419226845	0,6607096
27	PDGFRB		0,083555918	-0,0135324		0,578148072	-0,0683904		1,404416595	0,1264416
28	PPP1CA		0,073358964	-0,0096354		0,137788267	0,0172251		3,548018528	0,1824219
29	PPP1CC		0,989751256	-0,0891927		3,839576132	-0,2153383		1,401510072	-0,1127116
30	PRKCA		0,018326332	-0,0027817		0,578668307	0,0601030		0,11481118	0,0158617
31	PRKCC		0,192108401	0,0367188		1,027600425	0,1331055		0,716910323	-0,1034831
32	RAF1		0,476392382	0,0382487		1,664851708	0,0927058		0,452637769	0,0367839
33	RELN		0,281407993	-0,0428060		0,282227523	-0,0429077		2,26309733	0,1876221
34	PRKCB1		0,00336126	-0,0011489		0,720165501	-0,1559053	*	6,331929515	0,6135302
35	FYN		0,150338643	-0,0194336	*	9,699731232	-0,3542294		0,585538711	0,0584635
36	AKT2		1,324630599	-0,1190405		0,042931719	0,0070844		2,882343257	0,1944361
37	PDGFA		0,76491439	-0,1221029	*	6,857513934	-0,4913737		3,502079814	-0,3279297
38	PDGFRA		0,120550024	0,0408973		0,240150685	0,0743719		3,492458622	0,4859730
39	MAPK10		0,420141802	-0,0450846		0,040925808	0,0057943		0,290363119	-0,0336263
40	EGF		0,558205346	0,5370260		0,145846761	-0,1796875		3,502986015	-1,8065223
41	SPP1		1,07736006	0,2298177	*	12,64657969	1,4967448	*	13,47692415	1,6037326

42	CAV1		0,273842754	0,1160156		0,880046783	0,2808268		1,754626873	0,4448568
43	COL2A1		1,08819726	-0,1233259	*	7,734522385	-0,4283854		2,932908253	-0,2342820
44	BCAR1		0,638387761	-0,0600734		3,644120485	0,1884830		0,155363657	-0,0192945
45	PIK3R1		2,311501627	-0,4911386		0,130404705	0,0569300		1,091350265	0,3016855
46	ROCK2		0,003903984	-0,0006045		0,171833966	-0,0227400		3,838693142	0,2122861
47	TNR		0,447223524	0,0582090		0,386285521	0,0519650		0,528734029	-0,0660807
48	PPP1CB		0,166730731	-0,0319010		0,519361963	0,0803385		0,5005157	0,0781250
49	PTK2		0,043184894	0,0038767		1,401665858	-0,0680470		1,949573343	-0,0834517
50	COL11A1		0,116510678	-0,0352124		0,223410495	-0,0620622		4,946541746	0,5220551
51	FN1		0,01681382	-0,0092330		0,206316923	-0,0957115	*	6,115653445	0,9944957
52	ITGB7		1,364711939	-0,0979226		1,449978363	0,1018880		0,768415238	0,0661695
53	IGF1R		0,227140417	0,0229167		4,828379117	-0,1924368		1,97596125	0,1106771
54	ITGB4		0,172827382	0,0810547		0,110327642	0,0544922		5,60710408	0,9352444
55	CRKL		0,071462286	0,0089410		3,102148945	0,1587240	*	6,710624396	0,2512864
56	COL4A1		0,069098347	-0,0260417		0,09962229	0,0364946	*	6,495446098	0,7327474
57	CAPN2		0,665985984	0,0729980		2,476665643	-0,1756999		0,894196875	0,0900065
58	CAV3		1,102935014	-0,0903764		0,888709349	0,0779474		0,031305119	-0,0044685
59	VTN		0,0113143	-0,0032914		0,098802883	0,0263310		1,795994285	-0,2486256
60	CHAD		0,834300199	-0,1027669		2,548268339	0,2136719		0,515347784	-0,0724284
61	THBS4		0,655483564	0,1127387		0,346695679	0,0693902		1,708966607	-0,2176649
62	THBS2		1,22560058	0,1787471		4,484226869	0,4041160		3,48761874	0,3468967
63	ACTC1		0,414021337	-0,0620847		1,981188897	0,1837509		1,758342324	0,1704943
64	COL1A1		0,070537857	0,0331948		0,061563179	0,0292165		4,659048269	0,7561157
65	AKT3		1,45090492	0,1214658		0,097184628	-0,0145089		2,79714711	0,1848028
66	COL11A2		0,152436844	-0,0301288		0,353528045	-0,0608724		2,878593159	-0,2594763
67	PAK1		0,093675313	-0,0168383		0,274434104	0,0429096		3,787741374	0,2639678
68	PAK2		0,136271389	-0,0316569		2,395557655	0,2700081	*	6,256850668	0,4860026
69	PAK3		0,081182751	-0,0197266		0,628290413	0,1089518		1,269309251	-0,1777344
70	RAP1A		0,364046102	-0,0325087		1,009401684	-0,0687066		0,795378853	-0,0582465
71	PIK3R2		1,019784238	-0,0511556		2,11084018	-0,0819987		0,457063835	-0,0286947
72	ARHGAP5		1,012722036	0,2125947		1,620570098	-0,2903350		0,869974539	-0,1914358
73	COL4A4		0,169965682	0,0829486		0,178977132	0,0867365		2,533139703	-0,5983665
74	LAMB3		0,08594634	0,0688657		0,628875103	0,3612196		2,995995917	1,0177590

75	LAMA3		0,09941984	-0,0302734		0,649007861	0,1433377		0,388606993	0,0968967
76	ITGB6		4,655623937	0,3152018	*	22,50277445	0,8516940		5,337872792	0,3421875
77	TLN1		0,355880172	0,0572917		0,008223275	0,0017482		1,010977692	0,1235204
78	SOS1		1,839836353	0,0872053		0,85192224	-0,0525724		0,259819684	-0,0213085
79	ITGA5		0,185528225	0,0293265		1,408525475	0,1351503		0,594772127	0,0743371
80	LAMA1		0,09593866	0,0258198		3,669225253	-0,3912101		0,951301111	0,1636068
81	FIGF		0,040701064	-0,0115234		0,967603759	0,1656576		3,111137	0,3512695
82	PXN		0,078033515	-0,0178741		0,169965976	-0,0360152		1,946700341	0,2201705
83	COL6A2		0,060802484	-0,0185004		0,499488032	-0,1127930		4,928345592	0,5057509
84	CAV2		0,17765883	-0,0321960		2,548615447	0,2224121		0,020173091	-0,0042216
85	RAC1		0,12980553	-0,0329590		1,204297351	0,1880876	*	7,280722029	0,5801595
86	RAC2		0,307594381	-0,0743490		2,574160099	0,3300130	*	9,660588382	0,7350586
87	PTEN		0,629053349	0,0767299		0,401813769	-0,0546875		5,764962871	0,3261719
88	MAPK9		0,464628624	0,0563151		6,448124964	0,3138909		0,489533399	-0,0585938
89	MAPK3		0,422531009	-0,0458984		0,192778784	-0,0241970		1,371596883	0,1066623
90	CRK		0,23272584	0,0327000		3,004485564	0,2004025	*	15,32834539	0,5374645
91	FLT1		0,598339409	-0,0496807		1,52293805	0,0943855		0,003483903	-0,0004340
92	CCND1		0,372874754	0,0516680	*	5,965120906	-0,3191402	*	10,39477695	0,4368374
93	BIRC2		3,490097527	0,2148988		3,798998319	0,2244141		2,101420558	0,1564669
94	COL5A3		0,03138823	0,0100320		0,010041543	0,0032848		0,917901952	0,1785038
95	PIK3R3		0,891497012	-0,1176990		1,389476457	0,1590867		2,70288431	0,2437686
96	ACTN4		0,393720693	-0,0676491		0,526716371	0,0848589		2,956371907	0,2695946
97	BIRC4		1,707077574	-0,2729640		0,081797572	0,0251967		3,273710263	0,4092093
98	CDC42		0,734039136	0,0778646		0,095656086	0,0146484	*	6,31131146	0,3069661
99	BAD		0,205970528	0,0289418		0,376079687	0,0473485		2,864621066	0,1918547
100	PDGFD		0,798166082	0,1134115		0,010564451	0,0024089	*	9,680723223	0,5944010
101	BIRC3		0,118181932	0,0172201		2,739945352	0,1799805	*	13,99256293	0,4965477
102	PDGFC		0,297083508	-0,0705078		0,139493487	0,0371094		0,415655041	0,0920247
103	ITGA7		0,129002413	-0,0187603		0,383276882	0,0467893		5,17463841	-0,2619929
104	GRB2		0,040235413	0,0045030		0,605675352	0,0469021	*	7,77527715	0,2387424
105	PDPK1		0,177018684	0,0403350		2,609957725	-0,2861328		0,128626164	-0,0304806
106	ROCK1		0,531251312	0,0678385		2,186742249	0,1802083		4,32151277	0,2788411
107	ACTB		0,131560667	-0,0365710		0,103796556	0,0295596	*	8,852253377	0,6707841

108	VEGFA		0,203583522	-0,0748698		0,214071918	0,0781250		1,858977971	-0,3811553
109	SRC		0,005861807	0,0011268		0,136445951	0,0231120		0,919194692	0,1044421
110	GSK3B		0,076868602	0,0155888		1,430278232	-0,1599754		0,124547797	-0,0241970
111	COL3A1		0,159529166	0,0662109		0,283258405	-0,1076019		4,033301465	0,6713542
112	COL1A2		0,243150523	0,0994792		0,134174252	0,0596354	*	6,323800408	0,9228966
113	CTNNB1		0,019674384	0,0049293		1,023912632	0,1493676		5,345275531	0,4290365
114	COL5A2		0,128079234	0,0602214		0,570319088	-0,2047798		4,603783673	0,8029107
115	COL5A1		0,231688305	0,0868490		0,065142678	0,0279948		5,296270499	0,7876302
116	PGF		0,053391528	0,0107251		0,048369709	-0,0097656		0,071728163	0,0141516

Table 7: List of the focal adhesion pathway genes and the results obtained after statistical evaluation of the genome-wide expression analysis of whole kidney homogenates from 0, 6 and 24 day old transgenic rats PKD2 (1-703) (Mut) compared to TECs isolated from SD rats (SD).

Data were considered significant if the negative log of the p-value of Mut/SD was greater than 5.83. '*' denotes statistical significance after Bonferroni correction.

Panayiota Koupepidou

	Gene		neglogp Mut/SD T0	fold Mut/SD		neglogp Mut/SD T6	fold Mut/SD		neglogp Mut/SD T24	fold Mut/SD
1	CSNK1A1		1,484090347	-0,1264468		3,734211455	-0,2279053		3,8480476	0,2296730
2	WNT2		0,101040475	-0,0117398		0,960049193	0,0714571		4,935326447	-0,1974651
3	WIF1		0,195531726	-0,0287346		3,656842478	-0,2298177		0,114274137	0,0179332
4	WNT7A		0,180176493	-0,0527344		0,552113364	0,1297348		0,841565307	0,1758700
5	WNT2B		0,091784218	-0,0197384		0,712404036	0,1066229		0,749195647	-0,1105291
6	CSNK2A1		2,243694913	0,2135608		0,24573667	-0,0438304		1,922804926	0,1939721
7	MAPK8		3,28260558	-0,1062973		0,078972877	0,0064290		0,065863146	-0,0053859
8	PPP2R2C		0,232426645	0,0372179		0,692574439	0,0872396		0,248360886	0,0393338
9	PPP2R1A		0,69509621	-0,0954034		0,371311697	0,0594554	*	6,007844632	0,3730660
10	WNT11		1,790743161	-0,1694623		1,380162094	-0,1433249		0,480021588	-0,0681870
11	SIAH1A		0,883603302	-0,0974195		3,928743885	-0,2529001		1,528172209	0,1407138
12	CAMK2G		0,056774132	-0,0078532		0,426362102	-0,0452881		0,591999125	-0,0580241
13	PPP3CC		0,81794728	0,0752279		0,070047401	0,0098307		0,327960738	-0,0378581
14	APC		0,491325988	-0,0490560		2,224355473	-0,1378581		1,128944071	-0,0888346
15	CAMK2B		0,572172188	-0,0718678		1,514884826	0,1411675		4,474599105	-0,2771629
16	CAMK2D		0,152799969	-0,0135393		0,384400476	-0,0291401	*	12,81051821	0,2740025
17	JUN		0,022732108	-0,0098544		0,284767832	-0,0993826	*	6,071685313	0,7673356
18	MYC		0,265898367	0,2084310		0,016957528	-0,0164063	*	6,074967236	1,7522461
19	PPP2R2D		0,761219847	0,0850694		1,652222446	-0,1464844		0,962965612	0,1006944
20	PLCB1		0,224098992	0,0852273		0,486768568	-0,1585094		2,670122164	-0,5015980
21	PPP2CB		0,290593014	-0,0371094		1,208539665	-0,1067373		3,996899932	0,2250829
22	PPP3CA		2,005752872	-0,1109138	*	6,20644315	-0,2210977		1,915033414	0,1077178
23	PPP3CB		0,057121204	0,0110270		1,749307059	-0,1717264		0,709283122	0,0924072
24	PRKCA		0,018326332	-0,0027817		0,578668307	0,0601030		0,11481118	0,0158617
25	PRKCC		0,192108401	0,0367188		1,027600425	0,1331055		0,716910323	-0,1034831
26	PRKCB1		0,00336126	-0,0011489		0,720165501	-0,1559053	*	6,331929515	0,6135302
27	PLCB4		0,020326106	-0,0028987		3,130918802	-0,1720300		1,76004076	-0,1207527
28	MAPK10		0,420141802	-0,0450846		0,040925808	0,0057943		0,290363119	-0,0336263
29	MMP7		0,257387431	-0,1386068		0,799896253	0,3302083		1,013494739	0,3897559
30	CAMK2A		0,578486798	-0,0609131		1,250387051	0,1046549		0,20574061	-0,0267741
31	FOSL1		0,287309236	-0,0558712		2,255588568	0,2411518		0,286375564	0,0557232

Pour information supplémentaire

32	ROCK2		0,003903984	-0,0006045		0,171833966	-0,0227400		3,838693142	0,2122861
33	SMAD3		1,207491035	-0,1312145		1,249153382	0,1346199	*	5,823774162	0,3508237
34	PPARD		0,438867241	-0,0698686		0,116395305	0,0229936		2,807145586	-0,2468336
35	WNT5B		1,558858611	-0,0951705		0,993355774	-0,0705197		0,315820729	-0,0300959
36	CACYBP		1,454031329	-0,1443359		2,012991682	-0,1779856		1,170857502	0,1253942
37	AXIN2		0,110592651	-0,0360736		3,237070711	-0,4422940		0,503923761	0,1275154
38	PSEN1	*	7,301316523	0,2889083		3,048574733	0,1733484		1,200423301	0,0964056
39	PLCB3		0,37814356	-0,0926649		1,708371692	0,2773438		0,259734946	0,0683594
40	PRKACB		1,30222251	0,0784801		0,176803381	-0,0173112		1,730018939	0,0944010
41	SMAD2		0,075688746	0,0149148		0,168445849	0,0307769	*	6,203693299	0,3832639
42	CTBP1		0,008421309	-0,0008286	*	6,662879101	-0,1883339		1,869791587	0,0858191
43	PPP3R1		0,582850939	0,0610894		0,357076456	0,0419922		4,46282018	0,2320240
44	PPP3R2		1,180706633	-0,1046402		0,888638101	0,0862038		0,062707436	-0,0095881
45	RBX1		1,073560898	-0,1653646		2,426210761	-0,2818237		0,395751777	0,0799154
46	NFATC4		0,092966953	-0,0192308		0,604852547	0,0911458		0,417157666	-0,0688852
47	SFRP2		0,277390716	-0,1947206		0,035194139	0,0301403		3,14412895	-1,0522964
48	PRICKLE1		0,427240326	-0,0953776		0,463848308	-0,1015796		3,448769366	0,3868044
49	PPP2R1B		0,867899626	0,0669981		1,351455404	0,0914809		2,345933209	-0,1286103
50	FZD5		0,2360901	0,0257161		0,565846729	0,0512370		0,129096566	-0,0152669
51	BTRC		0,397138478	-0,0445602		0,442743535	-0,0489627		0,681588998	0,0675293
52	RAC1		0,12980553	-0,0329590		1,204297351	0,1880876	*	7,280722029	0,5801595
53	RAC2		0,307594381	-0,0743490		2,574160099	0,3300130	*	9,660588382	0,7350586
54	WNT16		0,116080701	0,0155362		2,575226919	0,1585582		2,101618609	-0,1397372
55	PRKX		0,463823285	0,0538249		0,670416497	0,0707357		5,048306754	0,2561849
56	SMAD4		0,006899696	-0,0012370		1,54336883	-0,1377387		3,649817377	0,2344184
57	MAPK9		0,464628624	0,0563151	*	6,448124964	0,3138909		0,489533399	-0,0585938
58	CREBBP		1,145873783	0,0906692		1,584346083	-0,1123009		1,213439344	-0,0941918
59	CSNK1E		0,353055038	-0,0475260		0,029753867	0,0051491		4,00622034	0,2486387
60	FZD1		1,216851716	0,1079545		0,270645282	0,0355280		0,77475046	0,0791607
61	CCND1		0,372874754	0,0516680	*	5,965120906	-0,3191402	*	10,39477695	0,4368374
62	PPP2R2B		0,301485635	0,0695431		0,530837012	-0,1080433		4,184197234	-0,4206913
63	FZD2		0,031377599	-0,0080078		0,741813302	-0,1232093		4,345175399	0,3840169
64	FZD4		0,383843605	-0,0902580		0,185647707	0,0496863		1,878280575	-0,2754794

65	WNT5A		0,013875459	-0,0083748		0,199433628	-0,1018759		0,00125677	0,0007694
66	CHD8		0,556514451	0,0426432		3,028088491	-0,1310136		0,3817734	-0,0321432
67	RUVBL1		0,095589846	-0,0218099		1,420282377	-0,1847331		3,813739614	0,3546549
68	SENP2		0,147803771	-0,0248210		0,554832007	0,0730794		2,812116159	0,2233887
69	AXIN1		0,085946854	-0,0092921		3,281791062	-0,1466787		1,65725923	0,0944898
70	CSNK2B		0,198177192	-0,0367188		0,819432274	-0,1108073		3,044410137	0,2607042
71	CTBP2		0,917210318	-0,0700955	*	6,041677856	-0,2370877		0,065534491	-0,0079210
72	ROCK1		0,531251312	0,0678385		2,186742249	0,1802083		4,32151277	0,2788411
73	DVL1		0,413916854	0,0660482		0,036659379	0,0077311		2,12230124	-0,2043783
74	CXXC4		0,355907206	-0,0463216		0,207198809	0,0297201		0,52245596	-0,0622721
75	GSK3B		0,076868602	0,0155888		1,430278232	-0,1599754		0,124547797	-0,0241970
76	CTNNB1		0,019674384	0,0049293		1,023912632	0,1493676		5,345275531	0,4290365
77	SFRP1		0,150516513	-0,0558860		1,309160187	-0,2934718		4,482149879	0,6256794
78	WNT4		0,648204596	-0,3177971		0,924668732	-0,4087950		1,136471274	0,4705256
79	SFRP4		0,047729272	-0,0138198		1,029090187	0,1779119		0,016413497	-0,0049124

Table 8: List of the Wnt signaling pathway genes and the results obtained after statistical evaluation of the genome-wide expression analysis of whole kidney homogenates from 0, 6 and 24 day old transgenic rats PKD2 (1-703) (Mut) compared to TECs isolated from SD rats (SD).

Data were considered significant if the negative log of the p-value of Mut/SD was greater than 5.83. '*' denotes statistical significance after Bonferroni correction.

	Gene		**neglogp Mut/SD T0**	**fold Mut/SD**		**neglogp Mut/SD T6**	**fold Mut/SD**		**neglogp Mut/SD T24**	**fold Mut/SD**
1	GSTO1		0,017555616	0,0050686		0,309035355	0,0703470		4,559294663	-0,4387429
2	OPLAH		0,364872164	0,0752279		0,70528024	-0,1236003		2,146028582	-0,2601563
3	GSR		0,733024373	-0,1280020		0,647494173	0,1170428		0,077816255	-0,0199291
4	GGTL3		0,71680898	-0,0871419		2,110916361	0,1794271		0,638410363	0,0801432
5	MGST1		0,3573793	0,0782434	*	7,410557147	0,5837175		0,006131538	-0,0017756
6	G6PDX		0,429049732	-0,1001302		0,008754768	-0,0027995		1,50218162	0,2449219
7	GSTA3		0,019182889	-0,0135239		0,581071053	0,2802734		5,617359218	-1,2166193
8	GSTM1		0,032582674	0,0253255		0,006430763	0,0051432		4,307734832	1,1645508
9	GSTM2		0,012718438	-0,0041775		0,066731348	-0,0207248		1,026496973	0,1949327
10	GSTT1		0,131480759	-0,0241247		0,873634572	0,1089048	*	6,785518213	-0,3987269
11	GCLC		1,047999759	0,3068774		0,239574759	0,1009114		3,356620153	-0,6395597

12	GSS		0,328087593	0,0943123		0,249978002	0,0756394		4,354075569	-0,5459280
13	GPX6		0,69950243	-0,0680043		1,229381593	0,1004380		0,544512759	-0,0566110
14	GPX2		0,600126294	-0,5558675		0,769297045	0,6654978		3,72651001	1,8597412
15	GPX4		0,322177546	0,0629340		0,127836631	0,0286458		0,417081461	0,0772569
16	GSTT2		0,080912982	-0,0278764		0,278407231	0,0822384		4,574103149	-0,5598662
17	GSTK1		0,027175809	0,0107422		0,216748541	-0,0726237		3,419158093	-0,5121094
18	TXNDC12		0,410517857	0,0649266		0,388789238	0,0622337		3,659371954	0,2837062
19	GSTO2		0,884711073	-0,0897461		1,375644138	0,1209635	*	6,955662574	-0,3288411
20	GSTM4		0,04685745	0,0080160		0,294339368	-0,0413411		0,288296977	-0,0406494
21	GPX3		0,83846731	0,2941985		0,810765888	0,2873264		0,150540598	-0,0755932
22	GSTM5		1,671039077	-0,2612124	*	13,43030158	-0,9489656		0,103818114	0,0303096
23	ANPEP		0,359375763	0,1457741		0,245620915	-0,1070668	*	9,646845174	-1,2655445
24	GSTM3		2,33499371	-0,2405895		5,712584549	-0,4132931		3,77759616	-0,3227391

Table 9: List of the glutathione metabolism pathway genes and the results obtained after statistical evaluation of the genome-wide expression analysis of whole kidney homogenates from 0, 6 and 24 day old transgenic rats PKD2 (1-703) (Mut) compared to TECs isolated from SD rats (SD).

Data were considered significant if the negative log of the p-value of Mut/SD was greater than 5.83. '*' denotes statistical significance after Bonferroni correction.

Panayiota Kotsogiannou

	Gene		neglogp Mut/SD T0	fold Mut/SD		neglogp Mut/SD T6	fold Mut/SD		neglogp Mut/SD T24	fold Mut/SD
1	TBP		1,549398444	0,091406		1,337172348	0,0830078		1,088564458	0,0729999
2	TAF2		1,116621795	0,077592		0,909290802	-0,0679830		0,252872597	-0,0255090
3	GTF2IRD1		1,913895704	-0,126953	*	9,693459257	-0,3454001		0,101983947	-0,0133168
4	TAF6		0,461263582	-0,052331		0,77908165	0,0770044		0,240231083	-0,0310950
5	GTF2H3		0,165790169	0,017193		1,123265284	-0,0751361		1,253276496	0,0808475
6	GTF2H4		1,175111422	0,097982		0,754031931	0,0720331		2,485770214	0,1593192
7	TAF11		1,120782939	-0,133268		1,582243742	-0,1673503		3,556343037	-0,2773438
8	GTF2I		0,069690796	-0,007017	*	5,938939351	-0,1869629		1,191893867	-0,0698657
9	TAF9		0,004113519	0,000977		0,168816531	-0,0343424		1,478585354	0,1783854
10	GTF2B		1,006749857	-0,087950		0,386750485	-0,0436790		0,909821164	0,0820313
11	GTF2F2		0,516267383	-0,083876		0,84579029	0,1207682		0,905855087	0,1268446
12	GTF2A1		1,188954479	-0,116211		4,052391719	0,2515299		0,940433779	0,0990885

Table 10: List of the basal transcription factors genes and the results obtained after statistical evaluation of the genome-wide expression analysis of whole kidney homogenates from 0, 6 and 24 day old transgenic rats PKD2 (1-703) (Mut) compared to TECs isolated from SD rats (SD).

Data were considered significant if the negative log of the p-value of Mut/SD was greater than 5.83. '*' denotes statistical significance after Bonferroni correction.

	Gene		neglogp Mut/SD T0	fold Mut/SD		neglogp Mut/SD T6	fold Mut/SD		neglogp Mut/SD T24	fold Mut/SD
1	CDK6		0,49380856	-0,1117622		3	0,3603516		0,076910323	-0,0228950
2	CDKN1A		0,265358669	-0,0654948		0,655110723	0,1317546		4	0,4141113
3	SHC3		0,510330843	-0,0944372		1,869587403	0,2313730		0,42551195	-0,0822121
4	MAPK1		0,278007726	0,0508174		2,879831529	0,2629485		3,354361086	0,2887370
5	MAP2K1		0,096443175	-0,0179332		0,300453402	0,0481066	*	6,691150146	0,3856037
6	PIK3CA		0,355668949	0,0412760		3,647181057	-0,1986793		2,896289983	-0,1733352
7	CBLB		0,042413131	-0,0061849	*	11,17777955	-0,4025472		0,301031061	-0,0357259
8	AKT1		0,313378976	-0,0790654		0,307772515	-0,0780037		4,281601863	0,4729456
9	MYC		0,265898367	0,2084310		0,016957528	-0,0164063	*	6,074967236	1,7522461
10	ACVR1C		0,056031527	-0,0140625		0,365926097	0,0728516		1,403165268	-0,1921084
11	NRAS		0,123204105	0,0393880		0,196414141	0,0592448		4,173836958	0,5406087
12	RAF1		0,476392382	0,0382487		1,664851708	0,0927058		0,452637769	0,0367839

13	RB1		2,443460343	0,2554525		0,384203185	0,0709352		2,543821061	-0,2619629
14	BCL2L1		0,870498808	-0,0809384		0,272596962	0,0335984		0,598829949	-0,0619420
15	STAT5A		0,088187644	-0,0200521		2,855663896	0,2804036		2,926817716	-0,2846680
16	STAT5B		0,261733542	0,0299805		0,471158386	0,0477865		1,025994144	-0,0837240
17	AKT2		1,324630599	-0,1190405		0,042931719	0,0070844		2,882343257	0,1944361
18	NFKBIA		0,127872829	-0,0256800		0,463044096	-0,0747613		5,384810363	0,3781467
19	PIK3R1		2,311501627	-0,4911386		0,130404705	0,0569300		1,091350265	0,3016855
20	PTPN11		0,849069975	0,0752249		0,042310114	0,0059482		0,855765906	0,0756392
21	SMAD3		1,207491035	-0,1312145		1,249153382	0,1346199	*	5,823774162	0,3508237
22	TGFB3		0,457552926	0,1465140		0,38375106	-0,1278705		3,007015614	0,5228456
23	CRKL		0,071462286	0,0089410		3,102148945	0,1587240	*	6,710624396	0,2512864
24	CBLC		0,315942178	0,0495877		1,595472139	0,1593967		3,01301677	0,2378111
25	CTBP1		0,008421309	-0,0008286	*	6,662879101	-0,1883339		1,869791587	0,0858191
26	AKT3		1,45090492	0,1214658		0,097184628	-0,0145089		2,79714711	0,1848028
27	TGFBR1		0,639592795	-0,0755894		0,421711227	0,0553214	*	6,282161976	0,3217516
28	PIK3R2		1,019784238	-0,0511556		2,11084018	-0,0819987		0,457063835	-0,0286947
29	RELA		0,104358486	0,0199160		1,023694714	0,1234975		2,827886301	0,2373917
30	NFKB2		0,593758314	0,0979492		0,312407778	-0,0597005		2,917324018	0,2826497
31	ABL1		0,280050447	0,0392992		1,770461845	-0,1486742		1,548790786	0,1364228
32	SOS1		1,839836353	0,0872053		0,85192224	-0,0525724		0,259819684	-0,0213085
33	E2F1		0,822280014	0,0997277		0,637626001	0,0835709		0,533236672	0,0728575
34	SMAD4		0,006899696	-0,0012370		1,54336883	-0,1377387		3,649817377	0,2344184
35	RUNX1		0,104935477	0,0560784		0,182963642	0,0916785	*	7,101706643	1,1540897
36	MAPK3		0,422531009	-0,0458984		0,192778784	-0,0241970		1,371596883	0,1066623
37	CRK		0,23272584	0,0327000		3,004485564	0,2004025	*	15,32834539	0,5374645
38	CCND1		0,372874754	0,0516680	*	5,965120906	-0,3191402	*	10,39477695	0,4368374
39	MAP2K2		0,024637647	-0,0029659		1,731917737	-0,1023963		3,103490683	-0,1469907
40	TGFB1		0,675317242	-0,1473130		0,411655429	-0,1016809	*	6,641991142	0,6339418
41	PIK3R3		0,891497012	-0,1176990		1,389476457	0,1590867		2,70288431	0,2437686
42	ARAF		0,068633533	0,0111003		0,314340578	-0,0422517		2,812916564	-0,1928322
43	BAD		0,205970528	0,0289418		0,376079687	0,0473485		2,864621066	0,1918547
44	GRB2		0,040235413	0,0045030		0,605675352	0,0469021	*	7,77527715	0,2387424
45	CTBP2		0,917210318	-0,0700955	*	6,041677856	-0,2370877		0,065534491	-0,0079210

Репозиторий БГМУ

46	NFKB1		0,448192002	0,0805220		0,328315373	0,0632209	*	7,815530809	0,5176669
47	TGFB2		0,107074086	-0,0420410		0,070577165	0,0286621		3,721984713	0,5718424
48	TGFBR2		0,271552192	-0,0459961		0,813003034	0,1060547		2,853915036	0,2407878
49	CDKN1B		0,777545263	0,0480867		0,645060496	-0,0422529		0,903391434	-0,0534035
50	IKBKB		0,52083626	0,0484138		1,365799363	-0,0952000		3,058711055	0,1582623
51	GAB2		1,247690093	-0,0996501		3,500554793	0,1920166		0,332898013	-0,0379639
52	HDAC2		0,242350225	0,0410156		1,034838377	-0,1234375		0,22770897	-0,0389323
53	CDK4		0,421782096	-0,1053060		0,80276501	-0,1695150		4,412363882	0,5094808

Table 11: List of the chronic myeloid leukemia pathway genes and the results obtained after statistical evaluation of the genome-wide expression analysis of whole kidney homogenates from 0, 6 and 24 day old transgenic rats PKD2 (1-703) (Mut) compared to TECs isolated from SD rats (SD).

Data were considered significant if the negative log of the p-value of Mut/SD was greater than 5.83. '*' denotes statistical significance after Bonferroni correction.

	Gene		**neglogp Mut/SD T0**	**fold Mut/SD**		**neglogp Mut/SD T6**	**fold Mut/SD**		**neglogp Mut/SD T24**	**fold Mut/SD**
1	GSTO1		0,017555616	0,0050686		0,309035355	0,0703470		4,559294663	-0,43874
2	ADH7		0,216295463	0,0314941		0,921390412	0,0958659		1,656082963	-0,14193
3	MGST1		0,3573793	0,0782434		7,410557147	0,5837175		0,006131538	-0,00178
4	ADH1	*	0,591769001	0,3269043		0,266860861	-0,1756185		6,931591074	-1,61515
5	CYP1A1	*	0,016100357	0,0179332		0,201099332	0,1897491		5,544830689	-1,90089
6	CYP1A2		0,299476621	-0,0591560		0,796910913	0,1241418		1,164656112	-0,16153
7	GSTA3	*	0,019182889	-0,0135239		0,581071053	0,2802734		5,617359218	-1,21662
8	GSTM1		0.0325826742	0.0253255		0.0064307627	0.005143		4,307734832	1,16455
9	GSTM2		0,012718438	-0,0041775		0,066731348	-0,0207248		1,026496973	0,19493
10	CYP2E1		0,863716493	0,3319010		1,712158862	0,5249102		1,840208879	-0,54934
11	GSTT1	*	0,131480759	-0,0241247		0,873634572	0,1089048		6,785518213	-0,39873
12	EPHX1		0,584514204	0,1360677		4,192160805	0,5205892		1,800227812	-0,29834
13	ALDH3A1		1,010747352	-0,0885417		0,720332887	0,0698686		0,679919803	-0,06703
14	CYP1B1	*	0,721042267	-0,2872070		1,132362992	-0,3931292		5,590550354	1,06806
15	GSTT2		0,080912982	-0,0278764		0,278407231	0,0822384		4,574103149	-0,55987
16	ADH4		0,529734053	-0,0843099		0,059456879	0,0129485		0,703298947	-0,10380
17	GSTK1		0,027175809	0,0107422		0,216748541	-0,0726237		3,419158093	-0,51211
18	ALDH3B1		0,056652743	0,0105054		0,580673962	0,0766158		0,411009171	-0,05898

19	GSTO2	*	0,884711073	-0,0897461		1,375644138	0,1209635		6,955662574	-0,32884
20	GSTM4		0,04685745	0,0080160		0,294339368	-0,0413411		0,288296977	-0,04065
21	UGT2A1		0,662915247	-0,0721209		0,428703293	0,0520472		0,497664909	-0,05881
22	GSTM5		1,671039077	-0,2612124		13,43030158	-0,9489656		0,103818114	0,03031
23	GSTM3		2,33499371	-0,2405895		5,712584549	-0,4132931		3,77759616	-0,32274

Table 12: List of the metabolism of xenobiotics by cytochrome P450 pathway genes and the results obtained after statistical evaluation of the genome-wide expression analysis of whole kidney homogenates from 0, 6 and 24 day old transgenic rats PKD2 (1-703) (Mut) compared to TECs isolated from SD rats (SD).

Data were considered significant if the negative log of the p-value of Mut/SD was greater than 5.83. '*' denotes statistical significance after Bonferroni correction.

Panayiota Koupepidou